Testing KIFC1 dependence across cancer types. Is cell survival more dependent on centrosome clustering or Survivin expression?

Name: Marcus Chorlton

Supervisor: Andrew Fielding

Biomedical Science MSc by Research

Biomedical and Life Sciences, Faculty of Health and Medicine

Lancaster University, United Kingdom

October 2024 – September 2025

1.0 – Abstract

Kinesin family member C1 (KIFC1) is a motor protein that helps crosslink microtubules, transports cargo such as vesicles to the cell nucleus, and promotes accurate chromosome alignment and segregation during mitosis in healthy cells. In cancer, however, KIFC1 facilitates the clustering of supernumerary centrosomes, enabling the formation of pseudo-bipolar spindles and supporting the survival of cancer cells. KIFC1 has also been reported to promote the stability of the protein Survivin. Survivin, encoded by BIRC5, is an anti-apoptotic protein and mitotic regulator also frequently expressed in cancer. Both proteins are of therapeutic interest due to their roles in mitotic progression and survival.

It is shown in the literature that many studies have focused greatly on breast cancer cell lines, but not as much compared to other cancer types, such as Ovarian, Colorectal and Central Nervous System (CNS) cancers. Therefore, this project aimed to investigate the dependency of cells on KIFC1 across Ovarian, Colorectal, and CNS cancer cell lines and determine whether KIFC1's influence on centrosome clustering or Survivin expression plays a more critical role in cell survival. While KIFC1 has been well-studied in breast cancer, its function in other cancer types remains less understood. Six cell lines from the NCI-60 panel were selected: OVCAR8 and OVCAR4 (Ovarian), COLO205 and HT29 (Colorectal), and U251 and SNB-19 (CNS), representing cells with either high or low levels of centrosome amplification (CA) in each cancer type.

Bioinformatic analysis using cBioPortal confirmed frequent alterations in KIFC1 and BIRC5 in cancers, with a weak correlation at the mRNA level. KIFC1 was knocked down using siRNAs, and the expression of KIFC1 and Survivin, as well as cell viability and apoptosis, were assessed using MTS assays and immunofluorescence staining. Other software, such as Fiji and GraphPad PRISM, was used to visualise, quantify, and interpret data findings from the experiments to fulfil the experimental design.

This project demonstrates that many cancer cell lines depend on KIFC1 for proliferation and survival, highlighting it as a key therapeutic target. Survivin contributed variably, but overall cell viability was more strongly dependent on non-clustering cellular mechanisms. The KIFC1–Survivin relationship differed across cell types and appeared influenced by p53 status, with mutant p53 lines showing greater sensitivity to KIFC1 loss, whereas wild-type p53 lines showed resistance. In CNS cancers, apoptosis was the primary driver of reduced cell viability. cBioPortal analyses further confirmed the clinical relevance of KIFC1 and Survivin, supporting their combined targeting at the protein level. These findings highlight both the therapeutic promise and complexity of disrupting the KIFC1–Survivin axis in cancer and support further studies targeting KIFC1 therapeutically, including the development of Proteolysis-Targeting Chimaeras (PROTACs) to target KIFC1 across various cancer types.

Table of Contents

2.0 – Acknowledgements

I want to thank Andrew Fielding for all the assistance he has provided in guiding me through this project. He is an excellent supervisor to have. I also want to thank fellow MSC by Research student Katie Mitchinson for the support through this project.

3.0 – Author's Declaration

Declaration:

This thesis is entirely my work and has not been submitted in whole or in part for the award of a higher degree at any other educational institution. No sections of this thesis have been published.

4.0 – Introduction

4.1 - Cancer overview

Cancer is the 2nd leading cause of mortality worldwide (World Health Organization, 2019). Whilst treatments and patient outcomes have improved significantly over the past 2-3 decades, treatment strategies require further improvement to enhance the prognosis of patients. Cancer cells acquire six main capabilities known as the hallmarks of cancer (Figure 1). These include evading apoptosis, self-sufficiency in growth signals, insensitivity to anti-growth signals, tissue invasion and metastasis, sustained angiogenesis, and limitless replicative potential (Figure 1). Uncontrolled cell proliferation is a significant process, driven by mutations in key proteins (Hanahan and Weinberg, 2011). For example, the tumour suppressor p53 promotes apoptosis, DNA repair, and cell cycle arrest in cells. It is also commonly mutated in cancer to evade apoptosis and survive in stressful conditions (Dorati, 2023). In addition to the six original hallmarks, genome instability and mutation were introduced as additional hallmarks in 2011 (Hanahan and Weinberg, 2000). Cancer cells frequently exhibit centrosome amplification (CA) and mitotic dysregulation, both of which can lead to genome instability, a phenomenon that will be discussed later.

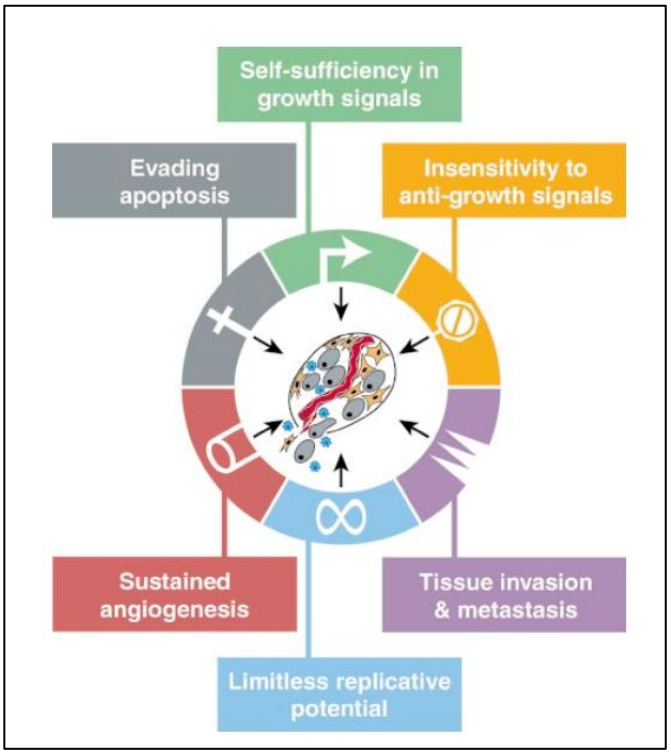

Figure 1: Hallmarks of cancer.

Cancer cells acquire six capabilities during their development. These include sustained angiogenesis, limitless replicative potential, evading apoptosis, self-sufficiency to growth signals, insensitivity to anti-growth signals and tissue invasion and metastasis.

4.2 – Ovarian, Colorectal and CNS Cancer

Ovarian, Colorectal and CNS cancers have been thoroughly studied in the literature, but in terms of centrosome amplification, not to a high degree compared to breast cancer research.

4.2.1 - Ovarian cancer

Ovarian cancer (OC) is prevalent primarily in women over the age of 50 and often presents with nonspecific pelvic or abdominal symptoms. Despite advancements in treatments, prevalence rates have been slowly increasing each year, with the highest incidence rates located in Northern, Central and Eastern Europe (Webb and Jordan, 2017). Various symptoms associated with OC include nausea, diarrhoea, fatigue, urinary symptoms, pelvic or back pain, and constipation. Risk factors for OC include smoking, obesity, and a high-fat or high-starch diet. In contrast, increased intake of vitamin C or E, regular physical activity, and fibre may reduce the risk of OC. However, there is limited evidence to

support the usefulness of specific lifestyle changes. Diagnostic screening for OC patients includes transvaginal ultrasonography and a serum CA-125 measurement. Approximately 85-95% of OCs are derived from epithelial cells, particularly in older women, while 5-8% arise from stromal cells and 3-5% from germ cells, which are more common in younger individuals (Webb and Jordan, 2017). Epithelial OC is most diagnosed during stages three or four, affecting approximately 70% of patients. Routine screening is generally not recommended, but women with a known family history of hereditary OC should be offered genetic counselling (Family, Roett and Evans, 2009). Interestingly, women who have given birth are at lower risk of developing OC, with each birth associated with a 10-20% reduction. Other studies have shown that menopausal hormone therapy increases OC risk by 40% (Webb and Jordan, 2017).

Recent studies have identified other genes that promote hereditary OC, including BRIP1, RAD51C and RAD51D, and BRCA1/2 (Paul, 2014). The RAD51D gene is essential for DNA repair through homologous recombination, and defects in this gene may increase OC risk. OC cells with a mutant RAD51D gene have shown increased sensitivity to PARP inhibitors (Pennington and Swisher, 2012). Mutated BRCA1 and BRCA2 genes are well-known to drive cell proliferation in ovarian and breast cancers (Paul, 2014). Both genes have essential roles in DNA damage repair and transcriptional regulation. Mutations in these genes promote abnormalities in DNA repair, thereby increasing OC risk. (Paul, 2014).

OC cells can exhibit multidrug resistance. These cells often possess ATP-active drug efflux pumps, such as p-glycoprotein inhibitors and multidrug resistance proteins, which enable them to expel drug molecules from the cells (Talib et al., 2021). Other resistance mechanisms may disrupt apoptotic pathways, immunity, cell cycle regulation, metabolism, oxidative stress, and autophagy. While the use of bevacizumab, which, in combination with chemotherapy, has been trialled as a treatment of epithelial OC, the prognosis did not improve (Yang et al., 2022). Similarly, the PARP inhibitor, Olaparib, was used to target OC cells with mutant BRCA genes, but its effectiveness was limited to patients who exhibit these mutations. Therefore, additional research is required to identify new biomarkers for treatment (Yang et al., 2022).

Surgery and chemotherapy remain the primary treatments for OC but often present significant challenges (Yang et al., 2022). Recent studies have explored immunotherapy, including CAR-T therapy and immune checkpoint inhibitors. Unfortunately, OC cells exhibit inhibitory signals that enable them to evade destruction by cytotoxic lymphocytes, thereby reducing the effectiveness of immunotherapy. CAR-T therapy also faces significant challenges, including antigen heterogeneity, physical barriers, and the complexity of the tumour microenvironment (Yang et al., 2020).

p53 gene therapy has been widely studied as a potential treatment for OC. Approximately 96% of cases of High-Grade Ovarian Cancer (HGOC) harbour p53 mutations, suggesting that p53 is a crucial gene for therapeutic targeting (Wallis et al., 2023). A clinical trial investigated the administration of adenoviral vectors with a wild-type p53 alongside standard chemotherapy to OC patients with a p53 mutation. The study found that approximately 77% of primary OCs exhibit impairments in cytochrome-c-dependent azotosome activation due to defects in the p53-induced caspase cascade (Zeimet and Marth, 2003). However, epigenetic changes, such as histone acetylation, may increase OC malignancy, thus making p53 gene therapy more challenging. Overall, more gene targets in OC are necessary to improve treatment strategies (Zeimet and Marth, 2003).

4.2.2 - Colorectal cancer

Colorectal cancer is the second most deadly cancer worldwide, with a mortality rate of almost 900,000 cases annually (Prashanth Rawla, Sunkara and Barsouk, 2019). Women experience approximately 25% lower incidence and mortality rates compared to men. By 2025, 2.5 million new cases are projected, making effective treatment and prevention strategies paramount. Incidence rates are increasing due to numerous factors. These include the ageing population, dietary changes in high-income countries, lack of physical activity, smoking and obesity. These factors have highlighted the need for effective screening programs, which are slowly becoming apparent, to increase early diagnosis rates (Dekker et al., 2019). Hereditary colorectal cancers exist, such as Lynch syndrome, a non-polyposis subtype

characterised by an impaired mismatch repair system due to the expansion of microsatellite repeats (Dekker et al., 2019).

Colorectal cancer originates from polyps and proliferates slowly. Eventually, two main pathways can lead to colorectal cancer, with the first being the adenoma-carcinoma pathway, accounting for approximately 70-90% of cases. This pathway involves mutations in tumour suppressors and oncogenes, including APC, TP53, KRAS, and BRAF, respectively. In approximately 10-20% of cases, the serrated neoplasia pathway is affected, involving mutations in the KRAS and BRAF oncogenes. In approximately 2-7% of cases, germline mutations in mismatch repair genes, such as MSH2, are associated with Lynch syndrome, as shown in Figure 2 (Dekker et al., 2019). Additional mutated genes are involved in promoting colorectal cancer progression and metastasis. Using cBioPortal, several key genes were identified in the TCGA database from colorectal cancer patients, including APC, KRAS, BRAF, PIK3CA, SMAD4, and TP53 (Huang et al., 2018). The APC tumour suppressor controls the Wnt/β-catenin signalling pathway to regulate cell proliferation and survival. APC genetic mutations are commonly observed in CRC, thus increasing cell survival through β-catenin accumulation (Zhao et al., 2022). Somatic TP53 mutations are also highly prevalent in approximately 60% of metastatic CRC cases, indicating many CRC cells depend on mutant TP53 for survival. Loss-of-function mutations in TP53 have been shown to promote metastasis by impairing DNA repair and inhibiting apoptosis (Shin, Giancotti and Rustgi, 2023).

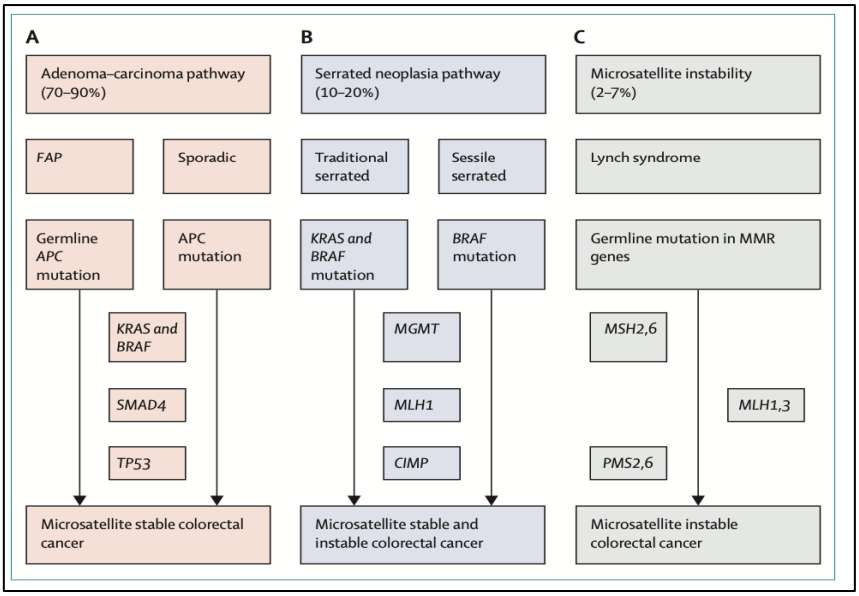

Figure 2: Colorectal cancer exhibits multiple pathways for tumorigenesis

The adenoma-carcinoma pathway (A) is highly prevalent in most sporadic colorectal cancers, caused by genetic mutations in the KRAS or BRAF genes, followed by methylation of tumour suppressor genes, such as TP53. Microsatellite stability remains apparent. The serrated neoplasia pathway (B) affects fewer cases associated with genetic mutations in KRAS or BRAF genes. Microsatellite repeats are either stable or unstable, depending on the level of epigenetic silencing activity. Lynch syndrome becomes apparent when microsatellite repeats are highly unstable (C) and caused by germline mutations in mismatch repair genes, affecting fewer cases (Dekker et al., 2019).

The epithelial-mesenchymal transition (EMT) contributes to the survival of CRC cells, specifically promoting motility, metastasis, and invasiveness. Commonly used drugs for metastatic CRC include 5-fluorouracil, capecitabine and oxaliplatin. However, genetic mutations may increase resistance, thereby reducing the efficacy of the drug. Epidermal growth factor receptor (EGFR) inhibitors are also frequently explored, as 60-80% of cancers exhibit EGFR overexpression (Shin, Giancotti and Rustgi, 2023). Cetuximab, a monoclonal antibody that binds to EGFR, is currently effective in clinical trials (Cancer Research Institute, 2023). However, EGFR-targeted therapies are selective and may not be effective in patients with mutated KRAS and BRAF genes. Immunotherapy strategies against CRC have also been explored. Although challenging, specific methods, such as PD1-blocking antibodies, have been granted FDA approval, including pembrolizumab and nivolumab. However, these treatments are

less effective in CRCs that express low microsatellite instability, which accounts for many CRC cases. Fewer neoantigens, low mutation burdens and reduced immune cell filtration are characteristics of these tumours, hindering efficacy levels in immune checkpoint inhibitors. Compared to the findings of (Yang et al., 2020), safety concerns are evident with CAR-T therapy, including cytokine release syndrome, which can result from off-target effects in healthy cells (Shin, Giancotti, and Rustgi, 2023). Given that this is evident from the literature, other treatments are necessary to minimise or eliminate the negative health impact of treatment in cancer patients, such as using siRNAs, which offer promising results.

4.2.3 - CNS cancers

CNS cancers are becoming increasingly prevalent at any age, affecting both children and adults (National Brain Tumor Society, 2024). Over 90% of cases exhibit a primary tumour in the brain, whereas fewer cases exhibit a primary tumour in the spinal cord, meninges or cranial nerves. Incidence and mortality cases globally in 2016 were 330,000 and 227,000, respectively. Incidence across all ages increased by 17.3% between 1990 and 2016. India, China and the USA reported the highest incidence of CNS cancers. Signs and symptoms of CNS cancer are diverse and include vision loss, blindness, headaches, seizures, speech disturbance and possible paralysis. Risk factors for acquiring CNS cancer include ionising radiation. Factors such as aspirin use, hormonal influences, cell phone radiation, pesticides, and dietary exposure have not been shown to increase the risk of CNS cancer (Fitzmaurice, 2019). Several diagnostic tests can be used to identify CNS cancer, such as brain MRI scans, biopsy and a lumbar puncture to examine cerebrospinal fluid levels (Tumors, 2023). There are several types of known brain tumours, such as gliomas, which are the most common type of CNS cancer. Glioblastoma, a high-grade glioma, can originate in astrocytes from the brain and is characterised as being fatal within two years of diagnosis. While gliomas are predominantly malignant, some can be benign. Other brain tumour types include pituitary, choroid plexus, embryonal, germ cell, pineal, meningiomas, and nerve tumours (Mayo Clinic, 2024).

Genetic syndromes have a minor but essential role in increasing CNS cancer risk, such as Neurofibromatosis types 1 and 2, Turcot syndrome, and Li-Fraumeni syndrome (Tumors, 2023). These syndromes are associated with germline mutations in tumour suppressor genes such as TP53, APC, NF1 and NF2. TP53 gene mutations, for example, promote brain tumour growth in Li-Fraumeni syndrome (Reilly, 2008), whereas APC gene mutations promote brain tumour growth in Turcot syndrome (Jovanović et al., 2023). Germline mutations in predisposition genes, such as IDH1/2 and CHEK2, increase the risk of CNS cancer. The CHEK2 gene plays a role in DNA damage repair, and its loss has been shown to downregulate apoptosis and disrupt cell cycle arrest mechanisms (Sameer Farouk Sait, Walsh, and Karajannis, 2021). In adult CNS cancers, mutated IDH1/2 genes are highly prevalent in low-grade and secondary high-grade gliomas, driving tumour growth (Cohen, Holmen, and Colman, 2013). Additionally, NF1 and NF2 genetic mutations can activate RAS/MAPK and PI3K/AKT pathways to promote cell proliferation in paediatric and adult CNS cancers (Jovanović et al., 2023). Interestingly, the PTEN gene, a tumour suppressor, is frequently mutated in glioblastomas to activate the PI3K/Akt/mTOR pathway, thereby increasing drug resistance and metastasis (Hashemi et al., 2023).

Glioblastoma-initiating cells are capable of proliferation, self-renewal and differentiation. The Aurora-A protein is a mitotic kinase required to modulate these cells, as it activates Cyclin B1-CDK, allowing cells to pass through the G2/M checkpoint in the cell cycle (Qin et al., 2008). Mutations in the AURKA gene, which encodes Aurora-A, promote CA, tumorigenesis and aneuploidy (Omim.org, 2015). Due to its characteristics in glioblastoma, inhibition of Aurora-A is a key therapeutic target for this disease. Alisertib, an Aurora-A inhibitor, has shown promising anti-tumour activity in glioblastoma by inhibiting Aurora-A (Kurokawa et al., 2016). However, patients exhibited several side effects, such as hypertension, diarrhoea, fatigue and febrile neutropenia (Willems et al., 2016). Immunotherapy is a widely researched treatment approach for many cancers. Most glioblastoma patients express tryptophan-degrading enzyme 2,3-dioxygenase (IDO), which is involved in immune evasion. Increased IDO activity may suppress the adaptive immune response by inducing apoptosis of cytotoxic lymphocytes, while decreased IDO expression may enhance T-cell-mediated tumour defence, thus

increasing cell survival in gliomas (Hosseinalizadeh et al., 2022). Currently, chemotherapy, radiotherapy, and surgery are commonly used treatment approaches in CNS cancers. For example, doxorubicin, a chemotherapeutic drug, is often used to treat cancer patients. However, epigenetic changes in gliomas may contribute to the development of increased drug resistance. Another challenge is that the blood-brain barrier can complicate the efficacy of treatment (He et al., 2022). Given the difficulties of overcoming multidrug resistance in Ovarian, Colorectal and CNS cancers, novel approaches are required.

4.3 – Centrosome Amplification

4.3.1 - Centrosome structure and function

Centrosomes are small, membrane-less organelles found in the cell cytoplasm. Each centrosome contains two cylindrical, microtubule-based structures known as centrioles, which exhibit nine-fold symmetry and help organise the surrounding pericentriolar material (PCM). Centrosomes promote accurate chromosome segregation by nucleating and anchoring microtubules during mitosis, promoting genomic stability. One centriole may transition into a basal body, forming a primary cilium or motile cilium, which is critical for tissue homeostasis (Vasquez-Limeta and Loncarek, 2021). Centrosome orientation and the microtubule network also establish cell polarity, which is important for directional cell migration. As cells reach the S and G2 phases, centrosomes duplicate, mature and localise to opposite poles to create a bipolar spindle for proper chromosome alignment and separation in mitosis, as shown in Figure 3 (Mónica Bettencourt-Dias and Glover, 2007). This current knowledge of centrosome dynamics is highly stable, regulated and apparent in healthy cells. In cancer cells, however, this is not the case.

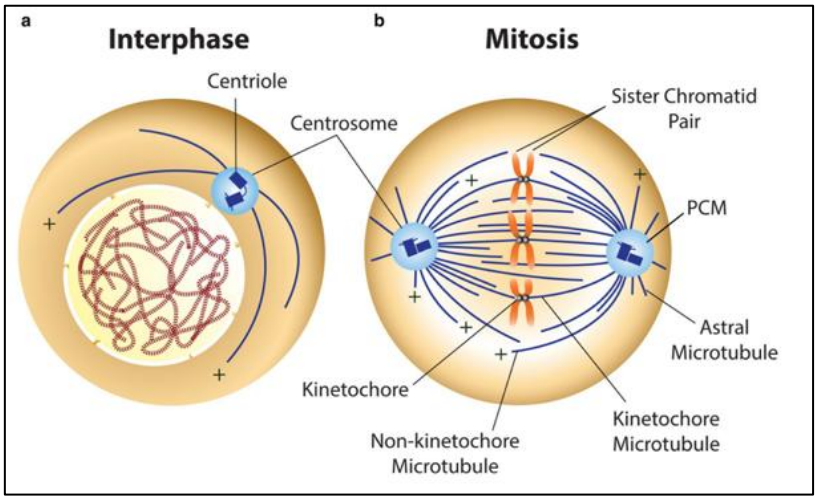

Figure 3: Centrosomes during interphase and mitosis

Centrosomes anchor microtubules at their minus ends, allowing microtubule-positive ends to extend outward in the cytoplasm. They nucleate microtubules in the PCM. During interphase (A), only one centrosome is present in healthy cells at the G1 phase and is duplicated during the S phase. Interphase centrosomes are essential for mediating organelle positioning and vesicle trafficking. During mitosis (B), healthy cells contain two centrosomes that are localised at opposite poles to one another. Microtubules attach to chromosomes during metaphase at their kinetochores, promoting chromosome segregation (Ryniawec and Rogers, 2021).

4.3.2 - Coping Mechanisms for Centrosome Amplification

Centrosomes are frequently dysregulated in cancer, which is referred to as CA. It is characterised by cells exhibiting more than two centrosomes and is a hallmark of several cancers, including Ovarian, Colorectal and CNS cancers. Metastasis, abnormal cell division and aneuploidy are associated with CA, contributing to cell survival and progression (Harrison, Bleiler, and Giardina, 2018). Cells undergoing mitosis may face challenges such as mitotic arrest, aneuploidy or apoptosis. To prevent cancer cells from exhibiting these outcomes, they develop coping mechanisms, such as centrosome clustering, to organise amplified centrosomes at two poles during mitosis, thereby maintaining a pseudo-bipolar spindle. Other coping mechanisms include centrosome loss by degradation or extrusion, as illustrated in Figure 4 (Qi and Zhou, 2021). There are two main types of CA, however. The first type is known as numerical CA, which is characterised by cells containing more than two centrosomes, often caused by centriole overduplication and cytokinesis failure, which leads to multipolar spindle formation. The

second type includes structural CA, which is characterised by abnormally large or hyperactive centrosomes, which can also occur even when centrosome numbers are normal (Sabat-Pośpiech et al., 2019).

Centrosome clustering relies on many cellular proteins, including KIFC1, cortical actin, and cell adhesion molecules. MYO10, for example, can directly bind to astral microtubules and coordinate their positioning with subcortical actin to promote centrosome clustering. The spindle-assembly checkpoint (SAC) plays a crucial role in preventing the cell cycle from advancing past metaphase until a pseudo-bipolar spindle with clustered centrosomes is formed (Qi and Zhou, 2021). Additionally, protein ubiquitination is required to regulate centrosome clustering. The Anaphase-promoting complex/cyclosome (APC/C) is a ubiquitin ligase involved in the ubiquitin-proteasome system, which marks proteins for degradation. Depletion of APC/C via declustering agents such as proTAME promotes centrosome declustering by initiating aberrant spindle pole movement during metaphase (Konstantinos Drosopoulos et al., 2014).

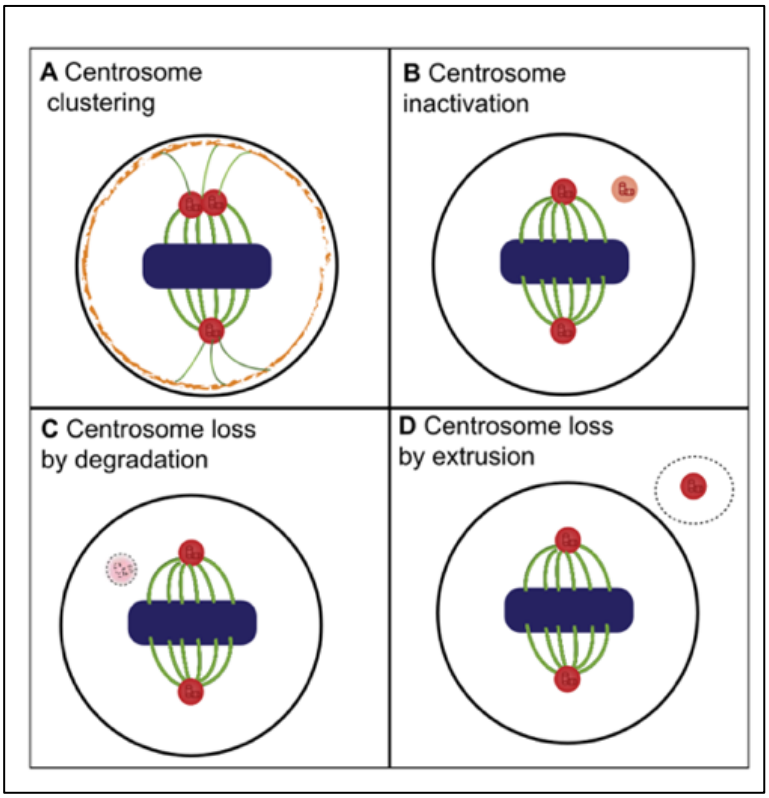

Figure 4: Cellular mechanisms associated with CA in cancer

Cancer cells exhibit coping mechanisms to sustain CA. Centrosome clustering and inactivation are highly characterised across several cancers. Cancer cells without these coping mechanisms fail to sustain CA, thus promoting multipolar mitosis and apoptosis (Konstantinos Drosopoulos et al., 2014).

4.3.3 - Consequences of CA

Colorectal cancer displays high levels of centrosome clustering and overduplication. Mutations in the BRAF oncogene, particularly the V600E point mutation, contribute to upregulated BRAF activity, causing aberrant RAF-MEK-ERK signalling in cells. This pathway induces hyperphosphorylation and stabilisation of Mps1, a protein that regulates the SAC, which may increase mitotic delay. Additionally, the loss of p53 hinders the regulation of centrosome duplication and integrity, thus promoting CA even further in cells (Harrison, Bleiler, and Giardina, 2018).

CA is highly prevalent in aggressive breast carcinomas and is often associated with p53 loss. These cancer cells exhibit centriole size deregulation, which promotes CA through mechanisms such as ectopic centriole formation and centriole fragmentation (Figure 5). Elongated centrioles also contribute to hyperactive centrosomes and promote the development of nucleated microtubules. Poor chromosome segregation during mitosis will likely drive chromosomal instability (Marteil et al., 2018).

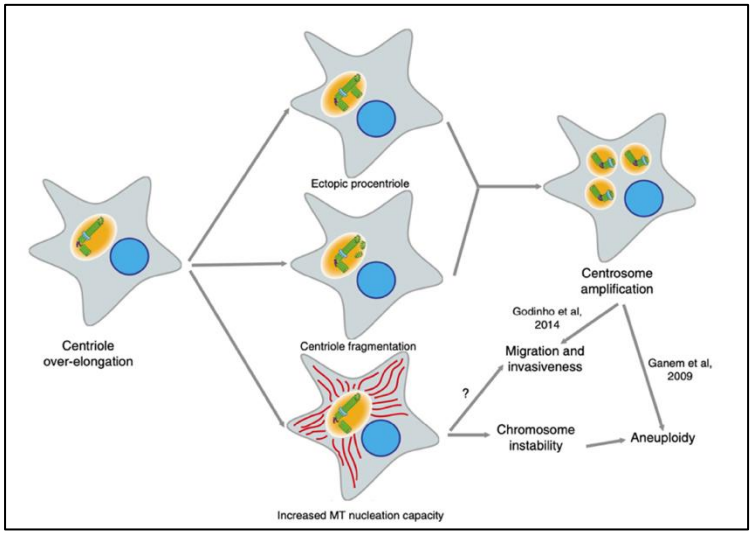

Figure 5: Centriole length deregulation is common in cancer

CA is induced by centriole elongation through ectopic procentriole formation or centriole fragmentation. Centriole elongation exhibits an increased capacity for microtubule nucleation in cells, promoting chromosomal instability during mitosis. As a result, CA becomes apparent, increasing tumour migration and invasiveness (Marteil et al., 2018)

The PLK4 kinase is required for regulating centrosome duplication. Following this, the PLK4 kinase localises to the proximal end of a parental centriole, phosphorylating the protein STIL for centriole elongation. The study by (Kim et al., 2019) investigated the role of the centrosome protein CEP131 in colon cancer cells. This protein has been previously explored in breast cancer and has been shown to elevate CA levels. Human U2OS cells tagged with CEP131 showed a 10% increase in CA and centriole development. Cells expressing higher levels of PLK4 resulted in a stronger interaction between CEP131 and STIL, ultimately driving tumorigenesis.

The APC tumour suppressor gene in colon cancer is frequently mutated, resulting in the loss of EB1 binding and C-terminal microtubule domains. This disrupts microtubule regulation, contributing to genomic instability and the development of tumours. Interestingly, β-catenin knockdown has been associated with reducing centrosome duplication, suggesting that APC is critical in maintaining centrosome stability (Harrison, Bleiler, and Giardina, 2018).

Centrosome-related proteins are also essential in cancer. Centromere protein J (CENPJ) is highly expressed in glioblastoma and plays a crucial role in regulating cellular proliferation and migration. Within CENPJ, a specific region known as PN2-3 has been shown to destabilise microtubules for cellular migration (Gabriella et al., 2022).

The RAP1 protein is a signalling molecule that aids cell adhesion, proliferation, and differentiation. It is activated in response to CA in the MCF10A breast cancer cell line. Activation of RAP1 has been shown to increase metastasis, motility, alterations, and invasiveness in cell adhesion proteins. Additionally, RAP1 activation disrupts epithelial barrier integrity by impairing the function of tight junctions. This suggests that CA can activate downstream proteins to promote tumour progression and cell survival (Prakash et al., 2023).

Aggressive uveal melanoma (UM) has been shown to exhibit high CA levels. In UM, loss-of-function mutations in the tumour suppressor gene BAP1 promote monosomy 3 in UM cells. It was discovered that the centrosome abnormality mitotic score was higher in cells with monosomy 3 than in cells without monosomy 3. Additionally, the Mel270 primary UM cells exhibited a frequency of 10% compared to the OMM2.3 metastatic UM cells, which had a frequency of 32%, suggesting that metastatic UM cells display higher levels of CA and monosomy 3. In comparison, metastatic and non-metastatic breast cancer cells did not display very high levels of CA compared to OMM2.3 cells (Sabat-Po Spiech et al., 2022).

A genome-wide RNAi screen was performed in *Drosophila* S2 cells to examine mechanisms that suppress multipolar divisions in cancer cells exhibiting CA. The SAC has been shown to prevent multipolar mitoses in cancer cells, preventing catastrophic chromosomal missegregation that would

initiate apoptosis. Additionally, specific proteins, such as Ncd, a kinesin-14 family member, enable centrosome clustering and prevent multipolar mitoses in S2 cells. Some kinesin proteins, such as KIFC1, promote centrosome clustering in human cancer cells, aiding survival (Kwon et al., 2008).

(Sauer et al., 2023) explores the degree of CA in high-grade serous ovarian carcinoma (HGSOC) cells. Among 93 HGSOC tumour sections, most showed a high degree of CA. Cells will likely show higher genome subclonality due to CA, which promotes genetic diversity in tumour cell populations. Furthermore, survival signalling pathways, such as the PI3K/AKT and MAPK pathways, are upregulated in cells with CA. Targeting proliferative genes in cancer could disrupt these signalling pathways, rendering cells more susceptible to apoptosis. Oxygen also plays a significant role in HGSOC cells, as it can promote the growth of cancer. This suggests that the tumour microenvironment is required for cell growth.

4.4 – Survivin

4.4.1 - Structure and function of Survivin

Apoptosis is a key mechanism for eliminating damaged cells through the activation of enzymes known as caspases, which cleave cellular proteins. Cells undergo a signalling cascade via either the intrinsic or extrinsic pathway. Specific treatments, like DNA damage or antimicrotubular agents, can help activate the intrinsic pathway. However, research has also identified an anti-apoptotic protein known as Survivin, which has been shown to contribute to drug resistance in cancer (Mita et al., 2008). Survivin is the smallest inhibitory apoptotic protein (IAP), 16.5-Kda in size, and is encoded at chromosome 17q25 by the BIRC5 gene. Survivin's structure contains an N-terminal Baculovirus IAP repeats (BIR) domain and a C-terminal alpha-helical region. The BIR domain is associated with anti-apoptotic function, whereas the alpha-helical region is associated with microtubule binding, as shown in Figure 6 (Jaiswal, Goel and Mittal, 2015).

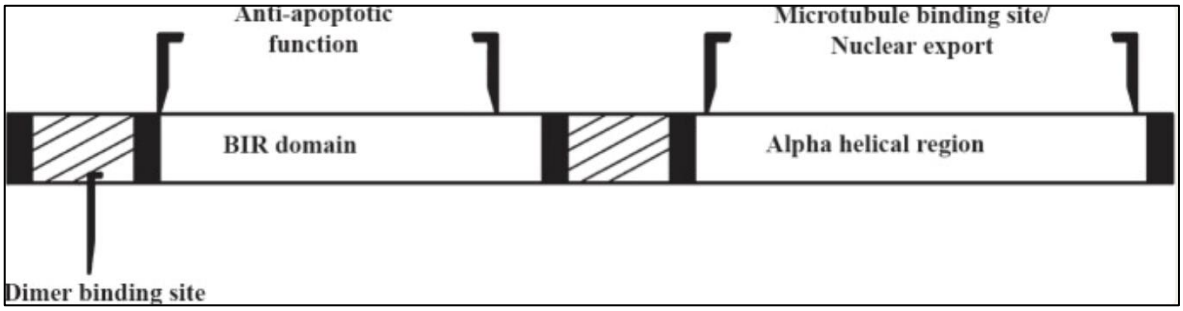

Figure 6: Structure of Survivin

Survivin has an N-terminal BIR domain and is associated with anti-apoptotic function. The C-terminal alpha-helical region is associated with microtubule binding (Jaiswal, Goel and Mittal, 2015).

Survivin expression is highly regulated throughout the cell cycle, peaking at the G2/M phase but declining in the G1 phase. It is released from the mitochondria in cells upon chemotherapy, contributing to drug resistance. As cells approach mitosis, Survivin is localised in the nucleus at kinetochores, microtubules, and centromeres by interacting with INCENP, Borealin, and Aurora-B to form the chromosomal passenger complex. This helps chromosomal alignment and stability of the mitotic spindle. During cytokinesis, Survivin is localised at the cell midbodies to ensure stability and proper mitotic division. CDK1 can also interact with and phosphorylate Survivin, leading to its activation (Chen et al., 2016). Survivin primarily aims to suppress apoptosis by inhibiting the activity of caspase enzymes. When cellular stress decreases, Survivin is inhibited by SMAC-DIABLO to suppress apoptosis (Figure 7). Overall, Survivin has a dual role in mitotic progression and regulation of apoptosis (Mita et al., 2008).

4.4.2 - The role of Survivin in cancer

Survivin has been shown to play a critical role in cancer progression. Several studies have found that Survivin protects cancer cells from therapeutic agents and environmental stress. For example, (Guindalini, Mathias Machado and Garicochea 2013) found that honokiol-induced apoptosis was downregulated when Survivin was upregulated. Furthermore, p53 promoted honokiol-induced apoptosis, suggesting a counteractive relationship between p53 and Survivin in cancer, as shown in

Figure 7. (Lai et al., 2014) An experiment was conducted to determine the effect of p53 and Survivin in colorectal cancer. The results were similar to those of (Guindalini, Mathias Machado, and Garicochea 2013), emphasising that Survivin is a key therapeutic target in cancers. In brain tumours, Survivin polymorphism -31C>G was genotyped in 82 patients and evaluated using ELISA. Survivin expression was significantly higher in malignant brain tumours than benign ones, suggesting that Survivin expression correlates with higher tumour severity (KAFADAR et al., 2018). Furthermore, the wnt/β-catenin signalling pathway is highly associated with colorectal cancers. Overexpression of β-catenin in the cell nucleus forms a β-catenin/T-cell factor transcriptional activator, which promotes Survivin expression to evade apoptosis (Chen et al., 2016). In recent studies, Survivin has been found in exosomes released from cancer cells. These exosomes transfer Survivin to surrounding cells, promoting therapeutic resistance, proliferation, and survival pathways. Furthermore, Survivin overexpression upregulates angiogenesis by interacting with endothelial cells to supply cancer cells with oxygen and nutrients for proliferation (Mahmoudian-Sani et al., 2019).

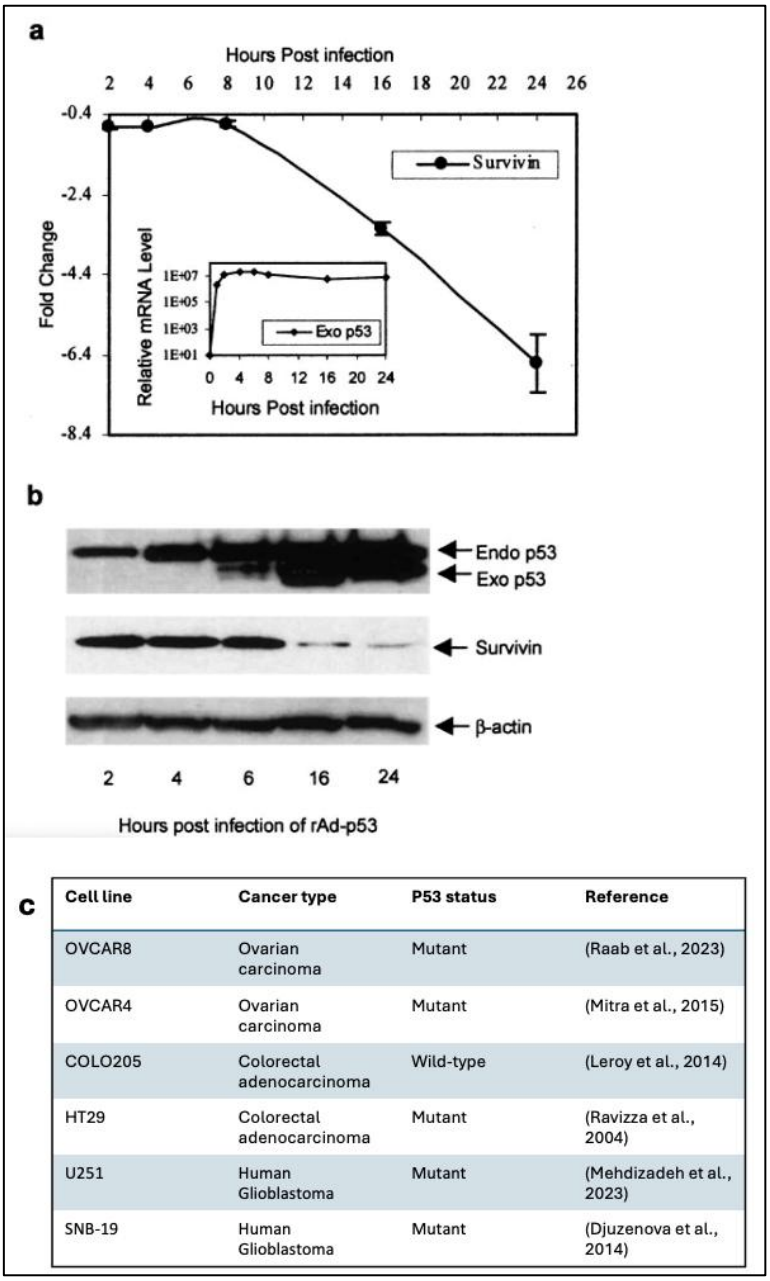

c

Cell line	Cancer type	P53 status	Reference
OVCAR8	Ovarian carcinoma	Mutant	(Raab et al., 2023)
OVCAR4	Ovarian carcinoma	Mutant	(Mitra et al., 2015)
COLO205	Colorectal adenocarcinoma	Wild-type	(Leroy et al., 2014)
HT29	Colorectal adenocarcinoma	Mutant	(Ravizza et al., 2004)
U251	Human Glioblastoma	Mutant	(Mehdizadeh et al., 2023)
SNB-19	Human Glioblastoma	Mutant	(Djuzenova et al., 2014)

Figure 7: Survivin at the protein and mRNA levels is repressed via increased p53 expression in cancer.

(A) showing RNA analysis from 2774qw1 cells using RT-PCR and revealed a continuous reduction in Survivin expression with exogenous p53. **(B)** showing a western blot analysis, which revealed a significant reduction in Survivin protein expression at 16 hours post-infection of rAd-p53. **(C)** showing a referenced table summary of p53 status in selected cancer cell lines.

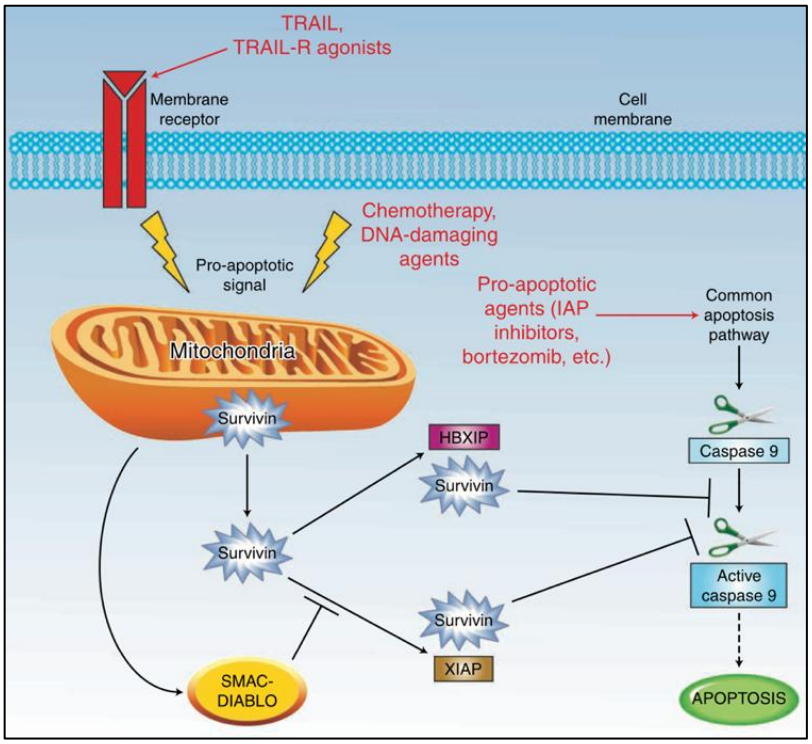

Figure 8: Survivin suppresses apoptosis.

When cells respond to chemotherapy and other DNA-damaging agents, Survivin is released from the mitochondria. In the cell nucleus, Survivin may interact with additional proteins, such as INCENP, Borealin, and Aurora-B, to promote chromosomal alignment and the stability of the mitotic spindle. Survivin also interacts with and binds to caspase 9 enzymes to inhibit apoptosis. When cellular stress decreases, SMAC-DIABLO inhibits Survivin (Mita et al., 2008).

4.5 – KIFC1

4.5.1 - Structure and function of KIFC1

Kinesin-14 motors are highly conserved in eukaryotes, from yeast to humans. They counteract Kinesin-5 motors, however, which exert opposing forces in spindle positioning and tension. Kinesin-5 pushes microtubules outward, whereas kinesin-14 pulls microtubules inward. Specific kinesin-14 members, such as Ncd, migrate to the positive end of microtubules while interacting with the EB1 protein to maintain microtubule stability and organisation. Kinesin-14 motors can cooperatively work with one another to maintain spindle structure and movement. This is critical in ensuring these motors can effectively transport cargo across microtubules. KIFC1 is a cell motor protein from the kinesin-14

subfamily which transports cargo from the plus end of microtubules to the negative end (She and Yang, 2017).

KIFC1 is localised in the nucleus during interphase (S phase) using its nuclear localisation signal (NLS) for chromosome alignment and spindle assembly. KIFC1's NLS is also required for binding to importin B, a protein that regulates spindle assembly. In mitosis, however, KIFC1 is localised at the mitotic spindle to allow effective centrosome clustering (Xiao et al., 2017). KIFC1's conserved C-terminal motor domain has a catalytic region for ATP hydrolysis and a microtubule-binding site. It has a stalk domain vital for regulating KIFC1's movement along microtubules. The N-terminal tail domain is used for binding to vesicles and y-tubulin, and it also has a microtubule-binding site to allow effective crosslinking, as shown in Figure 9 (Wei and Yang, 2019).

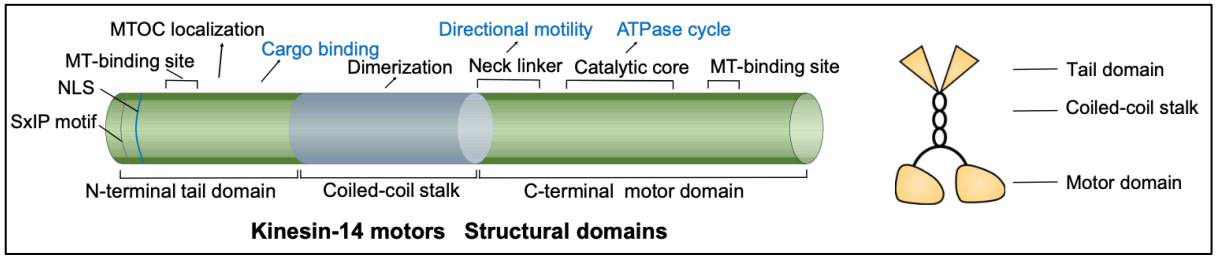

Figure 9: Overview of KIFC1 structural domains

Three domains are found in KIFC1. The C-terminal motor domain contains a catalytic region for ATP hydrolysis and a microtubule-binding site. The N-terminal tail domain promotes binding to vesicles and y-tubulin for cross-linking. The coiled-coil stalk domain regulates KIFC1 movement across microtubules (She and Yang, 2017).

KIFC1 facilitates nuclear membrane maintenance by regulating nuclear shape and positioning, thereby preventing nuclear deformation as KIFC1 migrates to opposing microtubule ends. Knockdown of KIFC1 has been shown to prolong the S phase in healthy cells, suggesting that genomic integrity may depend on KIFC1 expression, allowing DNA to be successfully repaired and synthesised before G2 entry. Therefore, KIFC1 can promote cell survival by facilitating proper cell cycle progression (Wei and Yang, 2019). Additionally, KIFC1 is required for meiotic maturation in mouse oocytes. A morpholino injection

and a KIFC1 inhibitor, AZ82, were used to determine KIFC1 expression. KIFC1 knockdown induced body extrusion defects in these oocytes, negatively affecting oocyte maturation. KIFC1 can interact with actin-related proteins, such as Fmn2, which is required for spindle migration. The expression of these proteins decreased in KIFC1-depleted oocytes, indicating that KIFC1 regulates the expression of specific proteins (Shan et al., 2022).

4.6 - KIFC1 function in cancer

4.6.1 - KIFC1 induces centrosome clustering

KIFC1 is an essential protein for CA in triple-negative breast cancer cells, regulating bipolarity and centrosome clustering during mitosis. KIFC1 knockdown was shown to increase multipolar mitoses in breast cancer, thus increasing the prevalence of chromosome missegregation. This suggests that KIFC1 is essential for maintaining the mitotic spindle. KIFC1 knockdown also promoted mitotic arrest. If cells remain in mitosis for too long, they may enter a state of senescence, thus limiting proliferative capacity and promoting centrosome clustering. KIFC1 dependency is increased in breast cancer cells exhibiting higher CA levels because the need for centrosome clustering is greater. Furthermore, CA was highly prominent in the EC109 breast cancer cell line overexpressing KIFC1. It further highlights that a higher KIFC1 expression is associated with higher levels of CA (Patel et al., 2018).

Cancer cells treated with DNA-damaging agents, such as chemotherapeutic drugs, promote KIFC1 clustering in vitro and *in vivo.* Under DNA damage, KIFC1 at serine 26 is phosphorylated via ATM and ATR kinases. Chemotherapeutic treatment revealed a delay in KIFC1 degradation, suggesting that DNA damage stabilises KIFC1 without increasing KIFC1 transcription levels. Moreover, KIFC1 exhibited lower ubiquitination levels in response to these drugs, thereby preventing degradation (Fan et al., 2021).

4.6.2 - KIFC1 interacts with Survivin to suppress apoptosis

Like other studies, KIFC1 is also overexpressed in hepatocellular carcinoma cells. Cell viability and apoptosis in HCC-LM3 and SMMC-7721 cell lines were evaluated via KIFC1 knockdown. siRNAs targeting KIFC1 showed a significant reduction in cell viability. Additionally, KIFC1 has been shown to

increase Survivin levels and prevent degradation via the ubiquitin ligase APC/C in hepatocellular carcinoma cells (Fu et al., 2018). KIFC1 binds to Survivin, preventing poly-ubiquitination and subsequent proteasomal degradation, thereby increasing cell stability and evading apoptosis. KIFC1-Survivin interaction can indirectly support the completion of mitosis even if genomic instability or CA is not highly expressed. More evidently, KIFC1 increases Survivin expression in breast cancer. Knockdown of KIFC1 may, therefore, downregulate Survivin expression as it can no longer protect Survivin from polyubiquitination and degradation (Fu et al., 2018). Targeting KIFC1 would be ideal in therapeutics to determine the relationship between Survivin and KIFC1 in future studies (Pannu et al., 2015).

4.6.3 - KIFC1 increases cell proliferation, invasiveness and metastasis

KIFC1 is required to promote cell proliferation in Oesophageal carcinoma. It also interacts with kinase proteins, such as Aurora-B. Aurora-B ensures proper microtubule attachment to chromosomes, thus acting as a cell quality control mechanism. It was discovered that KIFC1 knockdown suppressed Aurora-B expression. Overall, this study concluded that KIFC1 has a dual role in localising and regulating Aurora-B (Du et al., 2023).

The SKOV3 OC cell line was used to determine if KIFC1 knockdown suppressed cell proliferation. These cells were transfected with sh-KIFC1-1 to analyse cell viability and KIFC1 mRNA expression. Results showed that SKOV3 cells had a significantly lower proliferative capacity after transfection. Furthermore, CENPE expression was suppressed in response to KIFC1 knockdown. CENPE accumulates in the G2 phase and is highly abundant in breast and lung cancers, promoting chromosome alignment and kinetochore assembly (Li et al., 2020).

KIFC1 has been shown to regulate ZWINT in colorectal cancer. ZWINT is a protein in cells that is required for kinetochore assembly, enabling adequate chromosome segregation during mitosis. Immunohistochemical analysis revealed that ZWINT overexpression is associated with lower cell survival rates compared to cells with normal ZWINT levels. Furthermore, a KIFC1 inhibitor, kolavenic acid analogue, was used and showed a decline in proliferative capacity (Akabane et al., 2021). Figure

10 reveals that KIFC1 inhibition via KIFC1 siRNAs significantly reduces cell viability in two breast cancer cell lines, achieved by binding to KIFC1 mRNA. This effectively inhibits the translation of KIFC1 mRNA into protein, reducing KIFC1 expression and inhibiting its function (Li et al., 2015).

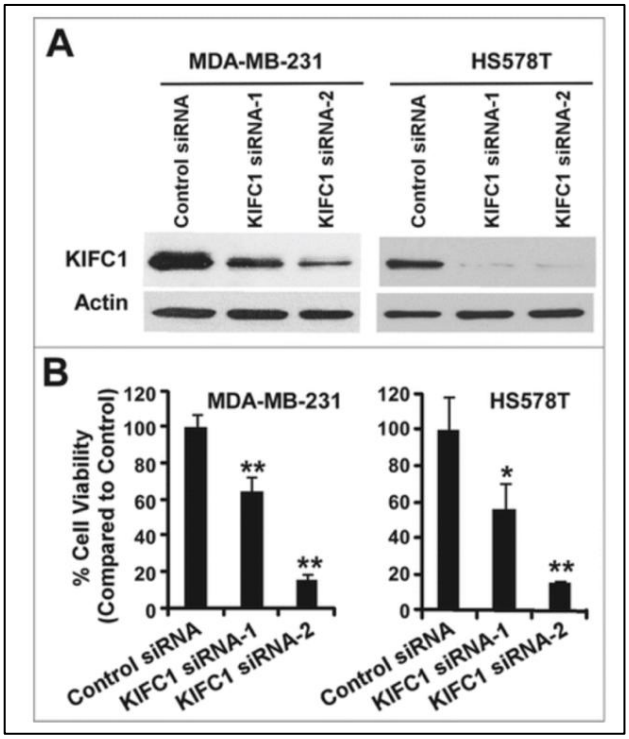

Figure 10: KIFC1 silencing significantly reduces cell viability in Triple-negative breast cancer cells. Western blot analysis to reveal KIFC1 expression in two Triple-negative breast cancer cell lines, MDA-MB-231 and HS578T, after KIFC1 siRNA treatment (A). KIFC1 silencing was apparent after KIFC1-siRNA treatment in both cell lines (B). The two cell lines were transiently infected with KIFC1 siRNAs in 96-well plates, and the CellTiter-Glo assay was used after 7 days of culture to measure cell viability.

4.6.4 - KIFC1 upregulates signalling pathways

Cancer cells upregulate the rate of glycolysis to provide energy and facilitate biosynthesis, even in a hypoxic environment, thereby increasing cell survival. They rapidly deplete glucose for DNA, RNA and protein synthesis. Glucose, lactate, ATP and LDH were upregulated in response to high KIFC1 levels, suggesting that KIFC1 significantly contributes to aerobic glycolysis. qRT-PCR and western blotting assays revealed KIFC1 expression in endometrial cancer cells. KIFC1 has been shown to upregulate GLUT1, HK2 and LDHA in aerobic glycolysis by promoting c-myc expression. KIFC1 can interact with

HMGA1 to regulate the expression of downstream genes, such as c-myc. This increases glucose metabolism in cancer cells, thereby promoting cell survival and growth. In contrast, the depletion of KIFC1 resulted in the suppression of aerobic glycolysis through the downregulation of HMGA1 and c-myc (Zhou et al., 2021).

KIFC1 is overexpressed in non-small cell lung carcinoma cell lines H1730, A549 and PC9. It is shown that the TGF-B/SMAD signal is aberrantly activated in cells overexpressing KIFC1. This promotes the production of ECM proteins and cytokines, enhancing cell survival, metastasis, and invasion (Liu et al., 2023).

4.6.5 - KIFC1 is associated with poor prognosis and drug resistance

The prognostic value of KIFC1 was analysed in bladder cancer cells after cystectomy. A correlation between KIFC1 and prognosis rates was established using a Kaplan-Meier analysis. Patients exhibiting higher KIFC1 expression exhibited worse patient outcomes, like lower survival rates (Sekino et al., 2021). In contrast, Kaplan-Meier curves were used to determine prognosis rates in prostate cancer and resulted in poorer prognosis rates in patients with high KIFC1 expression. This conclusion was apparent in other cancers like UM, thyroid carcinoma and mesothelioma (Kostecka et al., 2021).

Additionally, drug resistance is a significant issue in cancer therapeutics. Certain drugs, such as tamoxifen, taxane, and docetaxel, are becoming increasingly ineffective. Four kinesin proteins, KIFC1, KIF1A, KIFC3, and KIF5A, are overexpressed in breast cancer after drug treatment (Xiao and Yang, 2016). Overall, KIFC1 appears to have multiple functions in cancer, which is illustrated in Figure 11.

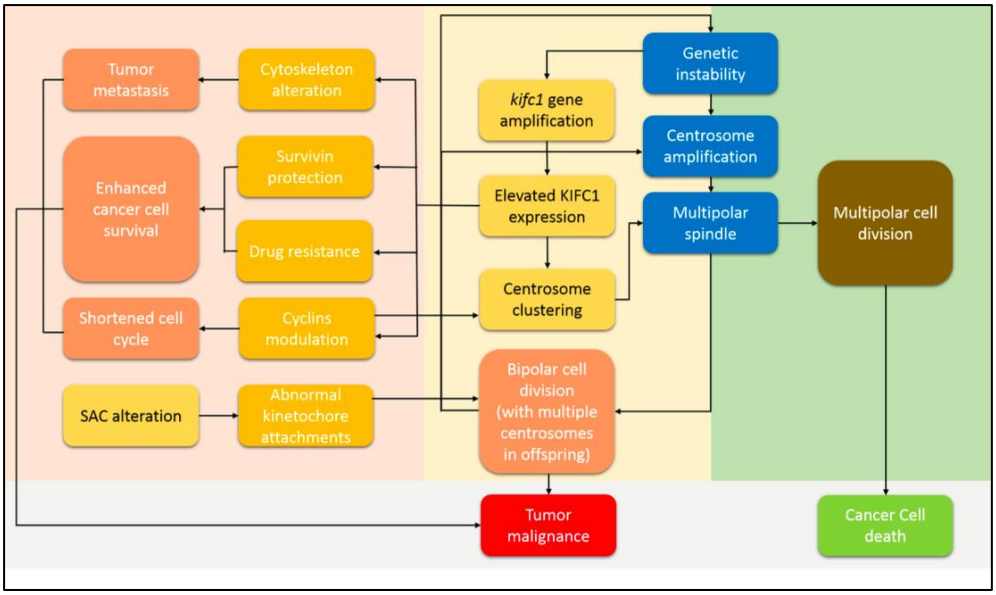

Figure 11: Schematic overview of KIFC1

KIFC1 can induce many characteristics in cancer cells. It is well-studied in the literature and is often associated with cell proliferation, invasiveness, metastasis, drug resistance, and signalling pathways. KIFC1 can also suppress apoptosis by protecting Survivin from ubiquitination and degradation. Increased KIFC1 expression may rescue cells by preventing the accumulation of multipolar spindles, which are often exhibited in CA. As such, KIFC1 also promotes centrosome clustering to achieve bipolar segregation and genetic stability (Xiao and Yang, 2016).

4.7 – KIFC1 inhibitors

A chemotherapeutic drug, paclitaxel, was used to determine cell viability in CRC cells. Low-dose paclitaxel was added to the HCT116 cancer cell line. It was found that cell viability was significantly lower in cells treated with the drug compared to cells without the drug, and the cells did not exhibit altered cell cycle or morphological properties (Chaoxiang Lv et al., 2017). Paclitaxel (Taxol) has been widely studied for its efficacy against various cancers due to its anti-microtubular properties; it binds to β-tubulin, thereby preventing microtubule depolymerisation (Drugbank.com, 2016). No studies have yet assessed whether Taxol can indirectly inhibit KIFC1 in cancer.

Additionally, the PJ34 drug is a potential therapeutic agent for the breast cancer cell line MDA-MB-231. It is a PARP inhibitor that promotes centrosome declustering and avoids damage to healthy cells. The

primary function of PJ34 is to suppress the poly-(ADP-ribose) polymerase, which acts as a transcriptional regulator. No studies have yet used this inhibitor to target KIFC1 (XIONG et al., 2014).

4.7.1 - SR31527

A small-molecule inhibitor, SR31527, promotes centrosome declustering and disrupts KIFC1 ATPase activity, rendering KIFC1 ineffective in cancer cells. SR31527 directly binds to KIFC1, independent of microtubule involvement, promoting multipolar mitosis and apoptosis in breast cancer cells. However, further questions remain, like the safety of drug administration. It remains unclear if cell cycle abnormalities are induced in normal cells (Zhang et al., 2016).

4.7.2 - CW069

The KIFC1 inhibitor, CW069, was synthesised and evaluated against neuroblastoma and breast cancer cell lines, N1E-115 and MDA-MB-231, respectively. It was discovered that multipolar spindles significantly increased in N1E-115 cells following CW069 treatment. Furthermore, CW069 has been shown to promote aberrant cell divisions and apoptosis in N1E-115 cells. It is yet to be verified as a potential chemotherapeutic agent. Further research is needed to evaluate this inhibitor across various cancer types and investigate the impact on healthy cells (Watts et al., 2013). CW069 has also been shown to reverse docetaxel resistance in prostate cancer cells, ultimately leading to an upregulation of apoptosis (Yohei Sekino et al., 2019).

4.7.3 - AZ82

Direct Inhibition of KIFC1 by the inhibitor AZ82 significantly downregulated transcription and translation activities, inducing multipolar mitosis via centrosome de-clustering in prostate cancer cells (Parvin et al., 2020). AZ82 specifically binds to KIFC1's motor domain, preventing ATP hydrolysis and thereby inhibiting movement along microtubules, which promotes apoptosis and decreases cell viability (Park et al., 2017). The study by (Yukawa et al., 2018) compared KIFC1 inhibitors AZ82, CW069, and SR31527. SR31527 displayed moderate levels of KIFC1 inhibition, whereas CW069 did not show significant activity. The specificity and efficacy of these drugs were not fully promising, as some

exhibited off-target effects. Overall, Inhibitors are ideal to a certain degree, but most recent studies have focused on newly synthesised protein-degrading molecules, known as proteolysis targeting chimaeras (PROTACs)

4.8 – PROTACs

4.8.1 - The ubiquitin-proteasome system

The ubiquitin-proteasome system (UPS) is essential for maintaining protein homeostasis, thereby preventing neurodegeneration and cancer. Three main cascade enzymes are associated with the UPS: the E1-activating enzyme, the E2-conjugating enzyme, and the E3 ubiquitin ligase. E1 is required to activate ubiquitin via ATP, and E2 is responsible for transferring the activated ubiquitin through transesterification reactions. The E3 ligase enzyme catalyses ubiquitin transfer to a lysine residue from E2, determining which proteins are tagged for degradation. This is because they bind to specific substrates and are highly selective in regulating protein homeostasis (Ramachandran and Ciulli, 2021).

4.8.2 - Structure and function of PROTACs

Studies have investigated PROTACs, bifunctional structures designed to recruit E3 ligases to the protein of interest (POI) for the selective degradation of target proteins. PROTACs exhibit three elements: a POI ligand, an E3 ubiquitin ligase ligand and a linker region for connecting both ligands. The POI ligand binds to the POI, followed by the E3 ligase ligand binding to the E3 ligase from the cytoplasm. The linker region then conjugates both ligands to activate the molecule. Doing so enables polyubiquitination from the E3 ligase to the POI, initiating destruction at the proteasome (Figure 12). PROTAC molecules can also detach and be recycled to bind to the next POI. This recycling ability suggests that PROTAC molecules remain active, allowing them to continue with additional rounds of protein degradation (Graham, 2022). In 2001, peptide-based PROTACs were used, which recruited the enzyme MetAP-2 to the E3 ligase complex. It was discovered that cell permeability and stability were not excellent, so improvements were necessary. In 2008, small-molecule PROTACs were synthesised

to selectively degrade protein targets, such as MDM2, CRBN, and VHL ligases. Cell permeability and stability were significantly improved (Li and Crews, 2022).

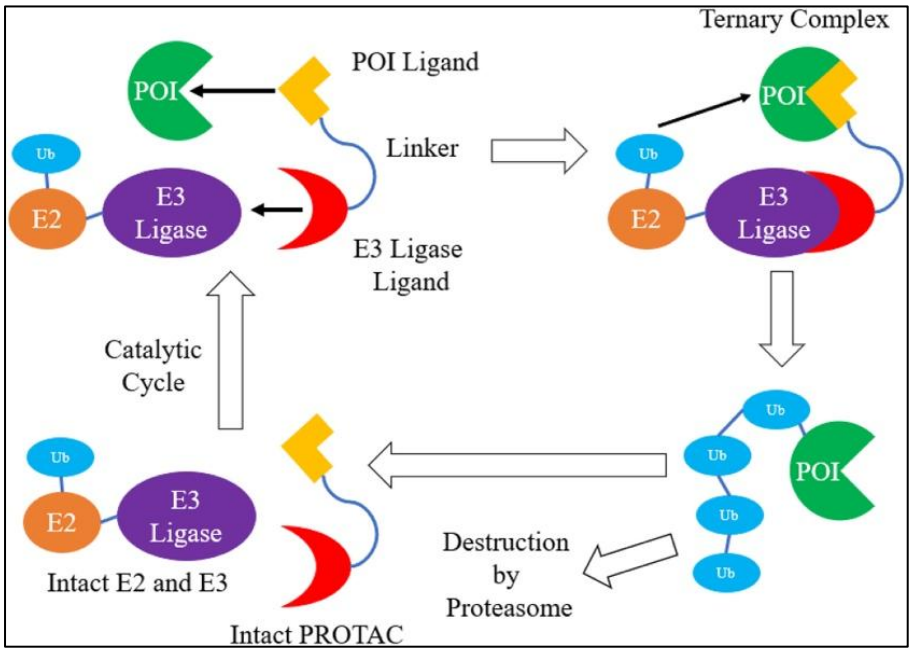

Figure 12: Structure and function of PROTACs

PROTAC molecules are unique; they contain an E3 ligase ligand, POI ligand and a linker region. Once bound to the E3 ligase and POI (ternary complex), polyubiquitination occurs at the POI to be marked for degradation by the 26S proteasome. The PROTAC molecule can be recycled for additional rounds of protein degradation (Graham, 2022).

4.8.3 - PROTACs against cancers

Focal adhesion kinase (FAK), encoded by the PTK2 gene, can be overexpressed in OC cells, making it a key therapeutic target. This led to the synthesis of a FAK kinase inhibitor, VS6063. However, it is not FDA-approved as it only showed modest effects. A FAK-PROTAC molecule was synthesised to investigate the impact on OC cells through FAK degradation rather than inhibition. It was found that the FAK-PROTAC molecule significantly reduced proliferation in OVCAR3 and OVCAR8 cell lines that exhibited high FAK expression, as shown in Figure 13 (Huo et al., 2022).

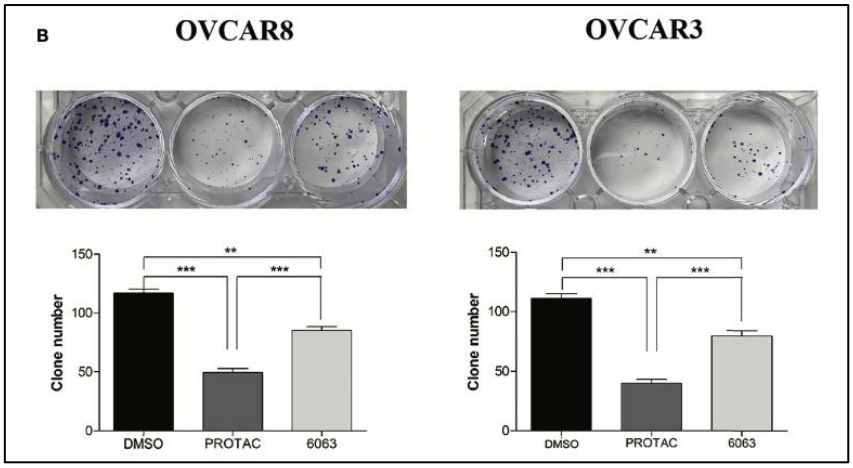

Figure 13: FAK PROTAC displayed fewer colonies than the VS6063 inhibitor.

Cell colonies stained with crystal violet for OVCAR8 and OVCAR3 cell lines treated with therapeutic drugs are shown. DMSO was added to the left cell plate as a control. 0.5 µm FAK-PROTAC and 0.5 µm VS6063 inhibitors were added separately to the other cell plates (Huo et al., 2022).

The transcription factor STAT3 promotes oncogenic processes, including immune evasion and treatment resistance in head and neck squamous cell carcinoma and CRC. STAT3 inhibitors are limited because of the lack of ligand-binding pockets and enzymatic catalytic sites. As a result, a PROTAC molecule prepared from toosendanin (TSM-1) has been synthesised to target STAT3 for degradation by the E3 ligase. The TSM-1 molecule effectively reduced cell viability via cell cycle arrest and promoted antitumour efficacy in STAT3-dependent cells. Combining TSM-1 with an anti-PD-L1 antibody enhances tumour regression, suggesting a high potential for immunotherapy strategies with TSM-1 (Jin et al., 2022).

PROTACs have also been explored in gliomas. The overexpression of the BRD4 gene promotes aberrant activation of downstream oncogenes like Bcl-2 and c-myc, increasing the risk of breast cancer, glioma and acute myeloid leukaemia. The production of nanoparticle cRGD-P, modified with cRGDfk peptides, was used in combination with two drugs: BRD4 PROTAC ARV-825 and doxorubicin. It was discovered that combining two drugs against this nanoparticle promoted cell cycle arrest at the G2/M phase and activation of apoptotic pathways. This suggests that the combination of PROTACs and chemotherapy may be a practical approach to treating cancer (He et al., 2022).

4.8.4 - Advantages and Disadvantages of PROTACs

In neuroblastoma, mitotic regulation is highly preserved due to AURKA gene overexpression, which promotes the stabilisation of the oncogene MYCN, thus providing a key target for PROTACs. The PROTAC molecule SK2188 strongly binds to AURKA for degradation. Furthermore, SK2188 induced MYCN degradation, apoptosis and high DNA damage. It significantly outperforms the AURKA gene inhibitor MK-5108, resulting in a more substantial reduction in cell viability (Rishfi et al., 2023).

Like other studies, PROTACs are more advantageous than small-molecule inhibitors because the POI is degraded rather than inhibited, thus potentially overcoming resistance and improving efficacy. Furthermore, PROTACs are useful against proteins that do not exhibit excellent binding pockets, such as transcription factors and oncogenes, as well as STAT3 and RAS, respectively. Arguably, the main advantage of PROTACs is that they can regulate multiple cycles of protein degradation, meaning one PROTAC molecule can degrade several POIs, thus successfully using lower drug concentrations.

Like other drugs, PROTACs are not perfect. Several challenges exist with them, including their large size, which leads to issues regarding bioavailability (Li et al., 2023). Additionally, PROTACs exhibit poor activity in permeability and aqueous solubility. On- and off-target toxicity in healthy cells may also be apparent because they require these targeted proteins for cell survival; therefore, protein degradation may not be ideal in specific settings. It is recommended that scientific studies continue to use drug inhibitors. Overall, extensive research must be carefully evaluated for PROTACs (He et al., 2022). It is important to note, however, that KIFC1 PROTACs are relatively new to cancer therapeutics and are not yet readily available for testing. In the case of this project, KIFC1 siRNAs still offer promising results by indirectly degrading the KIFC1 protein. This is achieved via complementary binding to its selected KIFC1 mRNA sequence, which consequently inhibits translation activity.

4.9 – Project aims

Many treatment options are available against Ovarian, Colorectal, and CNS cancers. However, treatment strategies such as immunotherapy and chemotherapy can make it challenging to achieve

high efficacy rates against commonly mutated oncogenes and tumour suppressors in cancer (Shin, Giancotti, and Rustgi, 2023). Recent research has identified CA as a key therapeutic target (Qi and Zhou, 2021) because cancer cells need to induce centrosome clustering to avoid aneuploidy, apoptosis, and multipolar mitosis, ultimately increasing cell survival (Marteil et al., 2018). A well-documented function of KIFC1 in cancer is to promote centrosome clustering (Patel et al., 2018). Much of the mechanistic work demonstrating the centrosome clustering effect has been conducted in breast cancer models, particularly TNBC. However, the centrosome clustering function has also been shown in several cancer types. Another significant, yet relatively unexplored, function of KIFC1 is to protect the anti-apoptotic protein Survivin from polyubiquitination and degradation at the 26S proteasome, thereby suppressing apoptosis. (Fu et al., 2018). This function has thus far been demonstrated exclusively in breast cancer. KIFC1 knockdown in many cancers induces multipolar mitosis in cells expressing high levels of CA. KIFC1 knockdown can also promote apoptosis as it can no longer protect and promote Survivin expression, thus highlighting two aspects of KIFC1 function as key therapeutic targets to examine further (Pannu et al., 2015). More cancer cell lines need to be evaluated to determine if the KIFC1-Survivin relationship is consistent across different cancer types.

To target KIFC1, small-molecule inhibitors have been designed against it, like AZ82, but have displayed off-target effects in cells (Yukawa et al., 2018). Current research has focused on PROTACs, which are designed to degrade targeted proteins. It exhibits higher efficacy rates against small-molecule inhibitors due to its more vigorous binding activity to selected proteins and is effective at low concentrations (He et al., 2022).

Overall, testing KIFC1 dependence in Ovarian, Colorectal and CNS cancers is of interest as fewer studies are currently present compared to breast cancer. Additionally, studies have not yet evaluated whether cancer cells rely more on centrosome clustering or Survivin expression in response to KIFC1 depletion. Therefore, the aims of this project are twofold:

1) Test the KIFC1 dependence in cell culture models of some common cancer types, including Ovarian, Colorectal and CNS, available from the NCI-60 cancer cell panel. Cell growth assays

will be performed through MTS cell survival assays. This will provide robust data on which cancer types are sensitive to KIFC1 depletion.

2) Assess whether cancer cells rely more on centrosome clustering or Survivin expression in response to KIFC1 depletion. Confocal microscopy will be used to examine cells for KIFC1 and Survivin expression. Figure 14 illustrates the experimental design and hypothesis in this project.

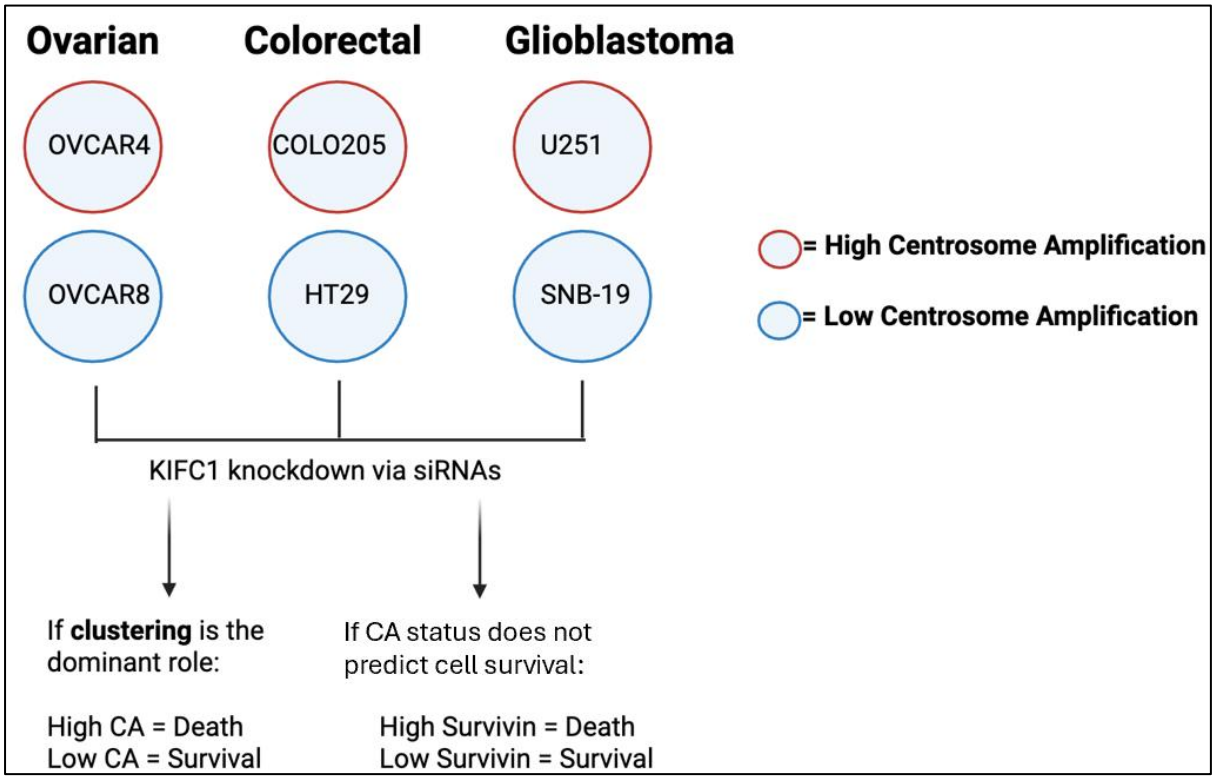

Figure 14: Overview of hypothesis and experimental design related to KIFC1 knockdown in six different cancer cell lines.

Two cell lines, each with a different CA status from three different cancer types, were selected. These were CNS, Ovarian, and Colorectal Cancers, and they were chosen to assess KIFC1 dependence and determine whether centrosome clustering or Survivin is the dominant factor. Cell lines with a red outline indicate high CA status, whereas cell lines with a blue outline indicate low CA status. If centrosome clustering is the dominant factor after KIFC1 knockdown, then we would expect cells with high CA to die and cells with low CA to survive. Conversely, if Survivin is the dominant factor after KIFC1 knockdown, we would expect The CA status of the cells to be a less important factor than Survivin expression.

5.0 – Methods and Materials

5.1 – Methods

5.1.1 - Cell culture

Cancer cells were cultured in RPMI medium containing 10% FBS and 1% penicillin/streptomycin and incubated at 37°C with 5% CO_2. For passaging, cells were first briefly rinsed with 1 mL of trypsin, which was aspirated, and then another 1ml trypsin was added, and the flask was returned to the incubator. After trypsinisation, cells were observed under a light microscope at 4X and 10X lenses, and then RPMI medium was added, depending on the dilution. Cells were pipetted up and down 3 times to remove cell clumps. A small volume of the single-celled suspension was dispensed into a new flask containing complete RPMI medium.

5.1.2 – Methanol Fixed IF staining

Cancer cells were plated onto glass coverslips containing 1ml media, 3 per cell line, into a labelled 6-well plate and incubated at 37°C with 5% CO_2 for 2 days. Cell media was removed from coverslips using the fume hood aspirator. 1 mL of methanol was added to all wells. The 6-well plate was placed in a freezer for 10 minutes, then aspirated, and replaced with 1 mL PBS. Parafilm was cut, labelled and put onto a large tray. Each coverslip was carefully placed face up on the parafilm using forceps. PBS with 5% Goat serum was used for blocking, primary and secondary antibody solutions. A 200µL aliquot from an Eppendorf tube containing PBS with 5% Goat serum and an appropriate primary antibody was dispensed to the appropriate coverslip, and this was repeated for the rest. The coverslips were left stained for 2 hours. Secondary antibodies were collected from a fridge at 4°C and made up in a new Eppendorf tube containing PBS with 5% Goat serum. Primary antibodies were removed from each coverslip and washed with 200µl PBS. 100µl of the secondary antibodies was dispensed onto each

coverslip for 1 hour. Secondary antibodies were removed and washed with 3x100µl PBS for each coverslip. Microscope slides were mounted with 25µL of Mowiol + 4',6-diamidino-2-phenylindole (DAPI). The coverslips were dabbed dry with Kimwipe tissue paper and placed face down on the microscope slide. The slides were dried overnight and then stored long-term at 4°C in the dark. All slides were imaged using a Zeiss LSM880 confocal microscope.

5.1.3 - Cell counting and protein quantification

Fiji software (The Fiji Team, 2019) was used to determine cell counting and protein quantification. The cell image file was opened. KIFC1 protein quantification was quantified in the DAPI channel by selecting 'image', 'adjust' and 'threshold' to highlight cell nuclei with 'dark background' and 'don't reset range' selected. Next, 'Analyse' and 'Analyse particles' were chosen. The size was '50-Infinity' with 'overlay', 'display results', 'add to manager', 'exclude on edges' and 'Include holes' selected. These steps were then applied to the KIFC1 channel to measure KIFC1 expression in cell nuclei. To measure Survivin expression from the cytoplasm and nucleus, the Survivin channel was opened, and it was then measured by selecting 'Analyse' and 'Measure' to calculate Survivin mean expression for the whole image. The rectangle tool in Fiji was used throughout all image analyses to provide a more in-depth look at cell structure, protein localisation and expression intensity at selected fields of view. Data visualisation and statistical analyses were performed using GraphPad PRISM (GraphPad, 2018). Bar graphs and scatter plots were generated using data from each experiment performed. Mean and/or standard deviation lines were visualised on the graphs. Statistical significance between experimental groups was assessed using unpaired two-tailed T-tests or one-way ANOVA with Dunnett's multiple comparison. P-values <0.05 were considered statistically significant. The same analysis parameters were kept constant for each experiment performed.

5.1.4 - MTS serial dilution

100µl of trypsinised cancer cells was carefully dispensed into a haemocytometer channel with a coverslip. The cells were counted under a light microscope using a 10X lens at one large

haemocytometer square. Cell counting was repeated 3 times at different squares to calculate the mean number of cells. Next, the cell dilution was calculated to achieve a cell count per 100µl. 100µl RPMI medium was dispensed into the cell and media-only wells, followed by 100µl diluted cells into well 9 to begin a serial dilution (Appendix 1). Next, the 96-well plate was placed in an incubator at 37°C with 5% CO_2 for 1 day. 20µl MTS agent was dispensed into all wells, and the plate was incubated for 4 hours. The plate was read using a spectrophotometer to obtain absorbance readings at 490 nm.

5.1.5 - Cancer Genomics

The cBioportal website was used to collect Genomic data from cancer patients. 'TCGA PanCancer Atlas studies' and 'query by gene' were selected with the following entered: 'KIFC1' and 'BIRC5' to explore the altered genes in several cancers. 'Mutations,' 'structural variant', putative copy-number alterations from GISTIC, and 'mRNA expression z-scores relative to diploid samples (RNA Seq V2 RSEM)' were selected before selecting 'submit query'. The 'Cancer type summary' tab was chosen to view the altered gene(s) in multiple cancers. Next, the 'plots' tab was chosen to look at mRNA expression in the altered gene(s) from the NCI-60 cancer cell panel. 'mRNA vs study' or 'mRNA vs Dx' were selected, followed by 'log scale', 'sort categories by median', ' mutation type' and 'copy number.' 'Structural variant' was unselected, and each gene was observed separately. The 'mutations' tab was selected to identify all mutations found in each gene. A series of graphs was used to display alteration frequencies, mRNA expression, and mutations of the KIFC1 and BIRC5 genes in several cancers (Cbioportal.org, 2021).

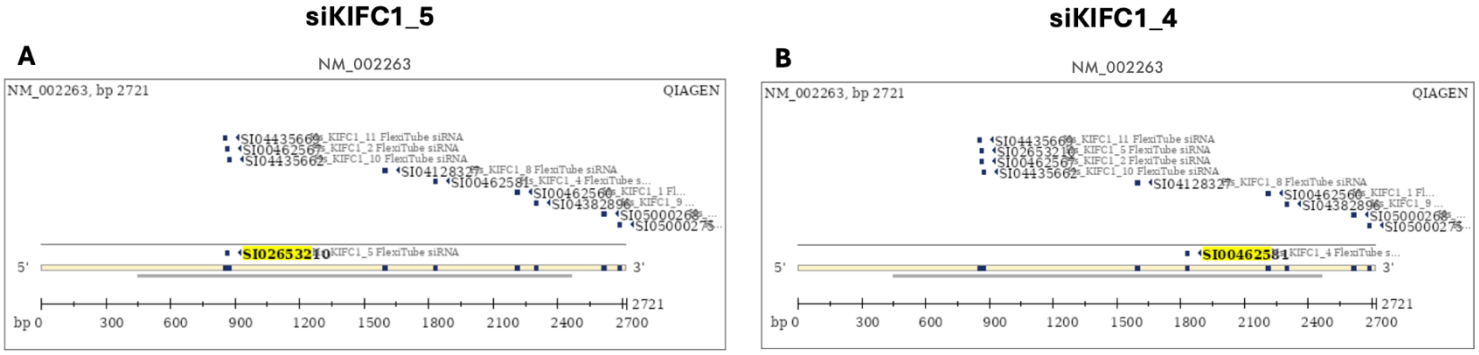

Figure 15: The binding sites of siKIFC1_5 and siKIFC1_4 to KIFC1 mRNA.

siRNA KIFC1 oligos were obtained from the Geneglobe website. Human KIFC1 siRNAs were selected, and the transcripts were observed. Parts A and B show detected KIFC1 transcripts NM_002263 (2721 bp). The locations of siKIFC1_4 and siKIFC1_5 binding sites on KIFC1 mRNA are highlighted (QIAGEN, 2025).

5.1.6 - siRNA transfection

Cancer cells were plated onto glass coverslips containing 1ml media into a labelled 6-well plate and incubated at 37°C with 5% CO_2 for 1 day. 2 wells were used for siRNA control, siKIFC1_5 or siKIFC1_4 per cell line. siRNA transfection mixtures were prepared from a stock concentration of 20µM to give a final concentration of 40nM: RNAiMAX and OptiMem were retrieved from a 4°C fridge, and the siRNA oligos were defrosted from a -20°C freezer. 4 tubes were labelled and added with the appropriate solutions (Appendix 3). 397µl RNAiMAX/OptiMem mixture from tube 1 was added to tubes 2-4, which were then incubated for 5 minutes at room temperature. Cell media from the 6-well plate was aspirated and replaced with 1.7 mL RPMI medium per cell line. 350µl from tubes 2-4 were added to the appropriate wells for each treatment condition. The 6-well plate(s) were incubated for 2 days before starting the methanol-fixed IF staining procedure.

5.1.7 - Reverse siRNA transfection

A 96-well plate and 4 tubes were labelled (Appendix 4). siRNA was prepared at a stock concentration of 20µM and a final concentration of 40nM. For 30 wells, 90µl of diluted RNAiMAX solution was prepared by performing a 1:20 dilution: 4.5µl RNAiMAX with 85.5µl OptiMEM in tube 1. The siRNA

conditions were prepared in 3 additional tubes: Mock (no siRNA), AllStars negative control siRNA, siKIFC1_4, and siKIFC1_5. For each tube, 152µl OptiMEM was mixed with 1.75µl of the appropriate siRNA. 21µl from tube 1 was added to tubes 2-4 to bring the final transfection mixture volume to 175µl. 25µl of the prepared transfection mixture was added to each appropriate well, which was gently tapped to distribute the transfection reagent evenly. The 96-well plate was incubated at room temperature for 20 minutes. Meanwhile, the cancer cells were trypsinised to count cells in a haemocytometer for 400 cells per 100µl for each appropriate well. Both cell lines were resuspended in RPMI medium. The 96-well plate was incubated at 37°C with 5% CO_2 for 5 days. Afterwards, 20µl MTS reagent was added to each well before reading the plate on a spectrophotometer to calculate absorbance at 490nm.

5.2 - Materials

Reagents and solutions:

Phosphate Buffered Saline (PBS) (Fisher Scientific)

Dimethyl Sulfoxide (DMSO) (Sigma-MERCK)

3-(4,5-dimethylthiazol-2-yl)-5-(3-carboxymethoxyphenyl)-2-(4-sulfophenyl)-2H-tetrazolium (MTS) (Promega)

Mowiol 40-88 (Fisher Scientific)

4’,6-diamidino-2-phenylindole (DAPI) (Sigma-MERCK)

Goat serum (Fisher Scientific)

Methanol (-20°C) (Fisher Scientific)

Cell culture:

RPMI medium (Fisher Scientific)

10% Fetal Bovine Serum (FBS) (Fisher Scientific)

1% Pen/Strep (Fisher Scientific)

Trypsin (Fisher Scientific)

siRNA transfection:

AllStars negative control (Qiagen)

RNase-free water (Qiagen)

siKIFC1_5 (Qiagen)

siKIFC1_4 (Qiagen)

OptiMem (Invitrogen, Thermo Fisher Scientific)

RNAiMax (Invitrogen, Thermo Fisher Scientific)

Primary antibodies:

CyclinB1 (mouse) (Millipore: 05-373)_

KIFC1 (rabbit) (Abcam: ab172620)

Survivin (rabbit) (Cell Signalling Technology: 2803)

Cleaved caspase-3 (rabbit) (Cell Signalling Technology: 9661)

Secondary antibodies:

Goat anti-mouse 488nm (A32723, Invitrogen, Thermo Fisher Scientific)

Goat anti-rat IgG 647nm (A21247, Invitrogen, Thermo Fisher Scientific)

Goat anti-rabbit IgG 568nm (A32732, Invitrogen, Thermo Fisher Scientific)

Other:

Fiji

GraphPad PRISM

Secondary antibodies and excitation laser	
Secondary antibody/Dye	**Laser**
Goat anti-Rabbit Alexa-Fluor Plus 555nm	DPSS 561nm
Goat anti-Mouse Alexa-Fluor Plus 488nm	Argon 488nm
Goat anti-Rat Alexa-Fluor 647nm	HeNe 633nm
DAPI	Diode 405nm
Microscopy Settings	
Microscope	Zeiss LSM 880
Acquisition Mode	Laser scanning confocal microscopy
Lens	Plan-Apochromat 20x/0.8 M27
Averaging	4
Image size	2048x2048
Pinhole	1 AU

Cancer cell lines: All from NCI-60 Panel (Charles River Labs, USA)

Cancer type	**Cell line**	**CA status (%)**	**p53 status**
Ovarian	OVCAR4	~60–70%	Mutant
	OVCAR8	~20–30%	Mutant
Colorectal	COLO205	~50–60%	Wild-type
	HT29	~20–25%	Mutant
Glioblastoma	U251	~60–70%	Mutant
	SNB-19	~20–30%	Mutant

6.0 – Results

6.1 – Bioinformatic analysis

Bioinformatic data from cancer patients were used to examine genetic and expression changes in the KIFC1 and BIRC5 genes, assessing their suitability as potential targets for cancer therapeutics. The cBioportal website was used to gather genomic data from cancer patients and to highlight genomic alterations in genes that enable cancer cell proliferation, centrosome clustering and survival. Genomic alterations in these genes include mutations, structural variants, amplifications, deep deletions, multiple alterations, and changes in mRNA expression.

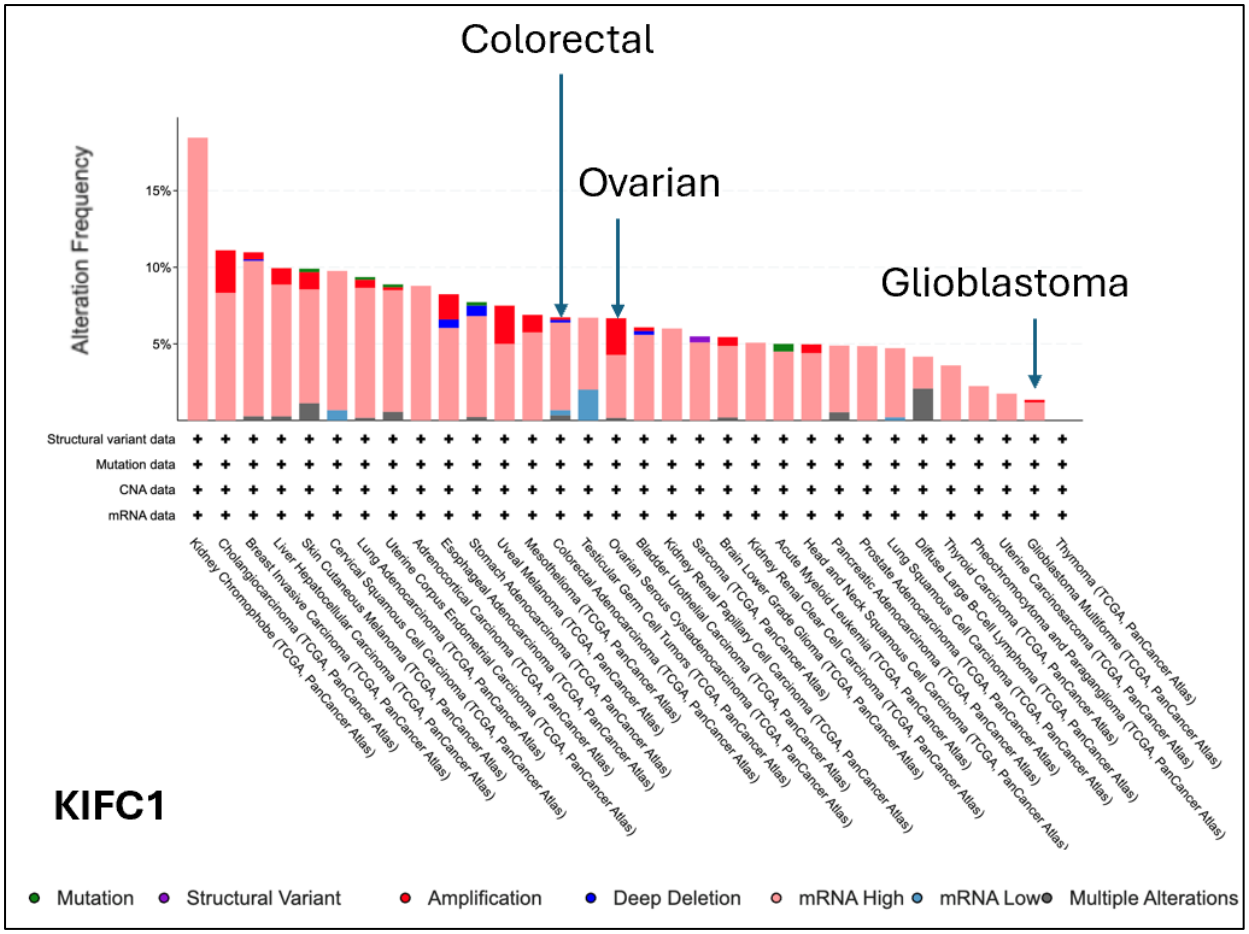

Figure 16: The KIFC1 gene is highly expressed in many cancers.

The cBioportal website was used to collect genomic data from cancer patients. TCGA PanCancer Atlas studies were used to query the KIFC1 gene, which is altered in 738 out of 10,967 patients. The KIFC1 gene was searched in the query box. Genomic profiles were selected: mutations, structural variants, putative copy-number alterations from GISTIC, and mRNA expression z-scores relative to diploid samples (RNA Seq V2 RSEM). The query was submitted to reveal a bar graph representing an overview of all cancer types with the KIFC1 gene found in the 'cancer type summary' tab (Cbioportal.org, 2021).

Figure 16 illustrates the alteration frequency (%) of the KIFC1 gene in various types of cancer. In Ovarian cancer, KIFC1 exhibited 2.4% amplification, 4.11% high mRNA expression, and 0.17% multiple alterations (i.e., gene altered in 6.68% of 584 cases). In Colorectal cancer, KIFC1 expressed 0.17% amplification, 0.17% deep deletion, 5.72% high mRNA expression, 0.34% low mRNA expression and 0.34% multiple alterations (gene altered in 6.73% of 594 cases). In Glioblastoma, KIFC1 expressed 0.17% amplification and 1.18% high mRNA expression (gene altered in 1.35% of 592 cases).

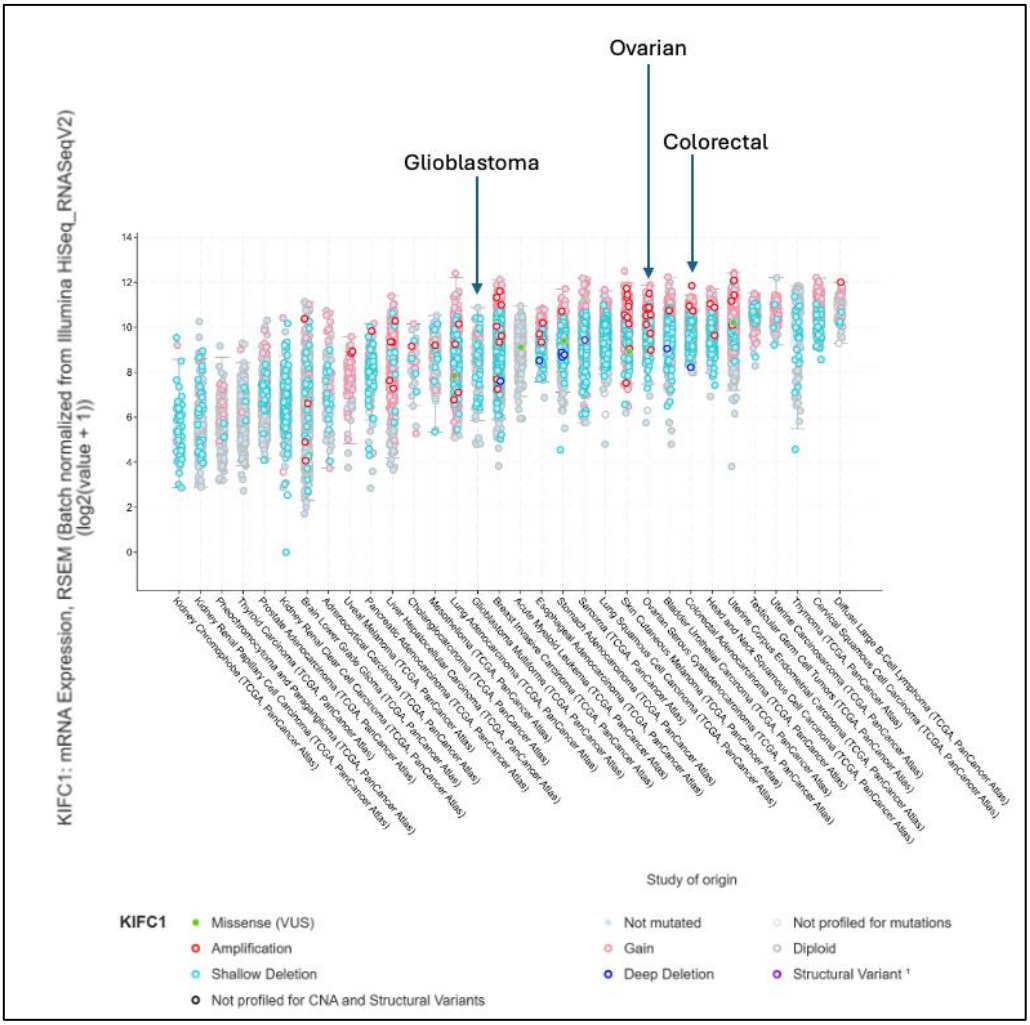

Figure 17: KIFC1 mRNA expression is highly expressed across all cancer types.

The cBioportal website was used to collect genomic data from cancer patients. TCGA PanCancer Atlas studies were used to query the KIFC1 gene, which is altered in 738 out of 10,967 patients. The KIFC1 gene was searched in the query box. Genomic profiles were selected: mutations, structural variants, putative copy-number alterations from GISTIC, and mRNA expression z-scores relative to diploid samples (RNA Seq V2 RSEM). The query was submitted to reveal a plot representing an overview of mRNA expression across cancer types. A log scale was used, and all categories were sorted by median. 'Mutation type', 'structural variants' and 'copy number' were also selected (Cbioportal.org, 2021).

Figure 17 shows KIFC1 mRNA expression across several cancer types. It is highly expressed in Ovarian, Colorectal and Glioblastoma cancers.

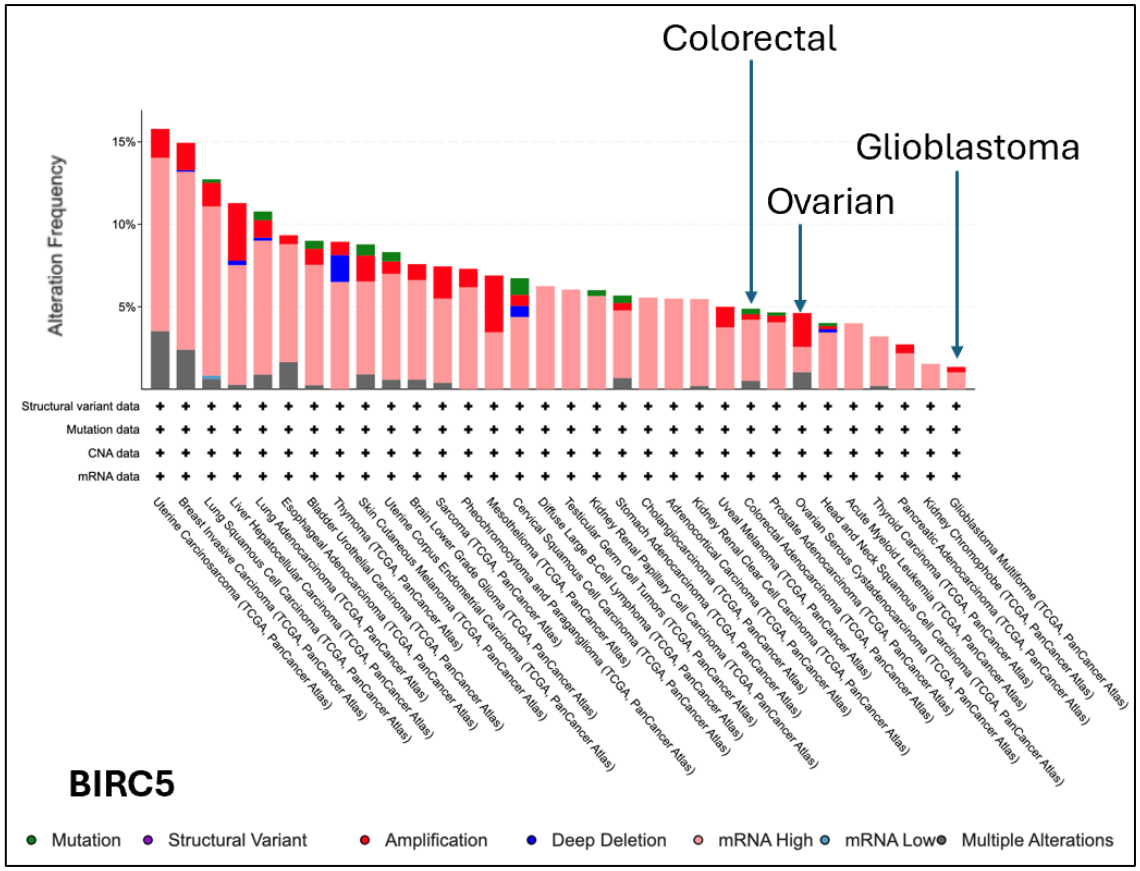

Figure 18: The BIRC5 gene is highly expressed in many cancers.

The cBioportal website was used to collect genomic data from cancer patients. TCGA PanCancer Atlas studies were used to query genes altered in 812 out of 10,967 patients. The BIRC5 gene was searched in the query box. Genomic profiles were selected: mutations, structural variants, putative copy-number alterations from GISTIC, and mRNA expression z-scores relative to diploid samples (RNA Seq V2 RSEM). The query was submitted to reveal a bar graph representing an overview of all cancer types with the BIRC5 gene, found in the 'Cancer Type Summary' tab (Cbioportal.org, 2021).

Figure 18 illustrates the alteration frequency (%) of the BIRC5 gene in various types of cancer. In Ovarian cancer, the BIRC5 gene expressed 2.05% amplification, 1.54% high mRNA expression and 1.03% multiple alterations (gene altered in 4.62% of 584 cases). In Colorectal cancer, the BIRC5 gene expressed 0.34% mutation, 0.34% amplification, 3.7% high mRNA expression and 0.51% multiple alterations (gene altered in 4.88% of 594 cases). In Glioblastoma, the BIRC5 gene expressed 0.34% amplification and 1.01% high mRNA expression (gene altered in 1.35% of 592 cases). Figure 19 shows

KIFC1 mRNA expression across several cancer types. Colorectal cancer has ~6-10 mRNA expression, Ovarian cancer has ~6-10 mRNA expression, and Glioblastoma has ~5-10 mRNA expression.

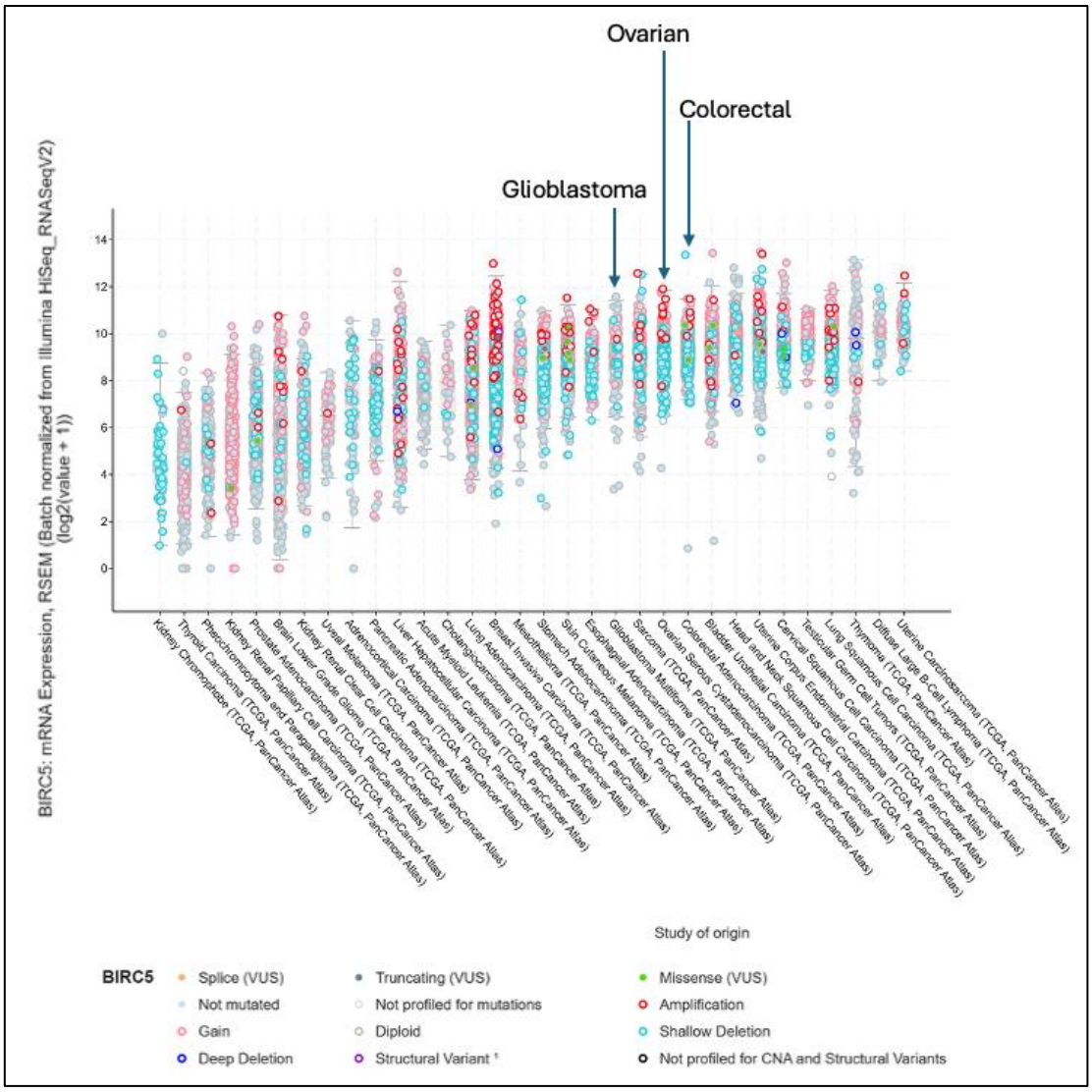

Figure 19: BIRC5 mRNA expression is highly expressed across all cancer types.

The cBioportal website was used to collect genomic data from cancer patients. TCGA PanCancer Atlas studies were used to query the KIFC1 gene, which is altered in 738 out of 10,967 patients. The KIFC1 gene was searched in the query box. Genomic profiles were selected: mutations, structural variants, putative copy-number alterations from GISTIC, and mRNA expression z-scores relative to diploid samples (RNA Seq V2 RSEM). The query was submitted to reveal a plot representing an overview of mRNA expression across cancer types. A log scale was used, and all categories were sorted by median. 'Mutation type', 'structural variants' and 'copy number' were also selected. (Cbioportal.org, 2021).

Figure 19 shows BIRC5 mRNA expression across several cancer types. It is highly expressed in Ovarian, Colorectal and Glioblastoma cancers.

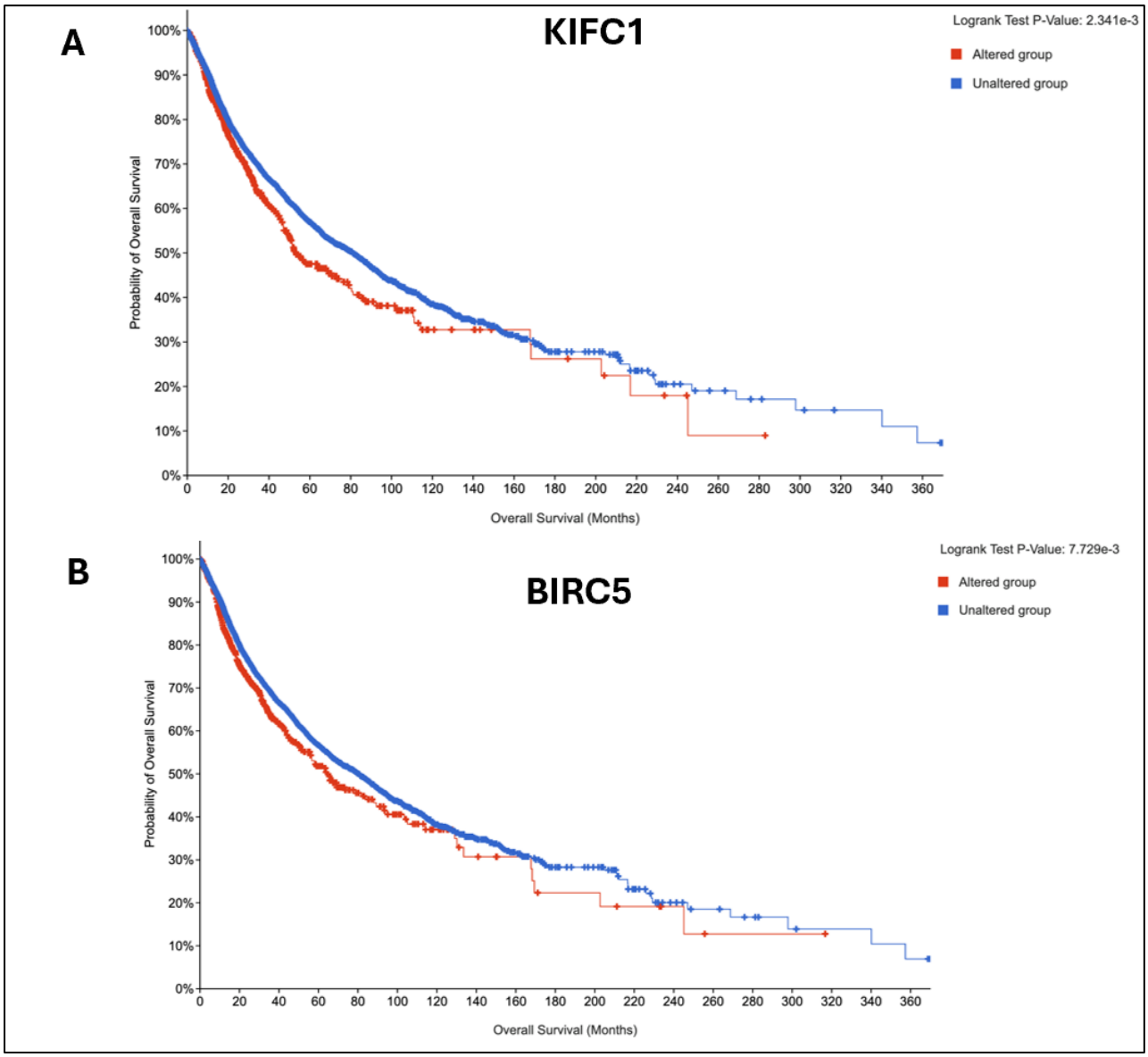

Figure 20: Patient prognosis rates are lower with altered KIFC1 and BIRC5 genes.

The cBioportal website was used to collect genomic data from cancer patients. TCGA PanCancer studies were used to query genes altered in 738 (KIFC1) or 812 (BIRC5) out of 10967 patients. The KIFC1 and BIRC5 genes were searched in the query box. Genomic profiles were selected: mutations, structural variants, putative copy-number alterations from GISTIC, and mRNA expression z-scores relative to diploid samples (RNA Seq V2 RSEM). The 'Comparison/survival' tab was selected to reveal a Kaplan-Meier plot for patient prognosis rates for the KIFC1 or BIRC5 gene, up to 370 months. A log-rank test p-value was generated to determine the statistical significance of patient survival between the two groups. KIFC1 p-value = 2.341e-3, BIRC5 p-value = 7.729e-3.

Figure 20 reveals the prognosis rates of cancer patients expressing altered or unaltered KIFC1 and BIRC5 genes. Log-rank tests were performed for both genes, with KIFC1 yielding a p-value of 2.341 × 10^ (-3) and BIRC5 yielding a p-value of 7.729 × 10^ (-3). Prognosis rates in the altered groups were significantly lower in both genes compared to their unaltered groups. After 120 months, the patient sample size in the altered groups decreased much quickly in both genes.

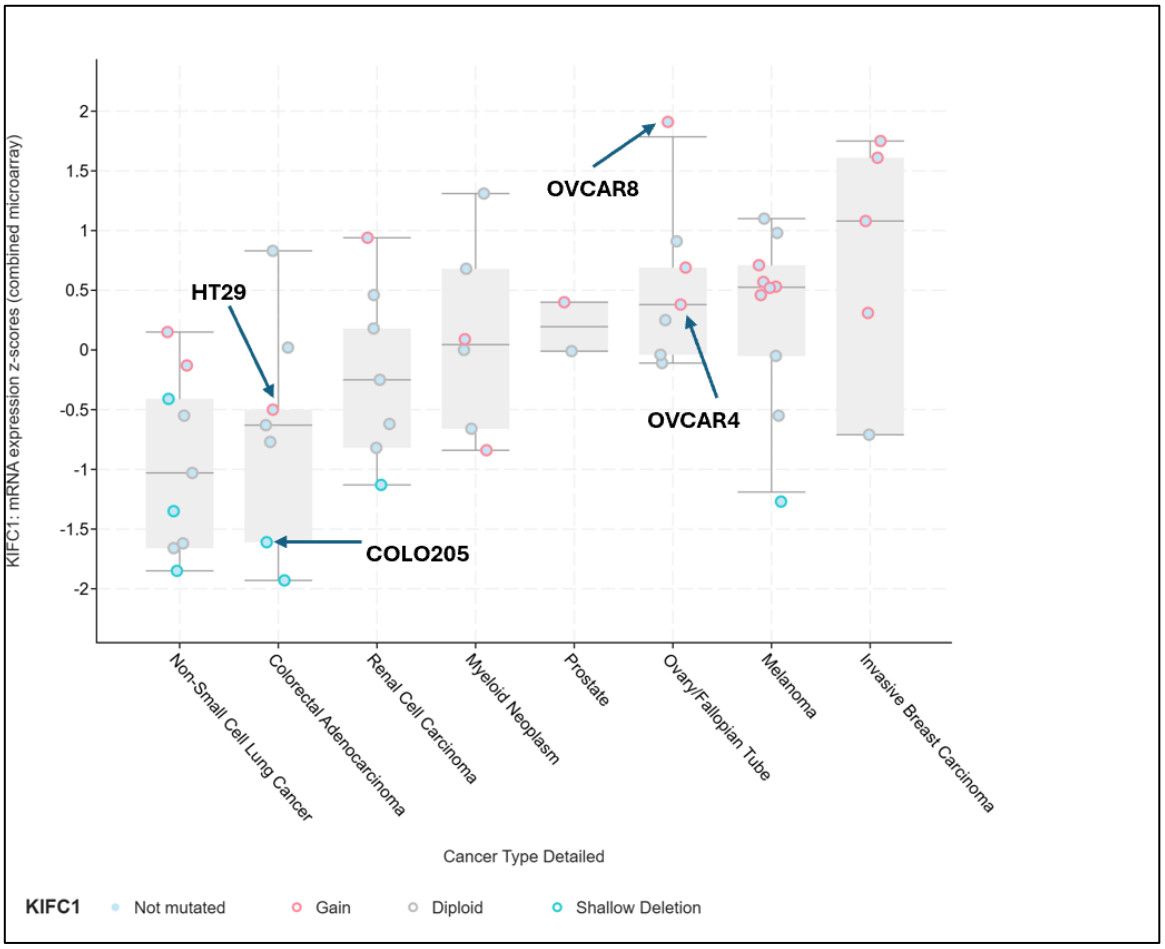

Figure 21: KIFC1 mRNA expression across the NCI-60 cancer cell line panel.

The cBioportal website was used to collect genomic data from cancer patients. The KIFC1 gene was searched in the query box to collect data from the NCI-60 cancer cell panel. Genomic profiles were selected: mutations, structural variants, putative copy-number alterations from GISTIC, and mRNA expression z-scores relative to diploid samples (RNA Seq V2 RSEM). The query was submitted to reveal a plot representing an overview of mRNA expression across cancer types. All categories were sorted by median. 'Mutation type', 'structural variants' and 'copy number' were also selected. Graph plot showing 53 complete patient samples out of 67 in total (Cbioportal.org, 2021).

Figure 21 shows mRNA expression z-scores from the NCI-60 cancer cell panel. OVCAR8 and OVCAR4 cells exhibit higher KIFC1 and BIRC5 mRNA expression compared to COLO205 and HT29 cancer cell lines, with OVCAR8 showing the highest expression and COLO205 the lowest.

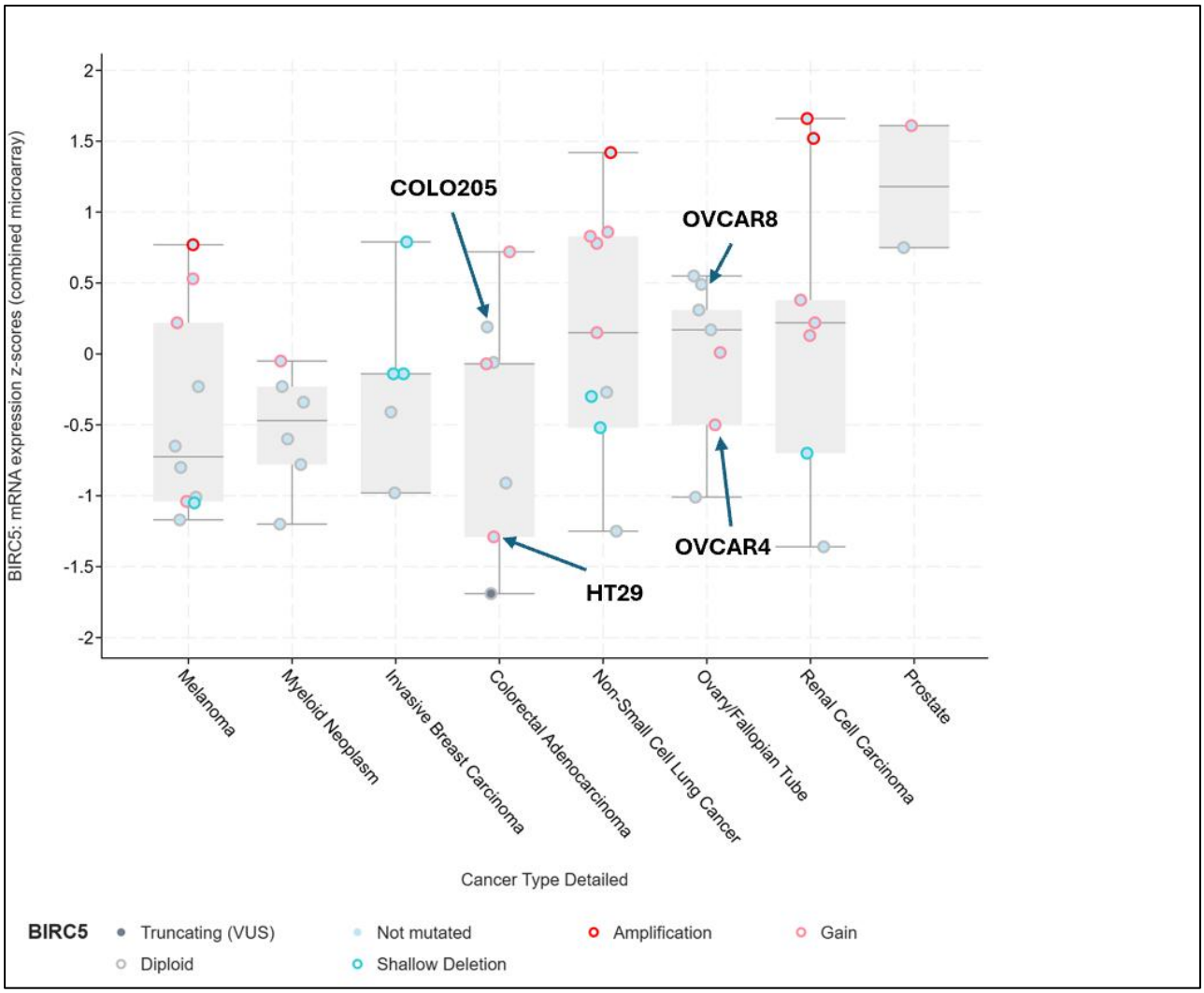

Figure 22: BIRC5 mRNA expression across the NCI-60 cancer cell line panel.

The cBioportal website was used to collect genomic data from cancer patients. The KIFC1 gene was searched in the query box to collect data from the NCI-60 cancer cell panel. Genomic profiles were selected: mutations, structural variants, putative copy-number alterations from GISTIC, and mRNA expression z-scores relative to diploid samples (RNA Seq V2 RSEM). The query was submitted to reveal a plot representing an overview of mRNA expression across cancer types. All categories were sorted by median. 'Mutation type', 'structural variants' and 'copy number' were also selected. Scatter plot showing 53 complete patient samples out of 67 in total (Cbioportal.org, 2021).

Figure 22 shows mRNA expression z-scores from the NCI-60 cancer cell panel. OVCAR8 and OVCAR4 cells exhibit higher KIFC1 and BIRC5 mRNA expression compared to COLO205 and HT29 cancer cell lines, with OVCAR8 showing the highest expression and COLO205 the lowest.

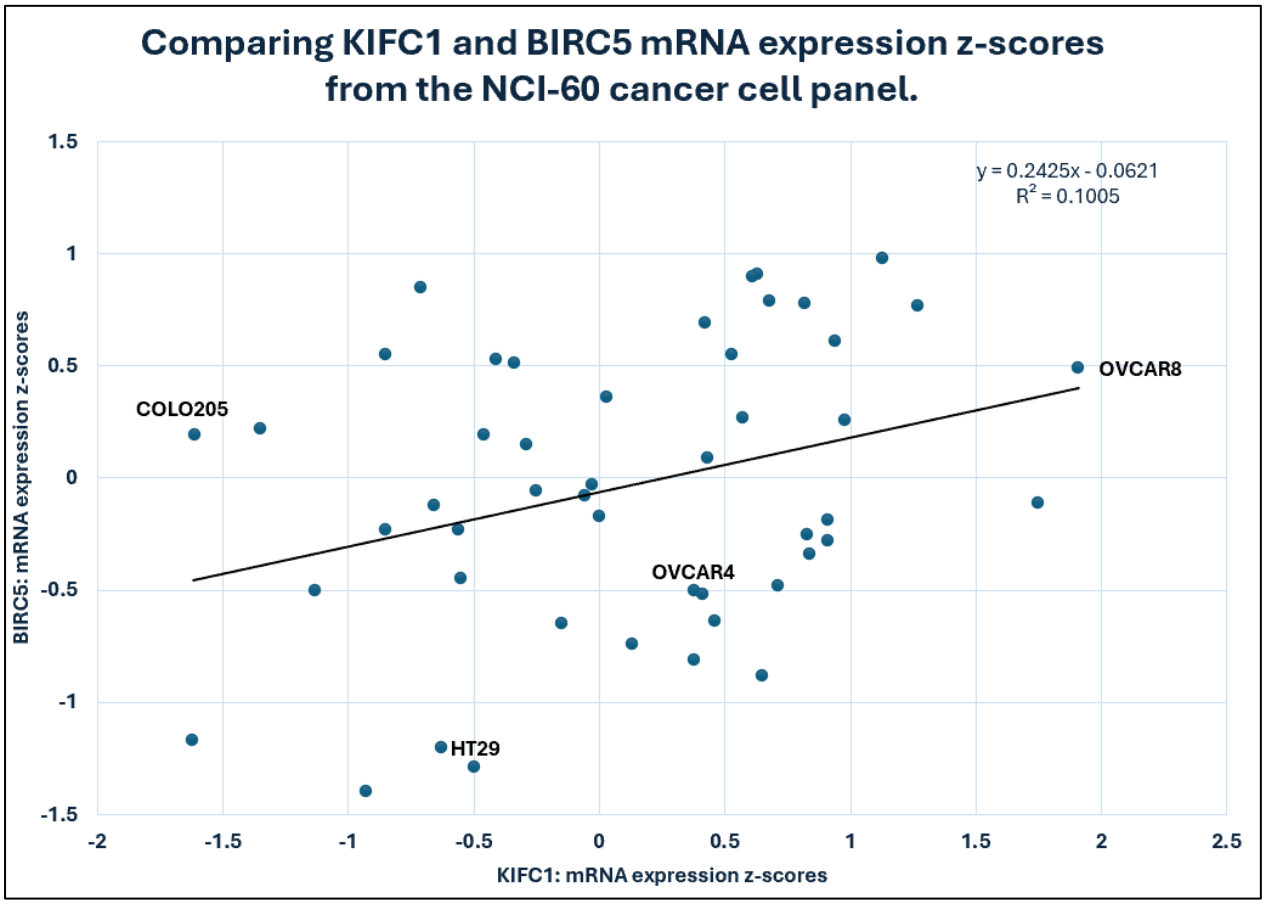

Figure 23: KIFC1 and BIRC5 mRNA expression correlation indicates weak linkage in cancer.

The cBioportal website was used to collect genomic data from cancer patients. The KIFC1 gene was searched in the query box to collect data from the NCI-60 cancer cell panel. Genomic profiles were selected: mutations, structural variants, putative copy-number alterations from GISTIC, and mRNA expression z-scores relative to diploid samples (RNA Seq V2 RSEM). The query was submitted to reveal a plot representing an overview of mRNA expression across cancer types. All categories were sorted by median. 'Mutation type', 'structural variants' and 'copy number' were also selected. Scatter plot showing 53 complete patient samples out of 67 in total (Cbioportal.org, 2021).

Figure 23 shows a scatter plot containing KIFC1 and BIRC5 mRNA levels. Increasing KIFC1 mRNA expression has a weak correlation with BIRC5 mRNA expression. Glioblastoma cell lines were not apparent in the data set.

6.2: Comparing the expression profile of KIFC1 and Survivin in Ovarian cancer cell lines with high and low centrosome amplification.

The first set of experiments was performed using two Ovarian cancer cell lines, which were OVCAR8 and OVCAR4. OVCAR8 is known to express low levels of CA (Mitra et al., 2015), whereas OVCAR4 expresses high levels of CA (Mitra et al., 2015). Initially, immunofluorescence staining and subsequent quantification were used to compare the expression of both KIFC1 and Survivin under control conditions between the two cell lines.

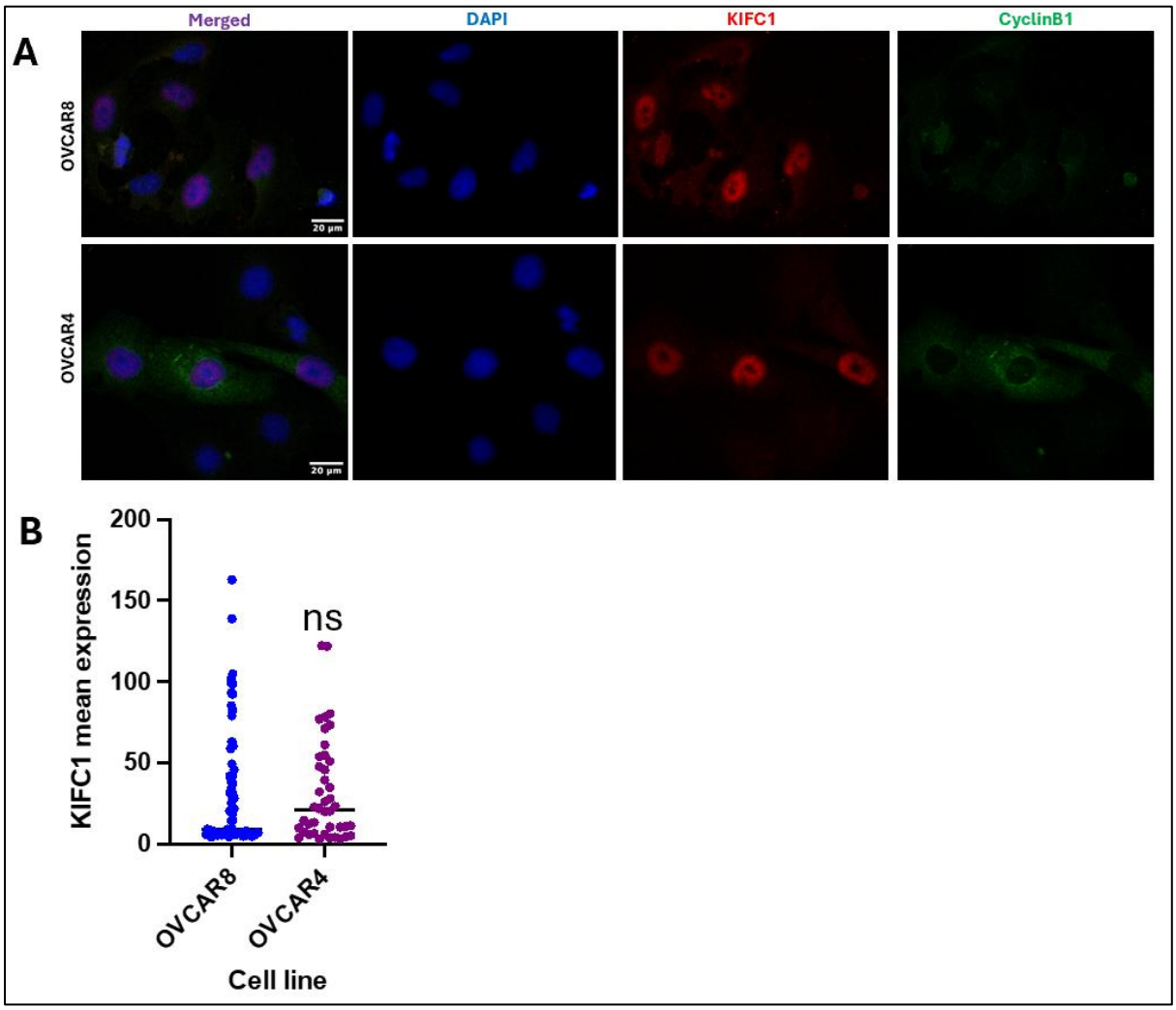

Figure 24: KIFC1 expression is similar between OVCAR8 and OVCAR4 cells.

OVCAR8 and OVCAR4 cells were treated with DMSO. They were incubated for 1 day before fixation with methanol. Cells were stained with primary antibodies: mouse anti-Cyclin B1, and rabbit anti-KIFC1, followed by secondary antibodies: Goat anti-mouse 488nm, and Goat anti-rabbit 568nm. Cells were mounted with Mowiol and DAPI on a microscope slide before being stored overnight at room temperature. Cells were imaged using a Zeiss LSM880 confocal microscope. **(A)** Zoomed-in fields of view of OVCAR8 and OVCAR4 cells were captured for KIFC1, DAPI and Cyclin B1. Scale bar of 20µm. **(B)** KIFC1 intensity was measured in FIJI in individual cells in 6 fields of view per cell line. Total n-number of cells = OVCAR8 = 70, OVCAR4 = 42. An unpaired T-test comparing KIFC1 expression between the two cell lines showed no significant difference, p-value = 0.4034.

Figure 24 shows OVCAR8 and OVCAR4 cells stained for DAPI, KIFC1 and Cyclin B1. KIFC1 expression is highly localised to cell nuclei in both cell lines. KIFC1 nuclear quantification was achieved using FIJI software by isolating the nuclei using the DAPI channel to create nuclear masks. KIFC1 intensity in each nucleus was automatically quantified. The mean value was then calculated across all cells for each cell line. Cyclin-B1 staining helped visualise KIFC1 localisation in cells, as KIFC1 migrates to the cell nucleus during S phase. Many cells expressing low/no KIFC1 are indicative of the G1 or early S-phase, while cells expressing moderate to high KIFC1 are indicative of the G2 phase or early mitosis. The mean expression of KIFC1 was similar between the two cell lines, showing no statistically significant difference.

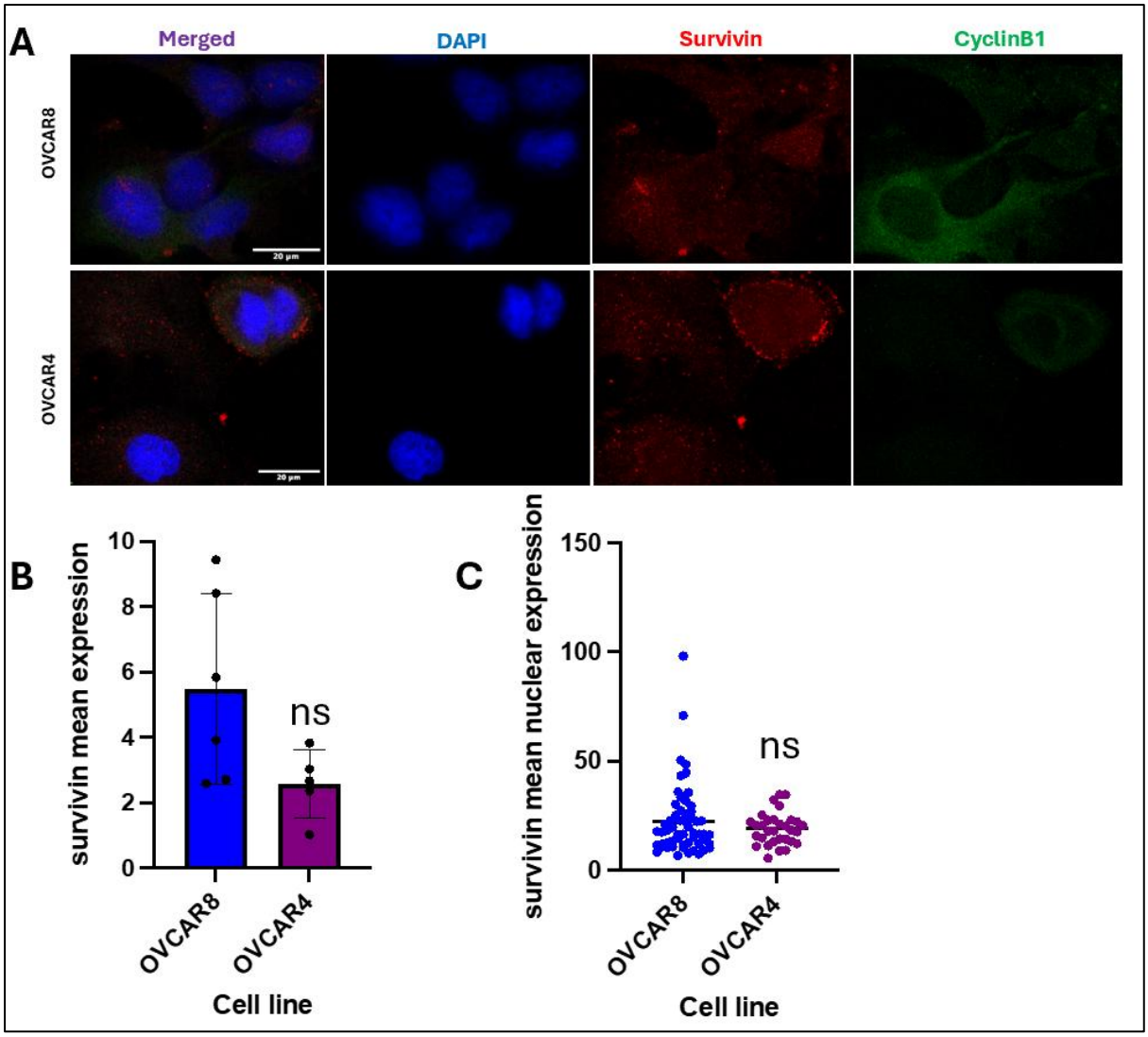

Figure 25: Survivin expression is similar between OVCAR8 and OVCAR4 cells.

OVCAR8 and OVCAR4 cells were treated with DMSO. They were incubated for 1 day before fixation with methanol. Cells were stained with primary antibodies: mouse anti-CyclinB1, and rabbit anti-Survivin, followed by secondary antibodies: Goat anti-mouse 488nm, and Goat anti-rabbit 568nm. Cells were mounted with Mowiol and DAPI on a microscope slide before being stored overnight at room temperature. The cells were then imaged using a confocal microscope. **(A)** Zoomed-in fields of view of OVCAR8 and OVCAR4 cells were captured for Survivin, DAPI and CyclinB1 with a scale bar of 20µm. **(B+C)** Survivin intensity was measured in FIJI in individual cells in 6 fields of view per cell line. Total n-number of cells = OVCAR8 = 52, OVCAR4 = 31. An unpaired T-test comparing Survivin expression between the two cell lines showed no significant difference **(B)** p-value = 0.0656, **(C)** p-value = 0.24.

Figure 25 shows OVCAR8 and OVCAR4 cells stained for DAPI, Survivin and Cyclin B1. Survivin nuclear quantification was achieved using FIJI software by isolating the DAPI channel. Each nucleus was automatically identified, along with its Survivin value, and the mean value was calculated across all cells from each cell line. Survivin mean expression was similar between each cell line and showed no significant difference. This was also apparent in the nuclear expression of Survivin. Cyclin-B1 staining was helpful in visualising Survivin localisation in cells, as Survivin migrates to the cell nucleus during the G2 phase or mitosis. Cells with no/low Survivin expression are indicative of G1 or early S-phase and are localised in the cytoplasm. Cells with moderate/high Survivin expression are indicative of G2 phase or mitosis and are localised to nuclei.

6.3: Using KIFC1 siRNAs to determine the effect of KIFC1 depletion on Survivin protein levels in Ovarian Cancer

Next, the effects of KIFC1 depletion on Survivin expression were examined in OVCAR8 and OVCAR4 cells. KIFC1 siRNAs were used to degrade KIFC1 mRNA in cells, leading to a depletion of KIFC1 protein expression.

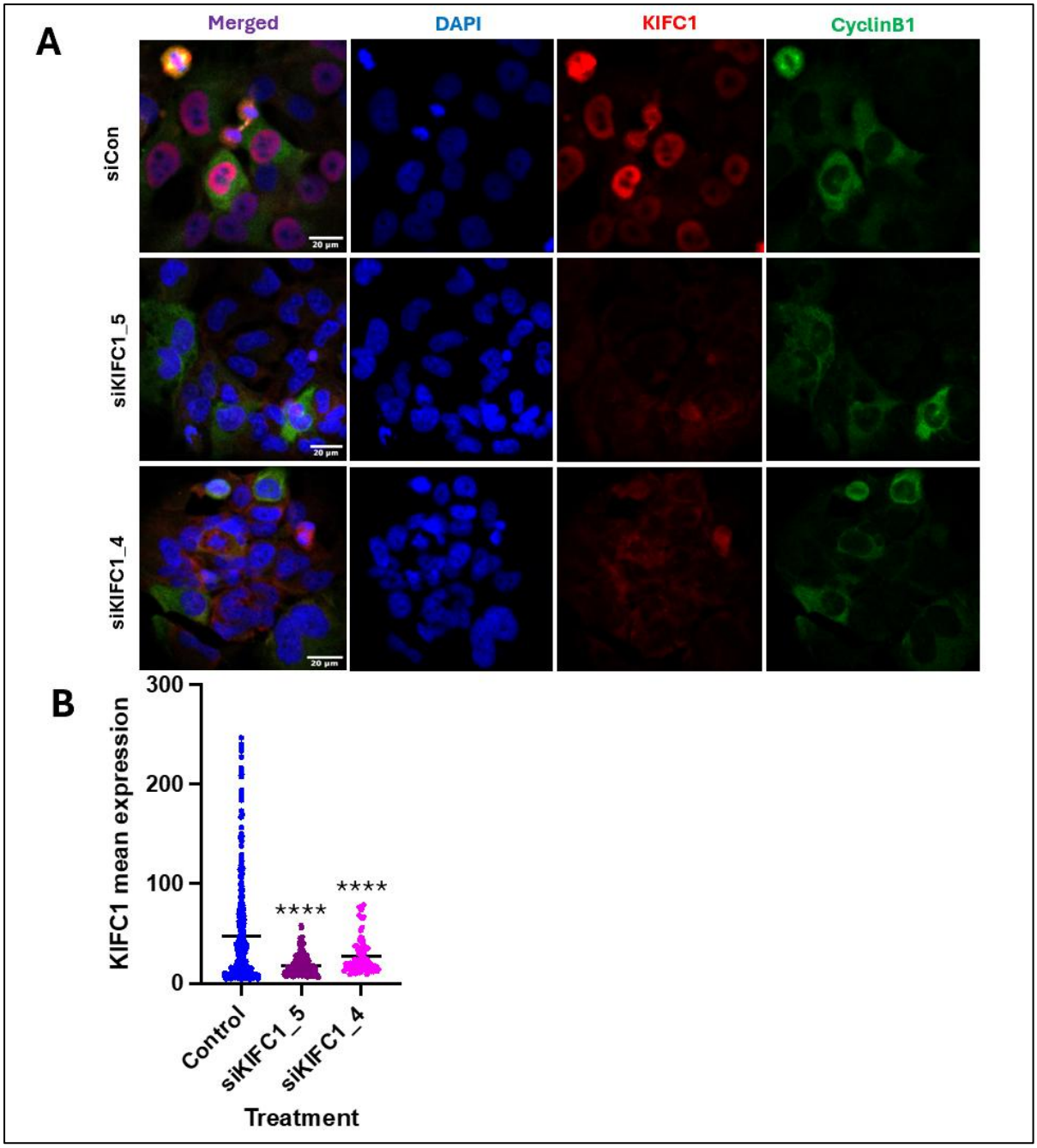

Figure 26: KIFC1 expression in OVCAR8 cells successfully knocked down using siRNAs.

OVCAR8 cells were transfected with siControl, siKIFC1_5 and siKIFC1_4 siRNAs. They were incubated for 2 days before fixation with methanol. Cells were stained with primary antibodies: mouse anti-CyclinB1, rabbit anti-KIFC1, followed by secondary antibodies: Goat anti-mouse 488nm, and Goat anti-rabbit 568nm. Cells were mounted with Mowiol and DAPI on a microscope slide before being stored overnight at room temperature. The cells were then imaged using a confocal microscope. **(A)** Zoomed-in fields of view of OVCAR8 cells were captured and stained for KIFC1, DAPI and CyclinB1 with a scale bar of 20µm. **(B)** KIFC1 intensity was measured in FIJI in individual cells across three fields of view per condition. Total n-number of cells = siCon = 362, siKIFC1_5 = 187, siKIFC1_4 = 91. A One-Way ANOVA statistical test with Dunnett's multiple comparison test was performed, **** p-value = <0.0001 for both siRNAs compared to the control.

Figure 26 shows OVCAR8 cells stained for DAPI, KIFC1 and Cyclin B1. Cells were treated with siControl and KIFC1 siRNAs. There was statistical significance in reducing KIFC1 mean expression with siKIFC1_5 and siKIFC1_4 (p-value = <0.0001). KIFC1 is highly localised to the cell nuclei.

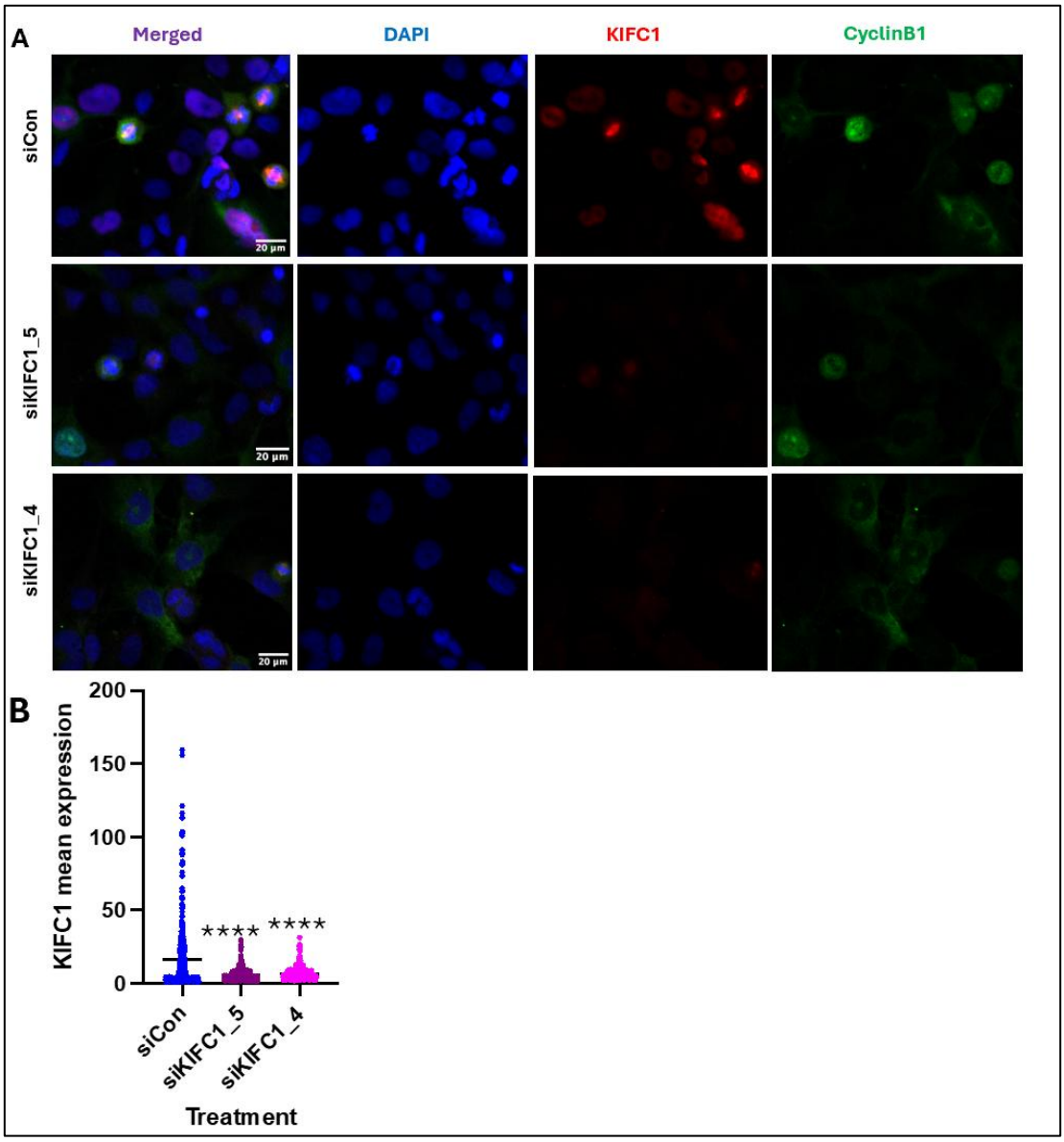

Figure 27: KIFC1 expression in OVCAR4 cells successfully knocked down using siRNAs.

OVCAR4 cells were transfected with siControl, siKIFC1_5 and siKIFC1_4 siRNAs. They were incubated for 2 days before fixation with methanol. Cells were stained with primary antibodies: mouse anti-CyclinB1, rabbit anti-KIFC1, followed by secondary antibodies: Goat anti-mouse 488nm, and Goat anti-rabbit 568nm. Cells were mounted with Mowiol and DAPI on a microscope slide before being stored overnight at room temperature. The cells were then imaged using a confocal microscope. **(A)** Zoomed-in fields of view of OVCAR8 cells were captured and stained for KIFC1, DAPI and CyclinB1 with a scale bar of 20µm. **(B)** KIFC1 intensity was measured in FIJI in individual cells across three fields of view per condition. Total n-number of cells = siCon = 393, siKIFC1_5 = 415, siKIFC1_4 = 371. A One-Way ANOVA statistical test with Dunnett's multiple comparison test was performed, **** p-value = <0.0001 for both siRNAs compared to the control.

Figure 27 shows OVCAR4 cells stained for DAPI, KIFC1 and Cyclin B1. Cells were treated with siControl and KIFC1 siRNAs. There was statistical significance in reducing KIFC1 mean expression with siKIFC1_5 and siKIFC1_4 (p-value = <0.0001). KIFC1 is highly localised to the cell nuclei.

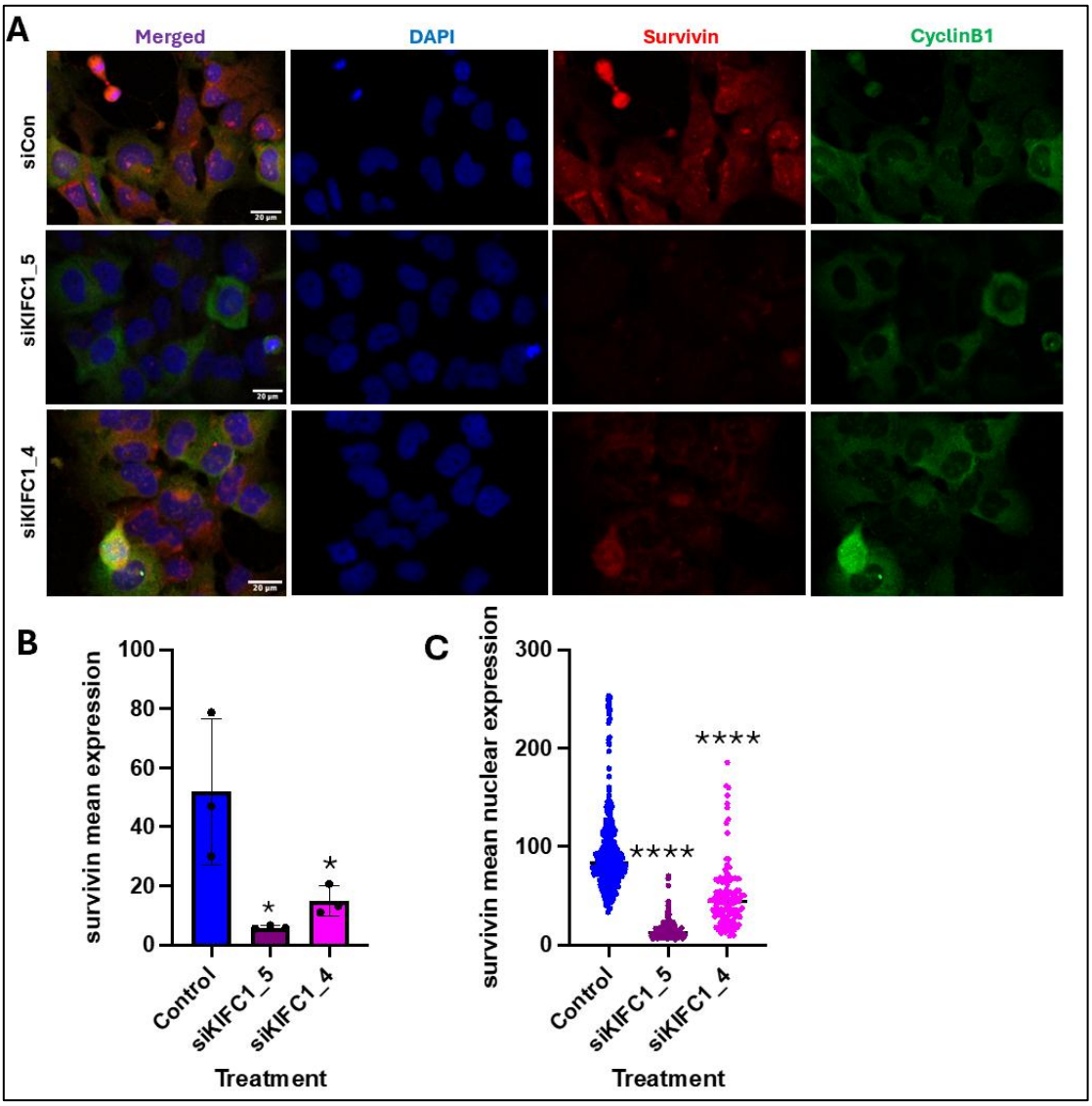

Figure 28: Survivin expression in OVCAR8 cells successfully knocked down using siRNAs.

OVCAR8 cells were transfected with siControl, siKIFC1_5 and siKIFC1_4 siRNAs. They were incubated for 2 days before fixation with methanol. Cells were stained with primary antibodies: mouse anti-CyclinB1, and rabbit anti-Survivin, followed by secondary antibodies: Goat anti-mouse 488nm, and Goat anti-rabbit 568nm. Cells were mounted with Mowiol and DAPI on a microscope slide before being stored overnight at room temperature. The cells were then imaged using a confocal microscope. **(A)** Zoomed-in fields of view of OVCAR8 cells were captured and stained for Survivin, DAPI and CyclinB1 with a scale bar of 20µm. **(B+C)** Survivin intensity was measured in FIJI in individual cells in 3 fields of view per condition. Total n-number of cells = siCon=400, siKIFC1_5 = 209, siKIFC1_4 = 126. A one-way ANOVA statistical test with Dunnett's multiple comparison test was performed **(B)** * p-value = 0.0149 (siKIFC1_5) and * p-value = 0.0370 compared to the control. **(C)** **** p-value = <0.0001 for both siRNAs.

Figure 28 shows OVCAR8 cells stained for DAPI, Survivin and Cyclin B1. Cells were treated with siControl and KIFC1 siRNAs. It revealed statistical significance in reducing Survivin mean expression with siKIFC1_5 and siKIFC1_4 (p-value = <0.0001). High levels of Survivin are localised to the cell cytoplasm and nuclei, particularly at the midbodies of cells during cytokinesis.

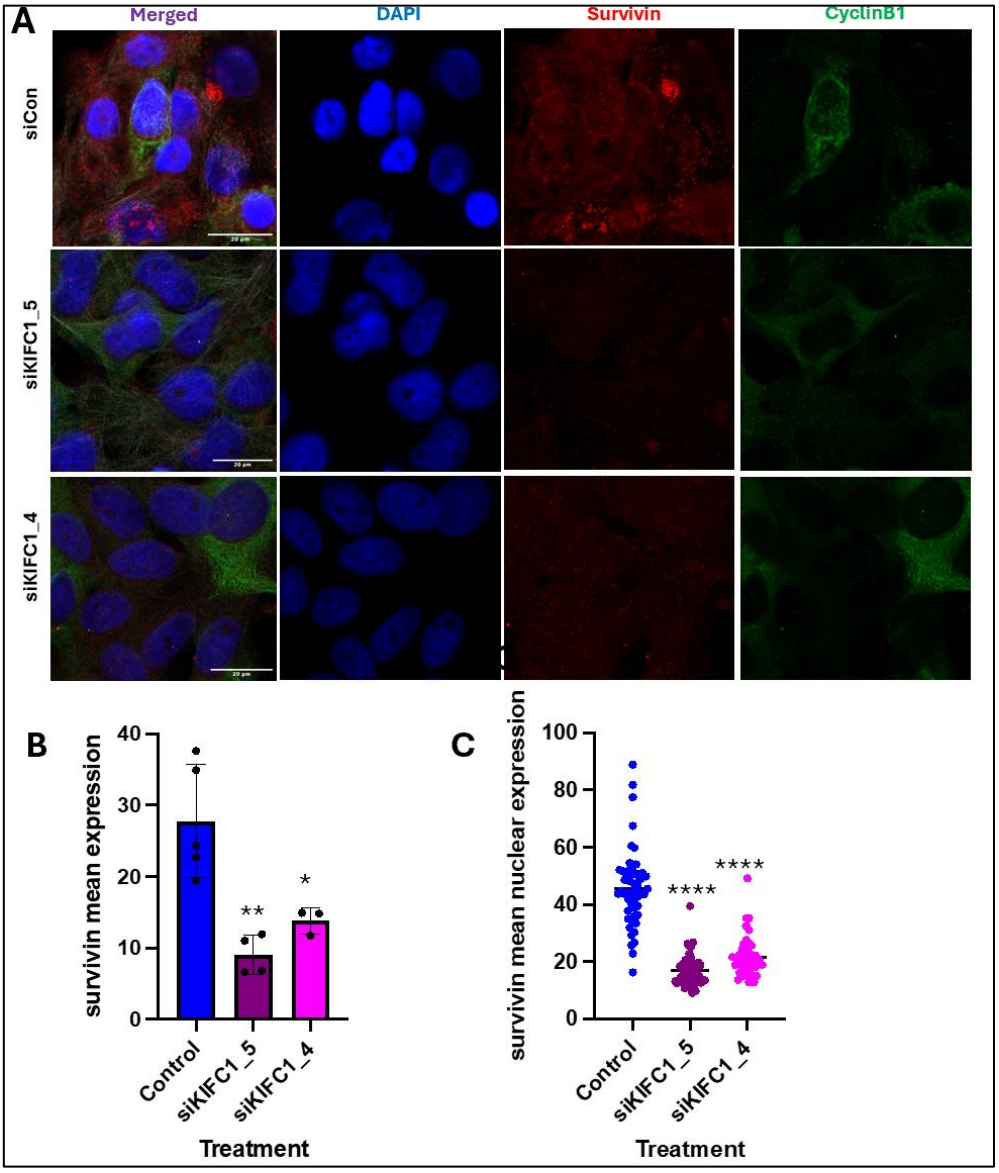

Figure 29: Survivin expression in OVCAR4 cells successfully knocked down using siRNAs.

OVCAR4 cells were transfected with siControl, siKIFC1_5 and siKIFC1_4 siRNAs. They were incubated for 2 days before fixation with methanol. Cells were stained with primary antibodies: mouse anti-CyclinB1, and rabbit anti-Survivin, followed by secondary antibodies: Goat anti-mouse 488nm, and Goat anti-rabbit 568nm. Cells were mounted with Mowiol and DAPI on a microscope slide before being stored overnight at room temperature. The cells were then imaged using a confocal microscope. **(A)** Zoomed-in fields of view of OVCAR4 cells were captured and stained for Survivin, DAPI and CyclinB1 with a scale bar of 20µm. **(B+C)** Survivin intensity was measured in FIJI in individual cells in 3 fields of view per condition. Total n-number of cells = siCon = 55, siKIFC1_5 = 51, siKIFC1_4 = 43. A one-way ANOVA statistical test with Dunnett's multiple comparison test was performed. **(B)** ** p-value = 0.0015 and * p-value = 0.0145 compared to the control. **(C)** **** p-value = <0.0001 for both siRNAs.

Figure 29 shows OVCAR4 cells stained for DAPI, Survivin and Cyclin B1. Cells were treated with siControl and KIFC1 siRNAs. It revealed statistical significance in reducing Survivin mean expression with siKIFC1_5 and siKIFC1_4 (p-value = <0.0001). High levels of Survivin are localised to the cell cytoplasm and nuclei.

6.4 – Assessing cell viability in Ovarian Cancer

The following experiment utilised an MTS assay, which aims to determine cell viability in OVCAR8 and OVCAR4 cells. While IF staining helps measure KIFC1 and Survivin protein expression and localisation, cell survival MTS assays help determine whether the effects of KIFC1 knockdown align more closely with clustering dependency, Survivin, or a combination of both. MTS is a colourimetric assay used to assess cell viability and proliferation by measuring the metabolic activity of live cells. Cell viability is quantified by measuring the absorbance of the cell wells at 490 nm.

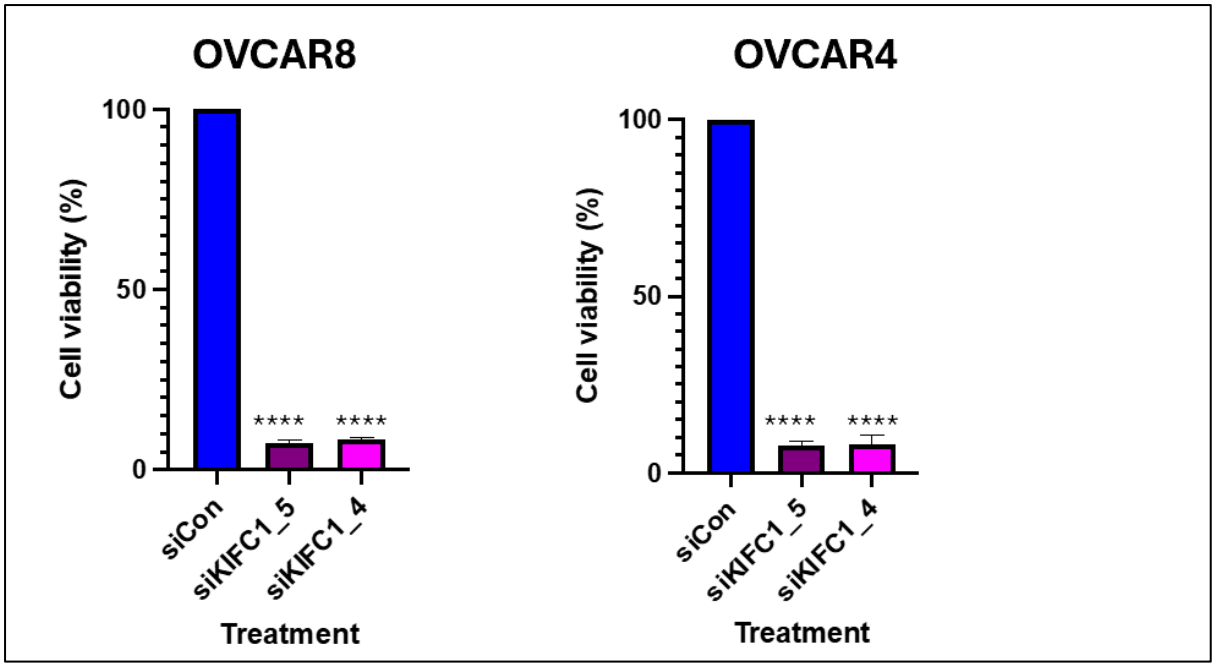

Figure 30: Cell viability in OVCAR8 and OVCAR4 successfully reduced by KIFC1 knockdown

OVCAR8 and OVCAR4 cells were reverse-transfected with siControl, siKIFC1_5, and siKIFC1_4 siRNAs in a 96-well plate. They were incubated for 5 days before the MTS reagent was added to each well. The 96-well plate was incubated for 4 hours before being read inside a spectrophotometer at 490 nm. Bar graphs showing OVCAR8 or OVCAR4 cells reverse transfected with siControl, siKIFC1_5 and siKIFC1_4 siRNAs. Cell viability for both siRNAs was normalised to the controls in each cell line. 3 well replicates were used per treatment condition with ≈400 cells per well. Two bar graphs were generated, one for OVCAR8 on the left and one for OVCAR4 on the right. A One-Way ANOVA statistical test with Dunnett's multiple comparison test was performed, **** p-value = <0.0001 for both siRNAs compared to the control in both cell lines.

Figure 30 shows OVCAR8 and OVCAR4 cells treated with siControl and two KIFC1 siRNAs in a 96-well plate with approximately 400 cells per well. Adding MTS reagent to the cells revealed a significant decrease in cell viability using KIFC1 siRNAs in both cell lines compared to their respective controls (p-values < 0.0001).

6.5: Comparing the expression profile of KIFC1 and Survivin in Colorectal cancer cell lines with high and low centrosome amplification.

The next set of experiments was performed using two Colorectal cancer cell lines, COLO205 and HT29. COLO205 is known to express high CA (Leroy et al., 2014), whereas HT29 expresses low CA (Ravizza et al., 2004). The same experimental procedures were performed, which included methanol-fixed immunofluorescence and MTS assays.

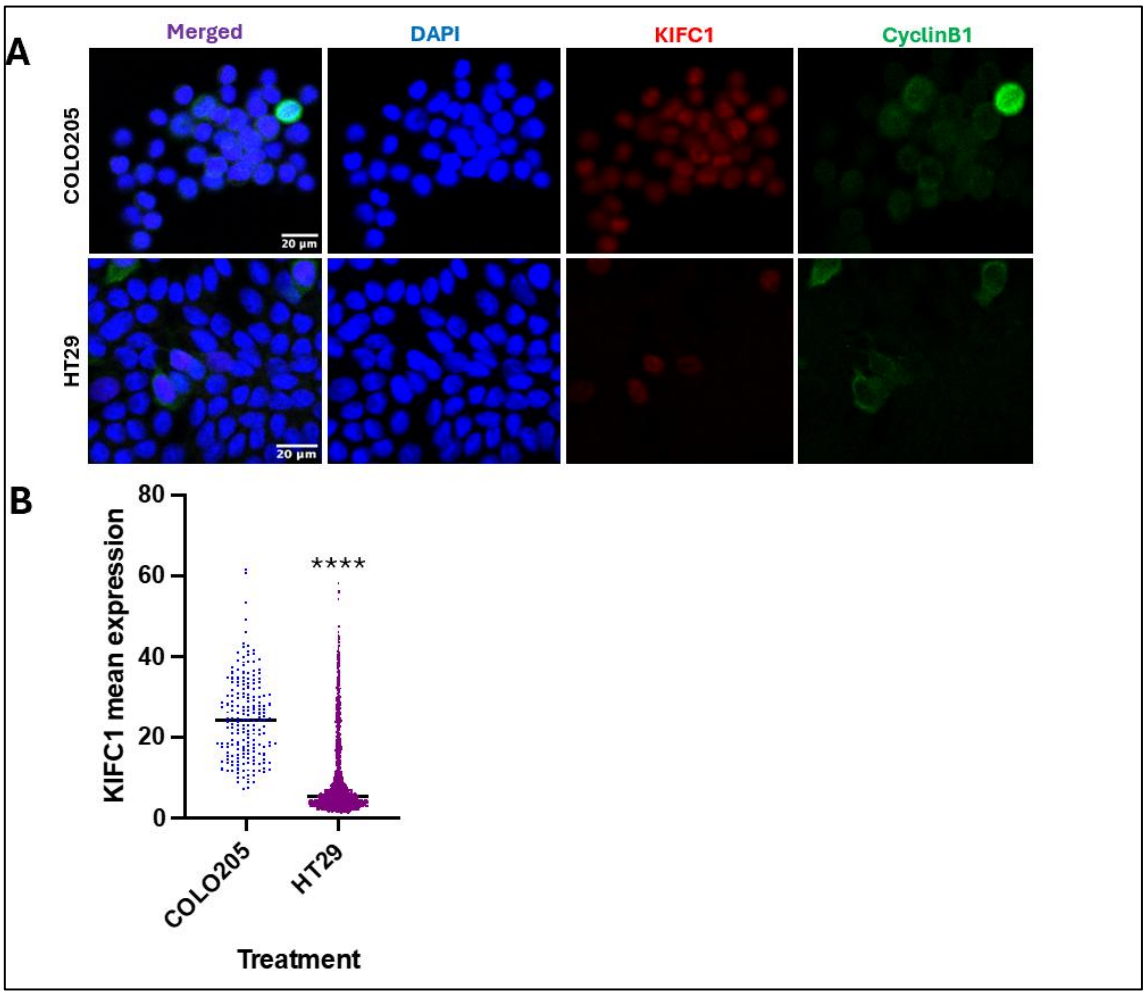

Figure 31: KIFC1 expression is higher in COLO205 cells.

COLO205 and HT29 cells were transfected with siControl siRNA. They were incubated for 2 days before fixation with methanol. Cells were stained with primary antibodies: mouse anti-CyclinB1, rabbit anti-KIFC1, followed by secondary antibodies: Goat anti-mouse 488nm, and Goat anti-rabbit 568nm. Cells were mounted with Mowiol and DAPI on a microscope slide before being stored overnight at room temperature. The cells were then imaged using a confocal microscope. **(A)** Zoomed-in fields of view of COLO205 and HT29 cells were captured and stained for KIFC1, DAPI and CyclinB1 with a scale bar of 20µm. **(B)** KIFC1 intensity in CyclinB1+ and CyclinB1- cells was measured in FIJI in individual cells in 3 fields of view per condition. Total n-number of cells, COLO205 = 197, HT29 = 1300. An unpaired T-test test was performed, **** p-value = <0.0001.

Figure 31 shows COLO205 and HT29 cells stained for DAPI, KIFC1 and Cyclin B1. KIFC1 mean expression is significantly higher in the COLO205 cells compared to the HT29 cells (p-value = <0.0001). KIFC1 is highly localised to cell nuclei but lacks localisation in the cytoplasm in both cell lines.

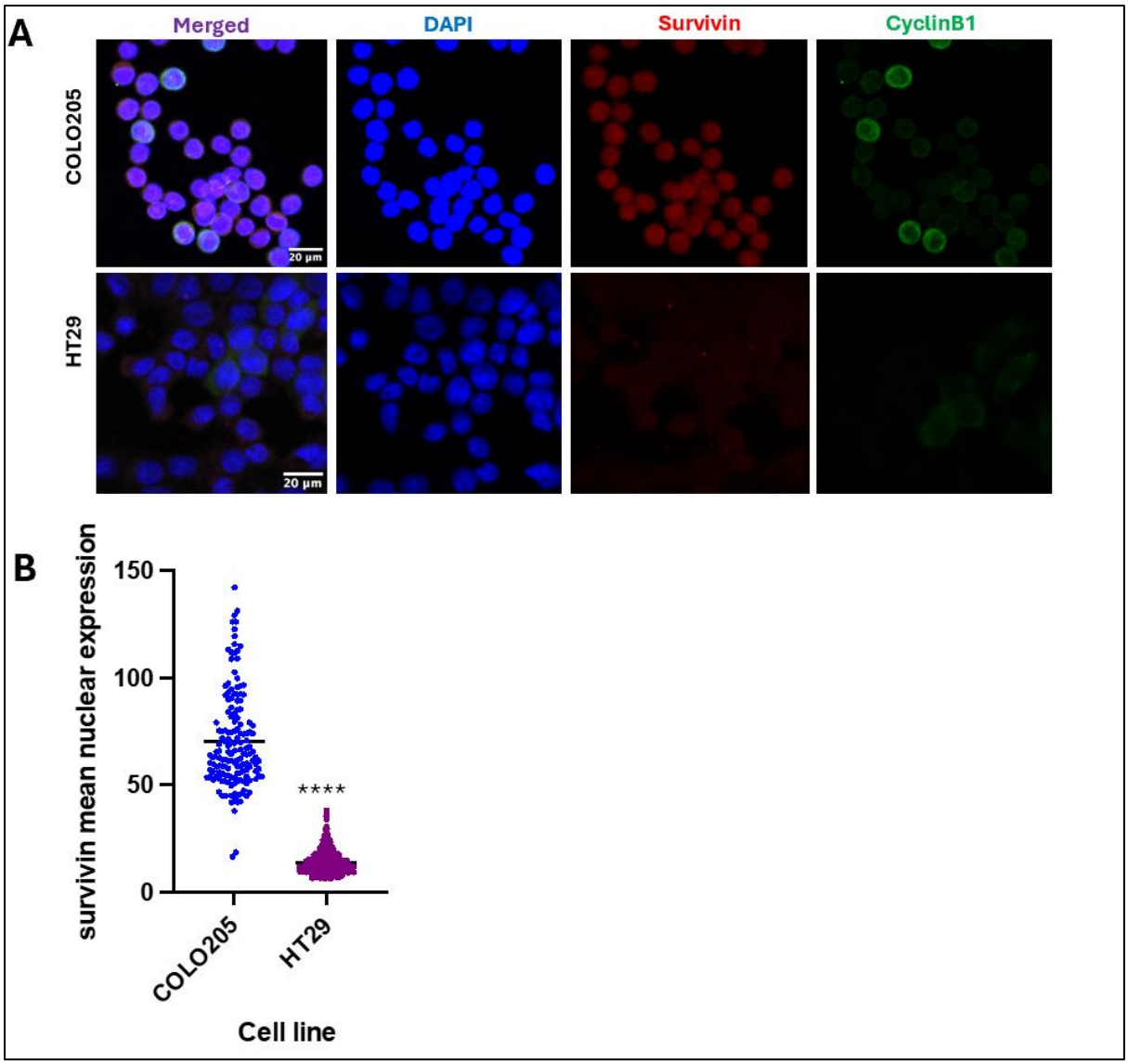

Figure 32: Survivin nuclear expression is higher in COLO205 cells.

COLO205 and HT29 cells were transfected with siControl siRNA. They were incubated for 2 days before fixation with methanol. Cells were stained with primary antibodies: mouse anti-CyclinB1, rabbit anti-Survivin, followed by secondary antibodies: Goat anti-mouse 488nm, and Goat anti-rabbit 568nm. Cells were mounted with Mowiol and DAPI on a microscope slide before being stored overnight at room temperature. The cells were then imaged using a confocal microscope. **(A)** Zoomed-in fields of view of COLO205 and HT29 cells were captured and stained for Survivin, DAPI and CyclinB1 with a scale bar of 20µm. **(B)** Survivin intensity in CyclinB1+ and CyclinB1- cells was measured in FIJI in individual cells in 3 fields of view per condition. Total n-number of cells, COLO205 = 155, HT29 = 806. An unpaired T-test test was performed, **** p-value = <0.0001.

Figure 32 shows COLO205 and HT29 cells stained for DAPI, Survivin and Cyclin B1. Survivin mean nuclear expression is significantly higher in the COLO205 cells compared to the HT29 cells (p-value = <0.0001). Survivin is highly localised to cell nuclei but lacks localisation in the cytoplasm in COLO205 cells. Next, COLO205 and HT29 cells were treated with KIFC1 siRNAs for further analysis.

6.6: Using KIFC1 siRNAs to determine the effect of KIFC1 depletion on Survivin protein levels in Colorectal Cancer

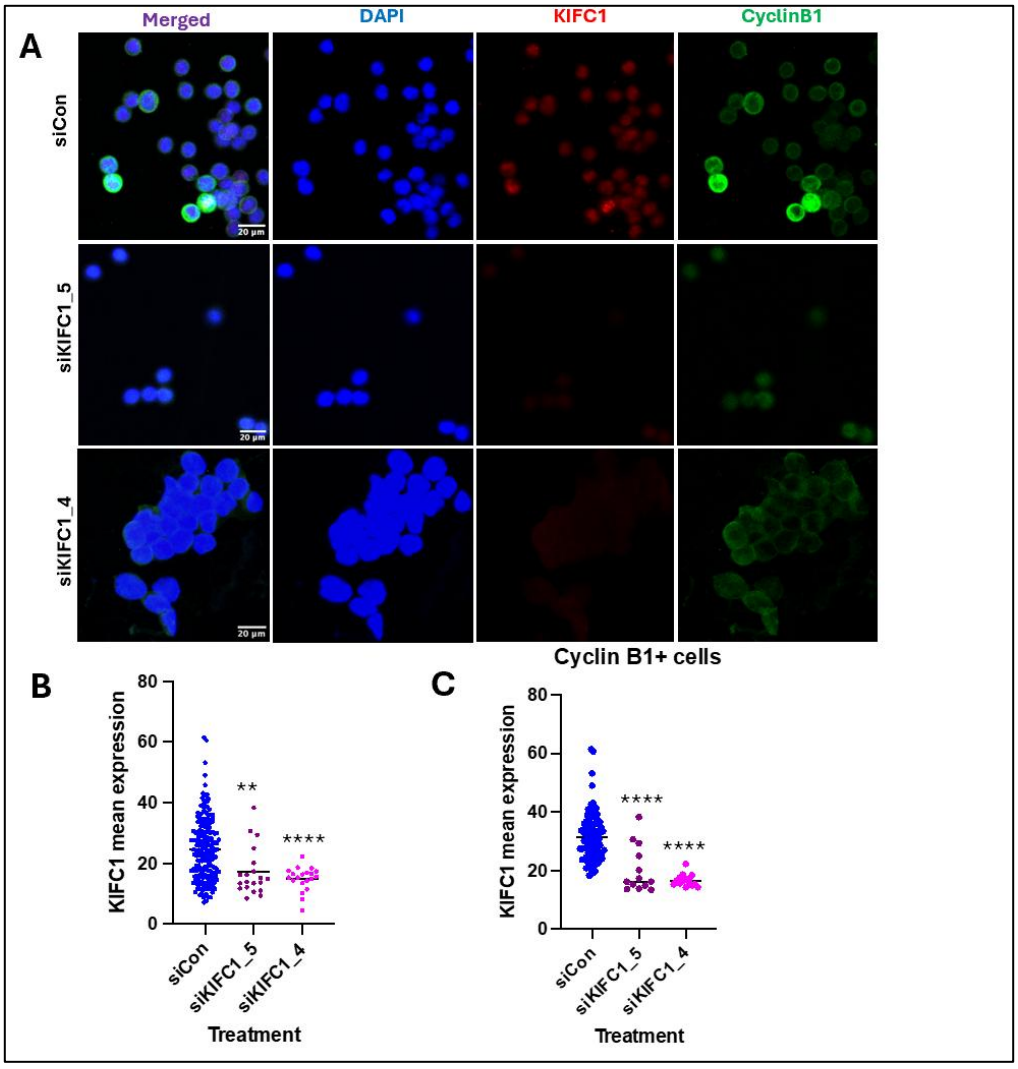

Figure 33: KIFC1 expression in COLO205 cells successfully knocked down using siRNAs.

COLO205 cells were transfected with siControl, siKIFC1_5 and siKIFC1_4 siRNAs. They were incubated for 2 days before fixation with methanol. Cells were stained with primary antibodies: mouse anti-CyclinB1, rabbit anti-KIFC1, followed by secondary antibodies: Goat anti-mouse 488nm, and Goat anti-rabbit 568nm. Cells were mounted with Mowiol and DAPI on a microscope slide before being stored overnight at room temperature. The cells were then imaged using a confocal microscope. **(A)** Zoomed-in fields of view of COLO205 cells were captured and stained for KIFC1, DAPI and CyclinB1 with a scale bar of 20µm. **(B+C)** KIFC1 intensity in CyclinB1+ and/or CyclinB1- cells was measured in FIJI in individual cells with 3 fields of view per condition. Total n-number of cells = siCon = 197, siKIFC1_5 = 20, siKIFC1_4 = 20. A One-Way ANOVA statistical test with Dunnett's multiple comparison test was performed, **(B)** **** p-value = <0.0001 and ** p-value = 0.0020 compared to the control. **(C)** **** p-value = <0.0001.

Figure 33 shows COLO205 cells stained for DAPI, KIFC1 and Cyclin B1. Cells were treated with siControl and KIFC1 siRNAs. Figure 33 showed statistical significance in reducing KIFC1 mean expression using siKIFC1_5 (p-value = 0.0020) and siKIFC1_4 (p-value = <0.0001) siRNAs in CyclinB1+/- cells.

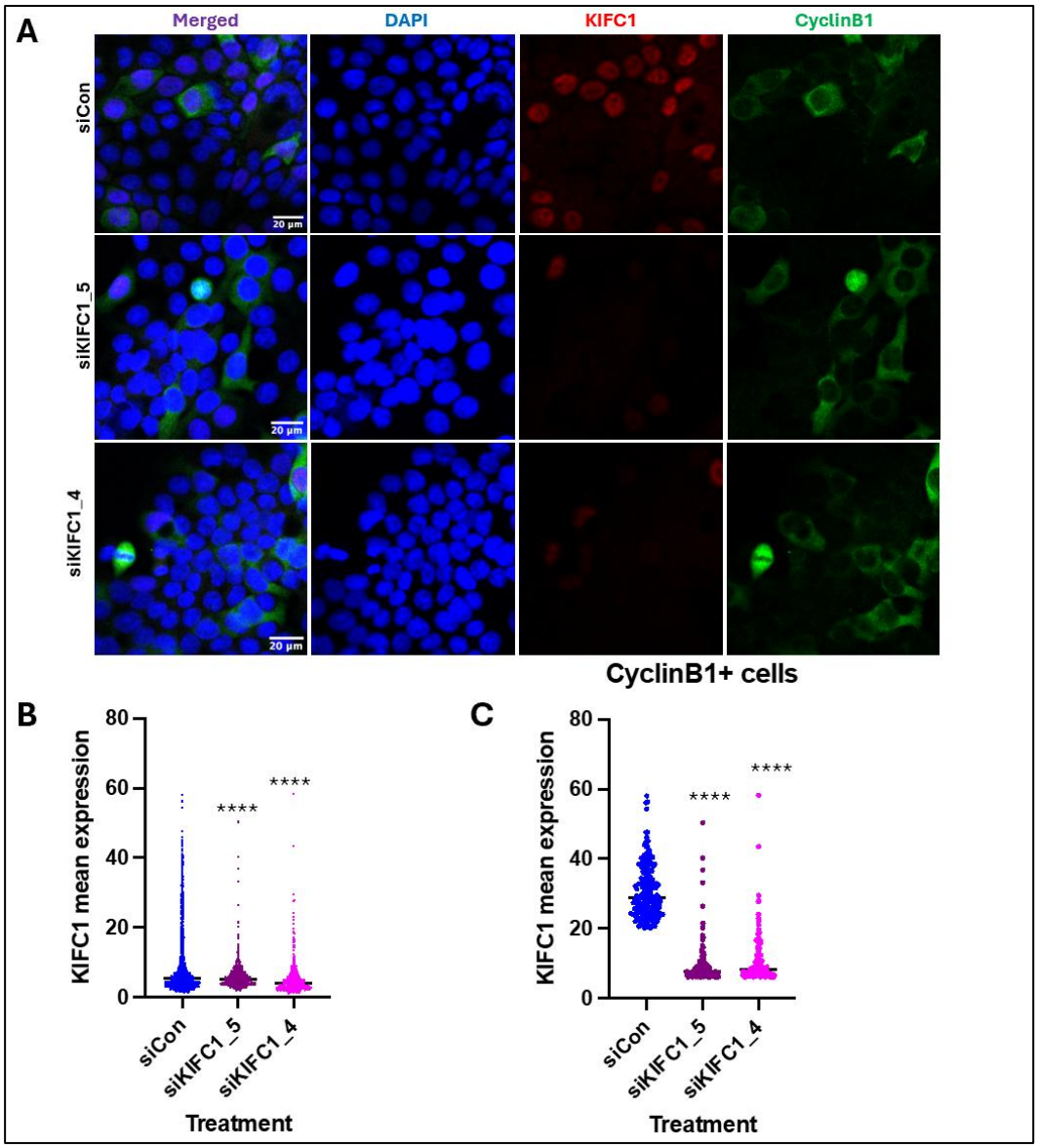

Figure 34: KIFC1 expression in HT29 cells successfully knocked down using siRNAs.

HT29 cells were transfected with siControl, siKIFC1_5 and siKIFC1_4 siRNAs. They were incubated for 2 days before fixation with methanol. Cells were stained with primary antibodies: mouse anti-CyclinB1, rabbit anti-KIFC1, followed by secondary antibodies: Goat anti-mouse 488nm, and Goat anti-rabbit 568nm. Cells were mounted with Mowiol and DAPI on a microscope slide before being stored overnight at room temperature. The cells were then imaged using a confocal microscope. **(A)** Zoomed-in fields of view of HT29 cells were captured and stained for KIFC1, DAPI and CyclinB1 with a scale bar of 20µm. **(B+C)** KIFC1 intensity in CyclinB1+ and/or CyclinB1- cells was measured in FIJI in individual cells with 3 fields of view per condition. Total n-number of cells = siCon = 1300, siKIFC1_5 = 506, siKIFC1_4 = 491. A One-Way ANOVA statistical test with Dunnett's multiple comparison test was performed. **(B)****** p-value = <0.0001 for both siRNAs compared to the control. **(C)** **** p-value = <0.0001.

Figure 34 shows HT29 cells stained for DAPI, KIFC1 and Cyclin B1. Cells were treated with siControl and KIFC1 siRNAs. Figure 34 showed statistical significance in reducing KIFC1 mean expression using siKIFC1_5 (p-value = 0.0020) and siKIFC1_4 (p-value = <0.0001) siRNAs in CyclinB1+/- cells.

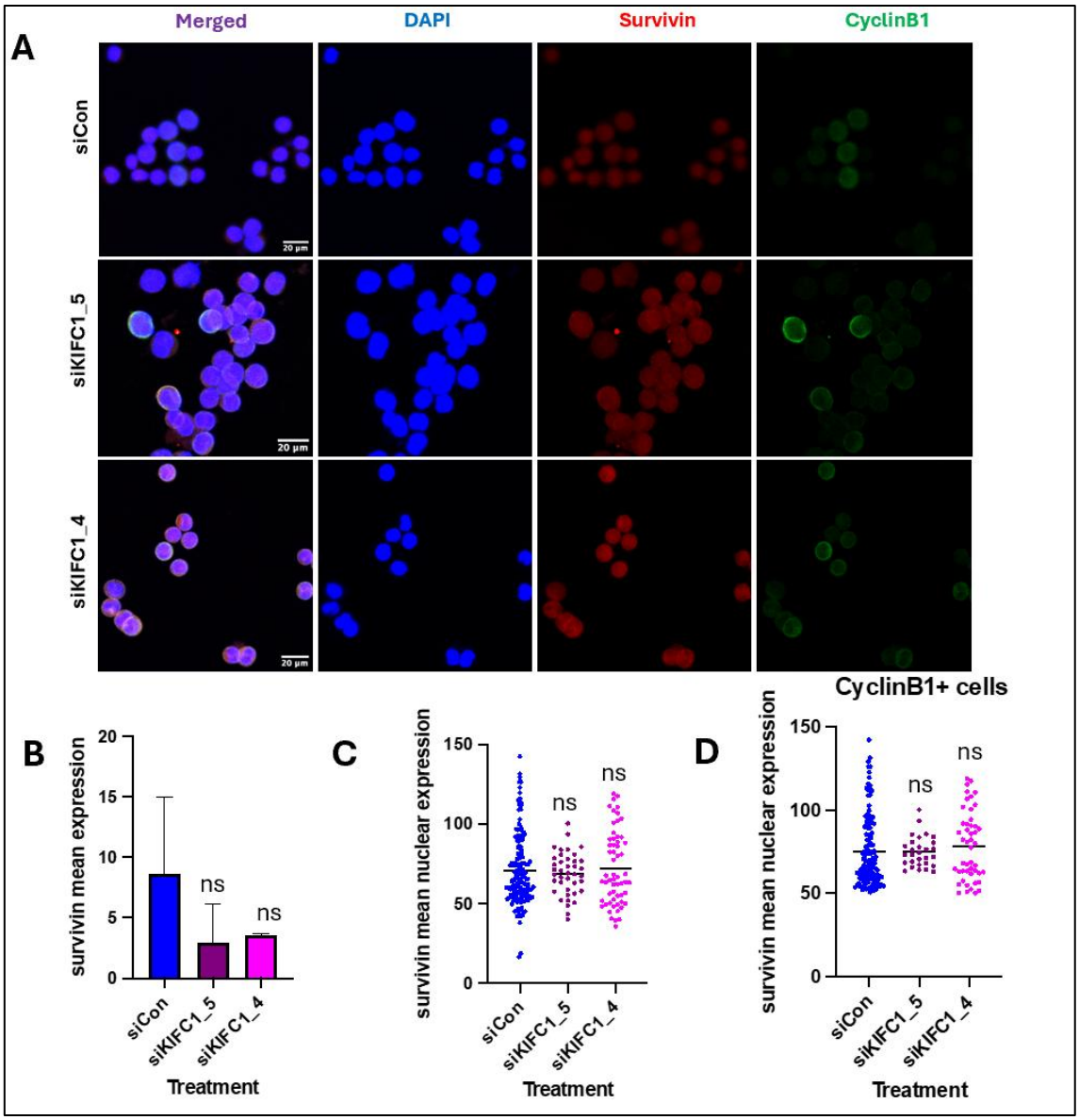

Figure 35: Survivin expression in COLO205 cells did not change using siRNAs.

COLO205 cells were transfected with siControl, siKIFC1_5 and siKIFC1_4 siRNAs. They were incubated for 2 days before fixation with methanol. Cells were stained with primary antibodies: mouse anti-CyclinB1, rabbit anti-Survivin, followed by secondary antibodies: Goat anti-mouse 488nm, and Goat anti-rabbit 568nm. Cells were mounted with Mowiol and DAPI on a microscope slide before being stored overnight at room temperature. The cells were then imaged using a confocal microscope. **(A)** Zoomed-in fields of view of COLO205 cells were captured and stained for Survivin, DAPI and CyclinB1 with a scale bar of 20µm. **(B-D)** Survivin intensity in CyclinB1+ and/or CyclinB1- cells was measured in FIJI in individual cells with 3 fields of view per condition. Total n-number of cells = siCon = 155, siKIFC1_5 = 40, siKIFC1_4 = 59. A One-Way ANOVA statistical test with Dunnett's multiple comparison test was performed, p-value = >0.05.

Figure 35 shows COLO205 cells stained for DAPI, Survivin and Cyclin B1. Cells were treated with siControl and KIFC1 siRNAs. Figure 35 showed no statistical significance in the increase or decrease of Survivin expression in CyclinB1+/ cells, and Survivin showed high localisation to cell nuclei but lacked localisation in the cytoplasm.

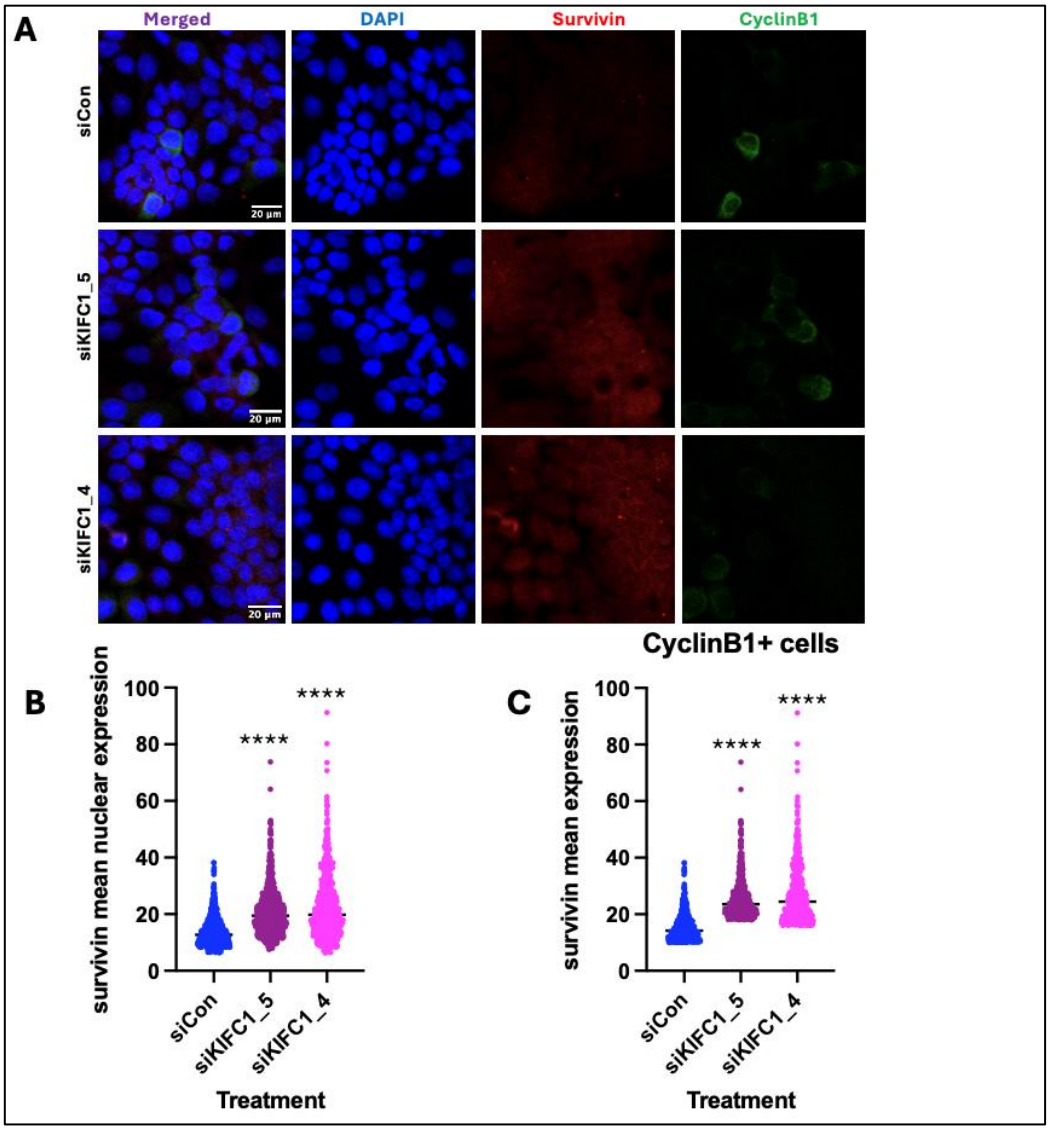

Figure 36: Survivin expression in HT29 cells increased using siRNAs.

HT29 cells were transfected with siControl, siKIFC1_5 and siKIFC1_4 siRNAs. They were incubated for 2 days before fixation with methanol. Cells were stained with primary antibodies: mouse anti-CyclinB1, rabbit anti-Survivin, followed by secondary antibodies: Goat anti-mouse 488nm, and Goat anti-rabbit 568nm. Cells were mounted with Mowiol and DAPI on a microscope slide before being stored overnight at room temperature. The cells were then imaged using a confocal microscope. **(A)** Zoomed-in fields of view of HT29 cells were captured and stained for Survivin, DAPI and CyclinB1 with a scale bar of 20µm. **(B+C)** Survivin intensity in CyclinB1+ and/or CyclinB1- cells was measured in FIJI in individual cells with 3 fields of view per condition. Total n-number of cells = siCon = 806, siKIFC1_5 = 976, siKIFC1_4 = 731. A One-Way ANOVA statistical test with Dunnett's multiple comparison test was performed. **(B)** **** p-value = <0.0001 for both siRNAs compared to the control. **(C)** **** p-value = <0.0001.

Figure 36 shows HT29 cells stained for DAPI, Survivin and Cyclin B1. Cells were treated with siControl and KIFC1 siRNAs. Figure 36 showed statistical significance in the increase of Survivin expression in CyclinB1+/ cells, and Survivin showed high localisation in cell nuclei and cytoplasm.

6.7: Assessing cell viability in Colorectal Cancer

Next, we investigated cell viability in Colorectal cancer cell lines after KIFC1 knockdown. This was achieved using MTS assays.

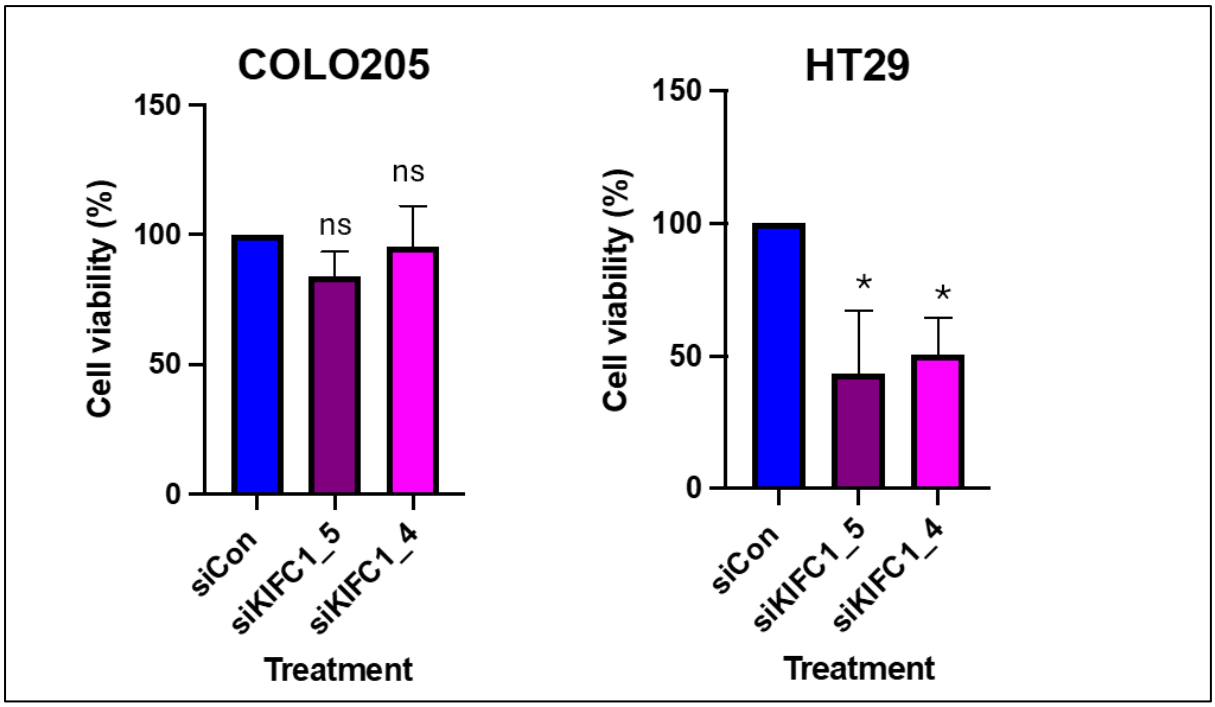

Figure 37: Cell viability in COLO205 remains unchanged when using KIFC1 siRNAs but decreases in HT29 cells.

COLO205 and HT29 cells were reverse-transfected with siControl, siKIFC1_5, and siKIFC1_4 siRNAs in a 96-well plate. They were incubated for 5 days before the MTS reagent was added to each well. The 96-well plate was incubated for 4 hours before being read inside a spectrophotometer at 490 nm. The experiment was repeated 3 times with 9 data points per siRNA for each cell line. Bar graphs showing COLO205 and HT29 cells reverse transfected with siCon, siKIFC1_5 and siKIFC1_4 siRNAs. Cell viability for both siRNAs was normalised to the controls in each cell line. 3 well replicates were used per treatment condition with ≈400 cells per well. A One-Way ANOVA statistical test with Dunnett's multiple comparison test was performed. COLO205: p-value = 0.1711 for both siRNAs. HT29: * p-values = 0.0195 (siKIFC1_5) and 0.0385 (siKIFC1_4).

Figure 37 shows COLO205 and HT29 cells treated with siControl and two KIFC1 siRNAs in a 96-well plate with approximately 400 cells per well. Adding MTS reagent to the cells revealed no significant decrease in cell viability in COLO205 cells. However, there was a significant decrease in cell viability in HT29 cells using both siRNAs (siKIFC1_5 p-value = 0.0195, siKIFC1_4 p-value = 0.0385) compared to the control siRNA.

6.8: Comparing the expression profile of KIFC1 and Survivin in Colorectal cancer cell lines with high and low centrosome amplification.

The next set of experiments was performed using two Glioblastoma cancer cell lines, U251 and SNB-19. U251 is known to express high CA (Mehdizadeh et al., 2023), whereas SNB-19 expresses low CA (Djuzenova et al., 2014). The same experimental procedures were performed, which included methanol-fixed immunofluorescence and MTS assays.

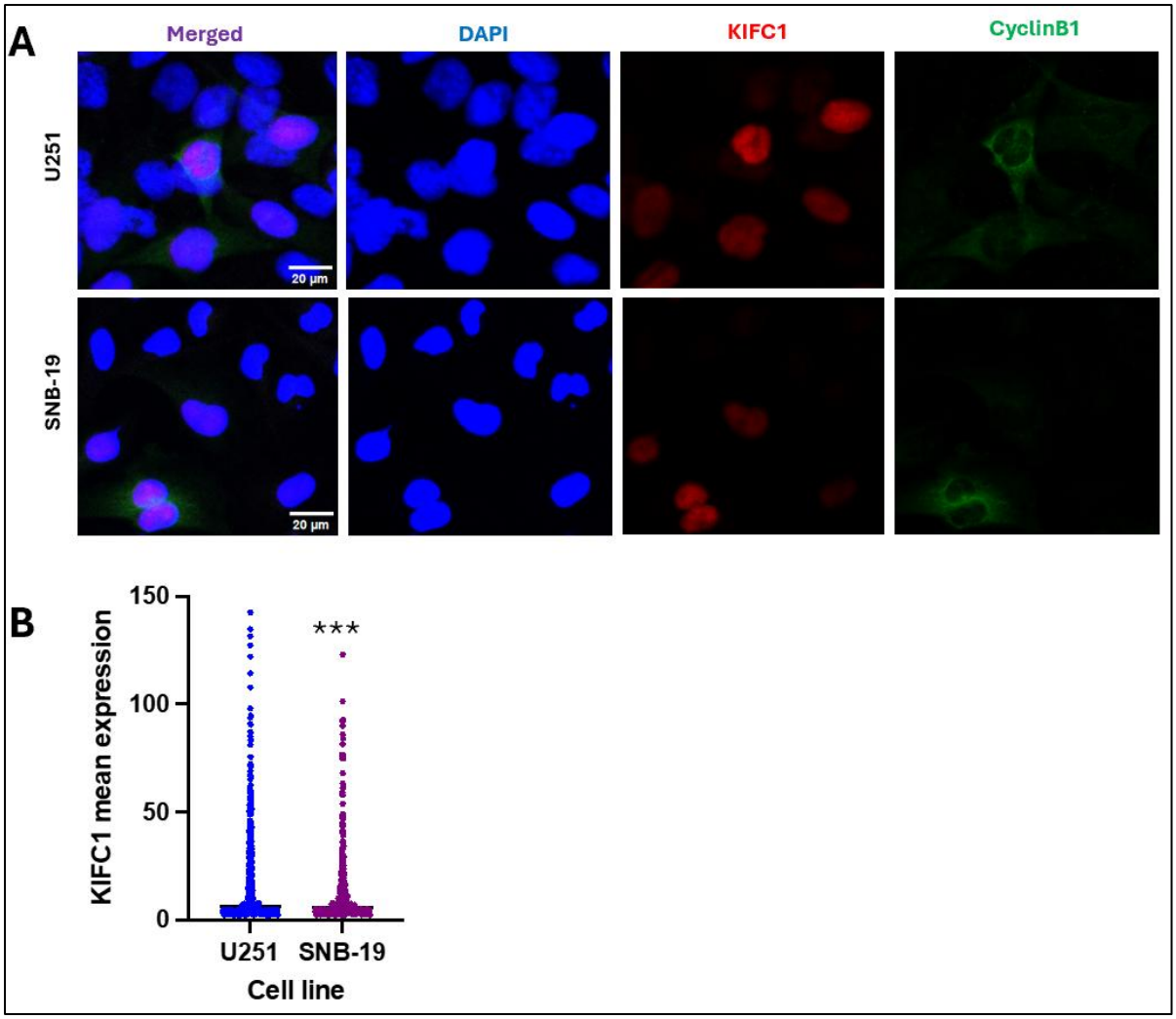

Figure 38: KIFC1 expression is higher in U251 cells.

U251 and SNB-19 cells were transfected with siControl siRNA. They were incubated for 2 days before fixation with methanol. Cells were stained with primary antibodies: mouse anti-CyclinB1, rabbit anti-KIFC1, followed by secondary antibodies: Goat anti-mouse 488nm, and Goat anti-rabbit 568nm. Cells were mounted with Mowiol and DAPI on a microscope slide before being stored overnight at room temperature. The cells were then imaged using a confocal microscope. **(A)** Zoomed-in fields of view of U251 and SNB-19 cells were captured and stained for KIFC1, DAPI and CyclinB1 with a scale bar of 20µm. **(B)** KIFC1 intensity in CyclinB1+ and CyclinB1- cells was measured in FIJI in individual cells in 3 fields of view per condition. Total n-number of cells, U251 = 490, SNB-19 = 390. An unpaired T-test was performed, *** p-value = 0.0005.

Figure 38 shows U251 and SNB-19 cells stained for DAPI, KIFC1 and Cyclin B1. KIFC1 mean expression is significantly higher in the U251 cells compared to the SNB-19 cells (p-value = <0.0005). KIFC1 is highly localised to cell nuclei but lacks localisation in the cytoplasm in both cell lines.

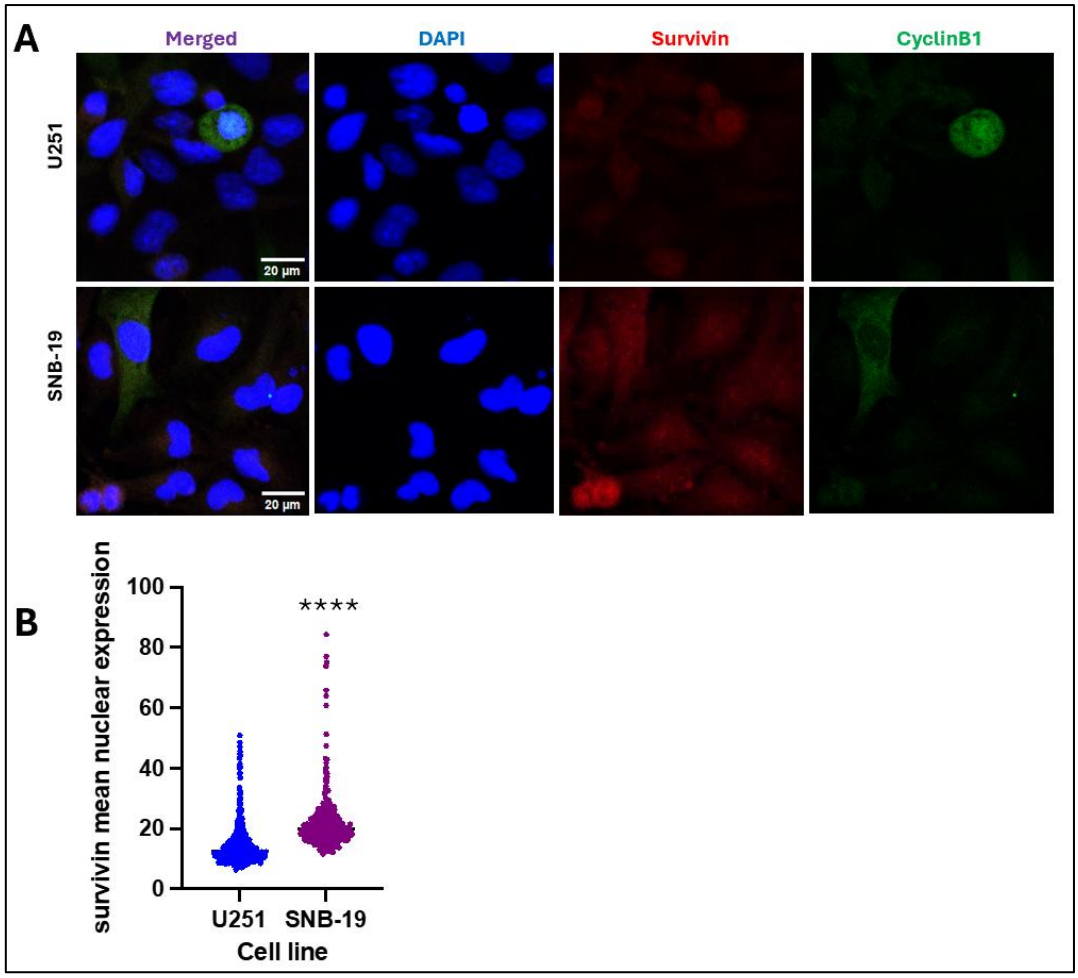

Figure 39: Survivin nuclear expression is higher in SNB-19 cells.

U251 and SNB-19 cells were transfected with siControl siRNA. They were incubated for 2 days before fixation with methanol. Cells were stained with primary antibodies: mouse anti-CyclinB1, rabbit anti-Survivin, followed by secondary antibodies: Goat anti-mouse 488nm, and Goat anti-rabbit 568nm. Cells were mounted with Mowiol and DAPI on a microscope slide before being stored overnight at room temperature. The cells were then imaged using a confocal microscope. **(A)** Zoomed-in fields of view of U251 and SNB-19 cells were captured and stained for Survivin, DAPI and CyclinB1 with a scale bar of 20µm. **(B)** Survivin intensity in CyclinB1+ and CyclinB1- cells was measured in FIJI in individual cells in 3 fields of view per condition. Total n-number of cells, U251 = 452, SNB-19 = 351. An unpaired T-test was performed, **** p-value = <0.0001 for both siRNAs compared to the control.

Figure 39 shows U251 and SNB-19 cells stained for DAPI, Survivin and Cyclin B1. Survivin mean nuclear expression is significantly higher in the SNB-19 cells compared to the U251 cells (p-value = <0.0001). Survivin is highly localised to cell nuclei and cytoplasm in both cell lines. Next, U251 and SNB-19 cells were treated with KIFC1 siRNAs for further analysis.

6.9: Using KIFC1 siRNAs to determine the effect of KIFC1 depletion on Survivin protein levels in CNS Cancer

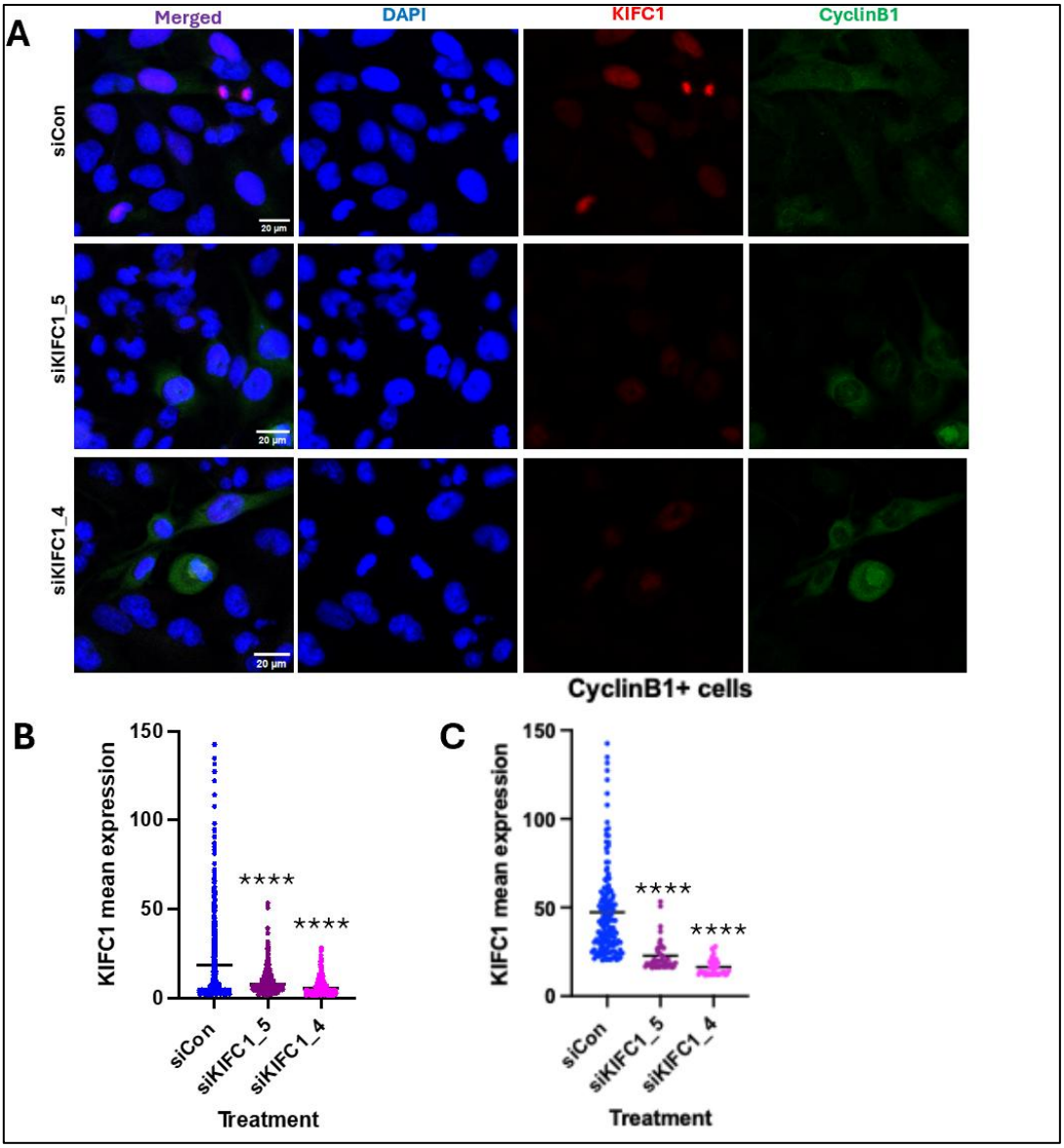

Figure 40: KIFC1 expression in U251 cells successfully knocked down using siRNAs.

U251 cells were transfected with siControl, siKIFC1_5 and siKIFC1_4 siRNAs. They were incubated for 2 days before fixation with methanol. Cells were stained with primary antibodies: mouse anti-CyclinB1, rabbit anti-KIFC1, followed by secondary antibodies: Goat anti-mouse 488nm, and Goat anti-rabbit 568nm. Cells were mounted with Mowiol and DAPI on a microscope slide before being stored overnight at room temperature. The cells were then imaged using a confocal microscope. **(A)** Zoomed-in fields of view of U251 cells were captured and stained for KIFC1, DAPI and CyclinB1 with a scale bar of 20µm. **(B+C)** KIFC1 intensity in CyclinB1+ and/or CyclinB1- cells was measured in FIJI in individual cells with 3 fields of view per condition. Total n-number of cells = siCon = 488, siKIFC1_5 = 539, siKIFC1_4 = 418. A One-Way ANOVA statistical test with Dunnett's multiple comparison test was performed, **** p-value = <0.0001 for both siRNAs compared to the control.

Figure 40 shows U251 cells stained for DAPI, KIFC1 and Cyclin B1. Cells were treated with siControl and KIFC1 siRNAs. Figure 40 showed statistical significance in the low KIFC1 mean expression using both KIFC1 siRNAs in Cyclin B1+/- cells. (p-value = <0.0001).

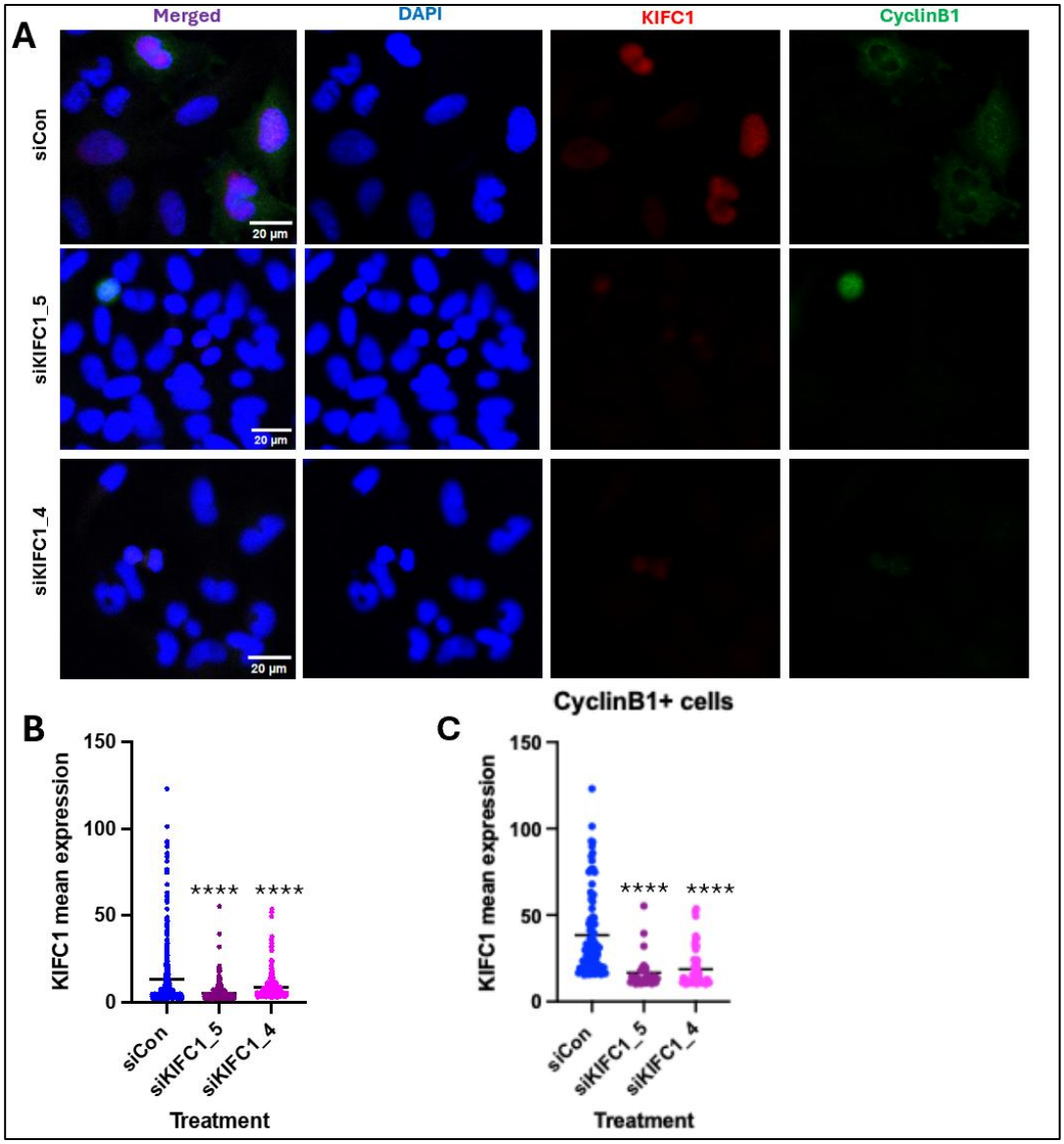

Figure 41: KIFC1 expression in SNB-19 cells successfully knocked down using siRNAs.

U251 cells were transfected with siControl, siKIFC1_5 and siKIFC1_4 siRNAs. They were incubated for 2 days before fixation with methanol. Cells were stained with primary antibodies: mouse anti-CyclinB1, rabbit anti-KIFC1, followed by secondary antibodies: Goat anti-mouse 488nm, and Goat anti-rabbit 568nm. Cells were mounted with Mowiol and DAPI on a microscope slide before being stored overnight at room temperature. The cells were then imaged using a confocal microscope. **(A)** Zoomed-in fields of view of SNB-19 cells were captured and stained for KIFC1, DAPI and CyclinB1 with a scale bar of 20µm. **(B+C)** KIFC1 intensity in CyclinB1+ and/or CyclinB1- cells was measured in FIJI in individual cells with 3 fields of view per condition. Total n-number of cells = siCon = 388, siKIFC1_5 = 355, siKIFC1_4 = 279. A One-Way ANOVA statistical test with Dunnett's multiple comparison test was performed, **** p-value = <0.0001 for both siRNAs compared to the control.

Figure 41 shows SNB-19 cells stained for DAPI, KIFC1 and Cyclin B1. Cells were treated with siControl and KIFC1 siRNAs. Figure 41 showed statistical significance in the low KIFC1 mean expression using both KIFC1 siRNAs in Cyclin B1+/- cells. (p-value = <0.0001).

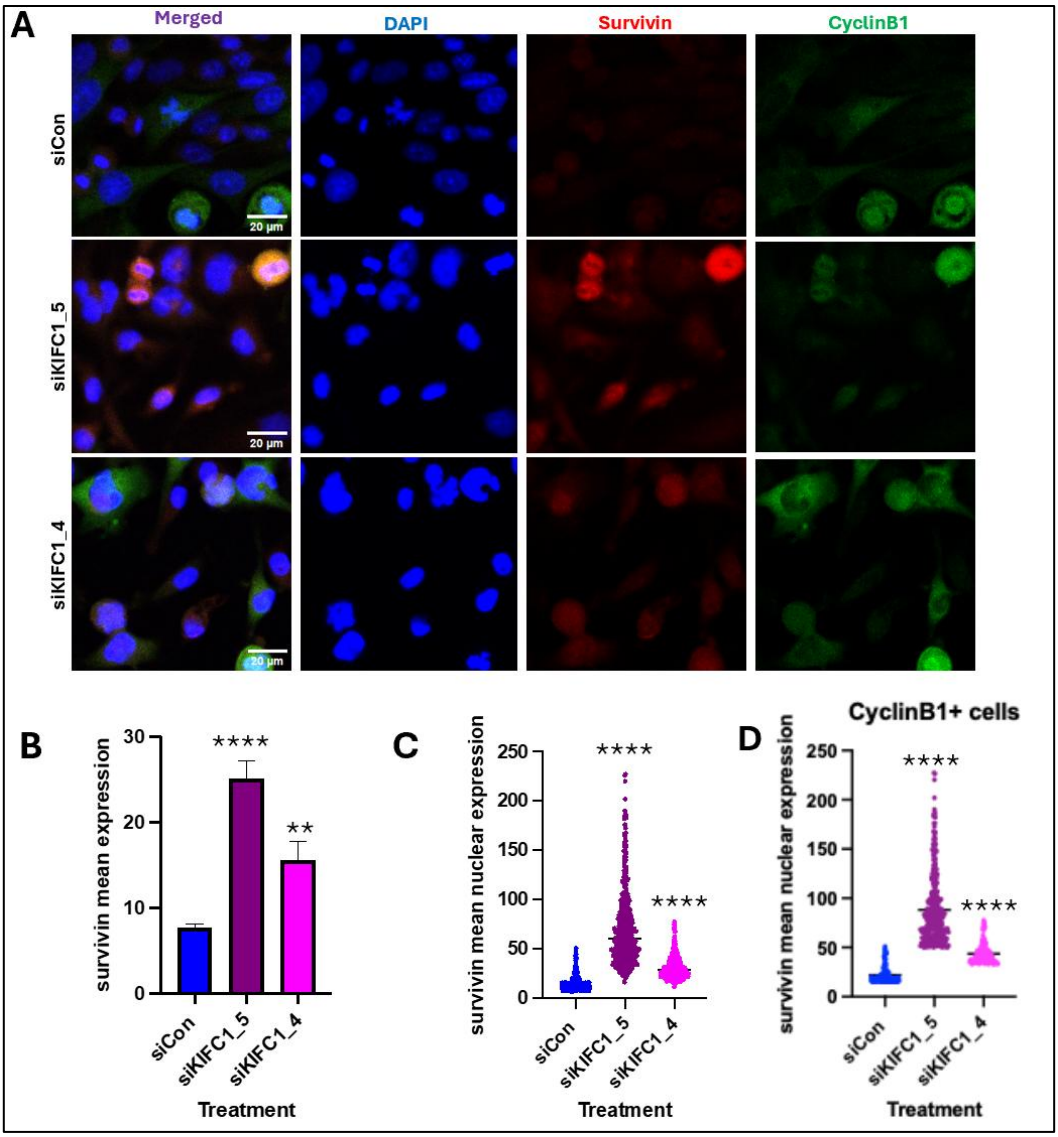

Figure 42: Survivin expression in U251 cells increased using siRNAs.

U251 cells were transfected with siControl, siKIFC1_5 and siKIFC1_4 siRNAs. They were incubated for 2 days before fixation with methanol. Cells were stained with primary antibodies: mouse anti-CyclinB1, rabbit anti-Survivin, followed by secondary antibodies: Goat anti-mouse 488nm, and Goat anti-rabbit 568nm. Cells were mounted with Mowiol and DAPI on a microscope slide before being stored overnight at room temperature. The cells were then imaged using a confocal microscope. **(A)** Zoomed-in fields of view of U251 cells were captured and stained for Survivin, DAPI and CyclinB1 with a scale bar of 20µm. **(B-D)** Survivin intensity in CyclinB1+ and/or CyclinB1- cells was measured in FIJI in individual cells with 3 fields of view per condition. Total n-number of cells = siCon = 452, siKIFC1_5 = 501, siKIFC1_4 = 411. A One-Way ANOVA statistical test with Dunnett's multiple comparison test was performed. **(B)** **** p-value = <0.0001 (siKIFC1_5), ** p-value = 0.0028 (siKIFC1_4). **(C+D)** **** p-value = <0.0001 for both siRNAs compared to the control.

Figure 42 shows U251 cells stained for DAPI, Survivin and Cyclin B1. Cells were treated with siControl and KIFC1 siRNAs. Figure 42 showed that there was statistical significance in the increase of Survivin expression in Cyclin B1+ cells (p-value < 0.0001).

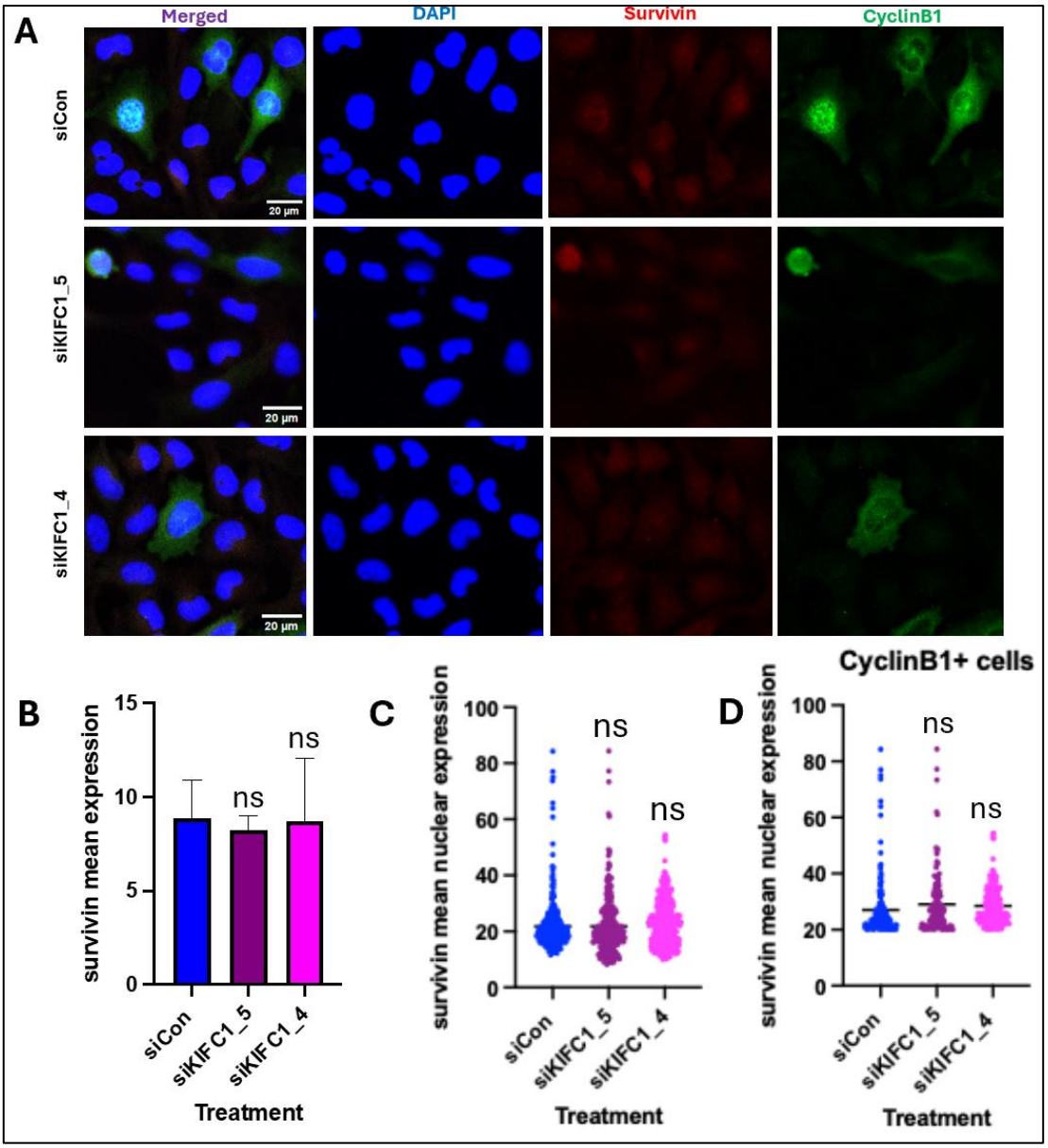

Figure 43: Survivin expression in SNB-19 cells did not change using siRNAs.

SNB-19 cells were transfected with siControl, siKIFC1_5 and siKIFC1_4 siRNAs. They were incubated for 2 days before fixation with methanol. Cells were stained with primary antibodies: mouse anti-CyclinB1, rabbit anti-Survivin, followed by secondary antibodies: Goat anti-mouse 488nm, and Goat anti-rabbit 568nm. Cells were mounted with Mowiol and DAPI on a microscope slide before being stored overnight at room temperature. The cells were then imaged using a confocal microscope. **(A)** Zoomed-in fields of view of SNB-19 cells were captured and stained for Survivin, DAPI and CyclinB1 with a scale bar of 20µm. **(B-D)** Survivin intensity in CyclinB1+ and/or CyclinB1- cells was measured in FIJI in individual cells with 3 fields of view per condition. Total n-number of cells = siCon = 351, siKIFC1_5 = 315, siKIFC1_4 = 353. A One-Way ANOVA statistical test with Dunnett's multiple comparison test was performed, p-value = >0.05.

Figure 43 shows SNB-19 cells stained for DAPI, Survivin and Cyclin B1. Cells were treated with siControl and KIFC1 siRNAs. Figure 43 revealed no statistical significance in the increase or decrease in Survivin expression after siRNA treatment in CyclinB1+/- cells.

6.10: Assessing cell viability in CNS cancer

Next, we investigated cell viability in Glioblastoma cancer cell lines after KIFC1 knockdown. This was achieved using MTS assays.

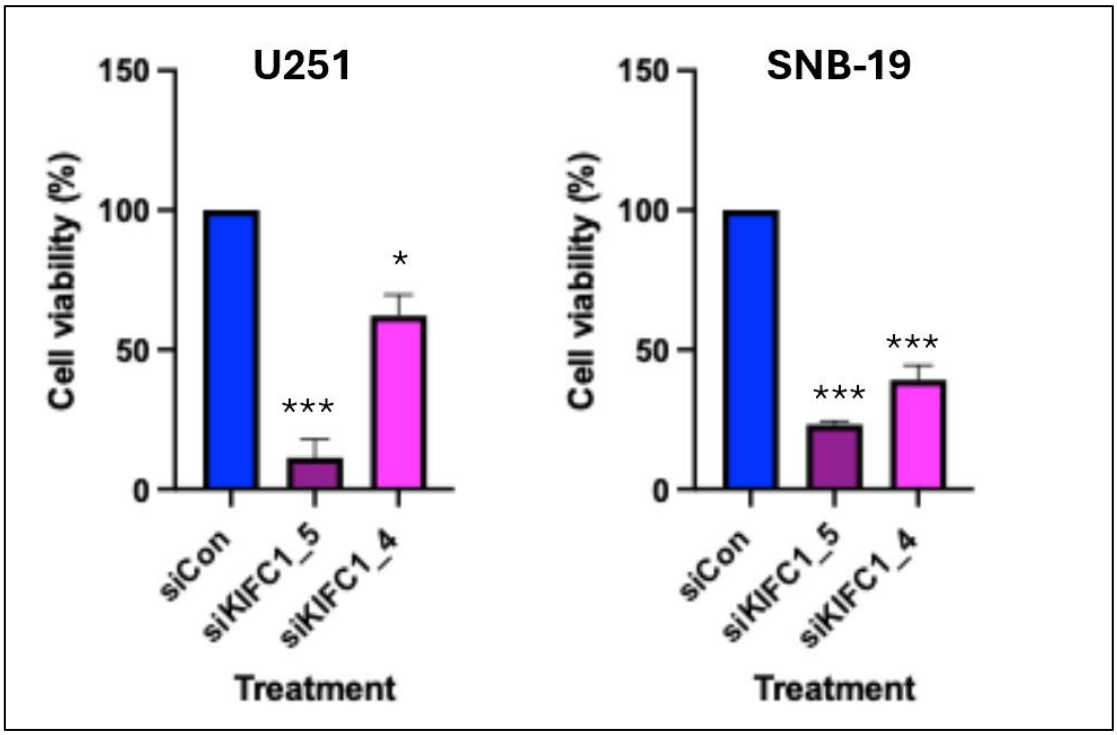

Figure 44: Cell viability in U251 and SNB-19 successfully reduced by KIFC1 knockdown.
U251 and SNB-19 cells were reverse transfected with siControl, siKIFC1_5 and siKIFC1_4 siRNAs in a 96-well plate. They were incubated for 5 days before the MTS reagent was added to each well. The 96-well plate was incubated for 4 hours before being read inside a spectrophotometer at 490 nm. Bar graphs showing U251 and SNB-19 cells reverse transfected with siControl, siKIFC1_5 and siKIFC1_4 siRNAs. Cell viability for both siRNAs was normalised to the controls in each cell line. 3 well replicates were used per treatment condition with ≈400 cells per well. A One-Way ANOVA statistical test with Dunnett's multiple comparison test was performed. U251: *** p-value = 0.0006 (siKIFC1_5) and * p-value = 0.0151 (siKIFC1_4). SNB-19: *** p-value = 0.0001 (siKIFC1_5) and *** p = 0.0003 (siKIFC1_4) compared to the control.

Figure 44 shows U251 and SNB-19 cells treated with siControl and two KIFC1 siRNAs in a 96-well plate with approximately 400 cells per well. Adding MTS reagent to the cells revealed a significant decrease in cell viability in both cell lines. The data presented show U251: (siKIFC1_5 p-value = 0.0195), (siKIFC1_4 p-value = 0.0385). SNB-19: (siKIFC1_5 p-value = 0.0001), (siKIFC1_4 p-value = 0.0003).

6.11 – Assessing cleaved Caspase 3 expression in Glioblastoma

The final experiment focused on assessing cleaved Caspase 3 expression in U251 and SNB-19 cancer cell lines to determine whether apoptosis is the primary factor contributing to low cell viability after KIFC1 siRNA treatment.

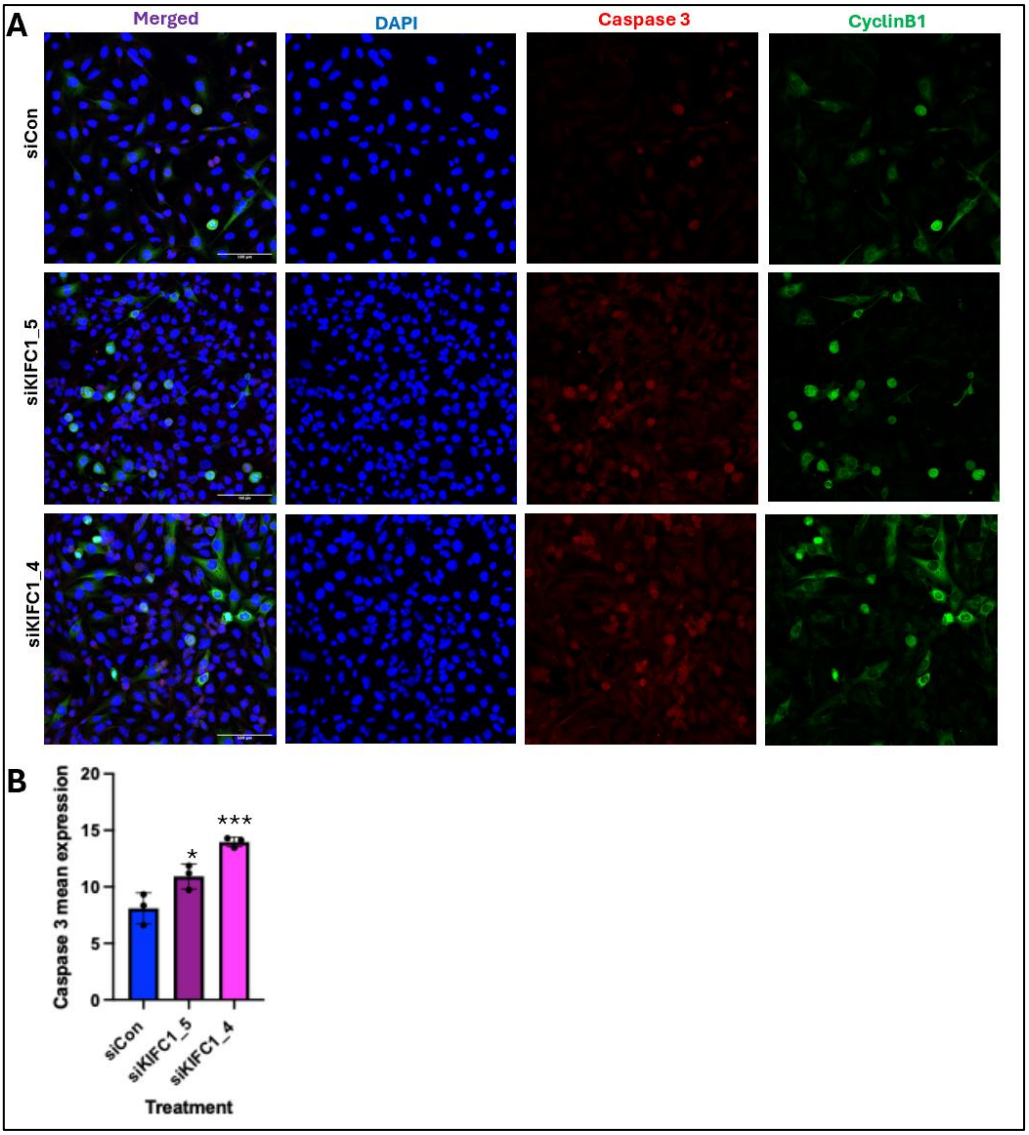

Figure 45: Cleaved Caspase 3 expression in U251 cells increased using siRNAs.

U251 cells were transfected with siControl, siKIFC1_5 and siKIFC1_4 siRNAs. They were incubated for 2 days before fixation with methanol. Cells were stained with primary antibodies: mouse anti-CyclinB1, rabbit anti-cleaved Caspase 3, followed by secondary antibodies: Goat anti-mouse 488nm, and Goat anti-rabbit 568nm. Cells were mounted with Mowiol and DAPI on a microscope slide before being stored overnight at room temperature. The cells were then imaged using a confocal microscope. **(A)** Whole fields of view of U251 cells were captured and stained for cleaved Caspase 3, DAPI and CyclinB1 with a scale bar of 100µm. **(B)** Cleaved Caspase 3 intensity in Cyclin B1+ and/or Cyclin B1- cells was measured in FIJI using individual cells with three fields of view per condition. A One-Way ANOVA statistical test with Dunnett's multiple comparison test was performed, * p-value = 0.0282 (siKIFC1_5), *** p-value = 0.0008 (siKIFC1_4).

Figure 45 revealed that cleaved Caspase 3 expression was significantly higher in U251 cells after KIFC1 siRNA treatment. U251: p-value = 0.0282 (siKIFC1_5) and p-value = 0.0008 (siKIFC1_4).

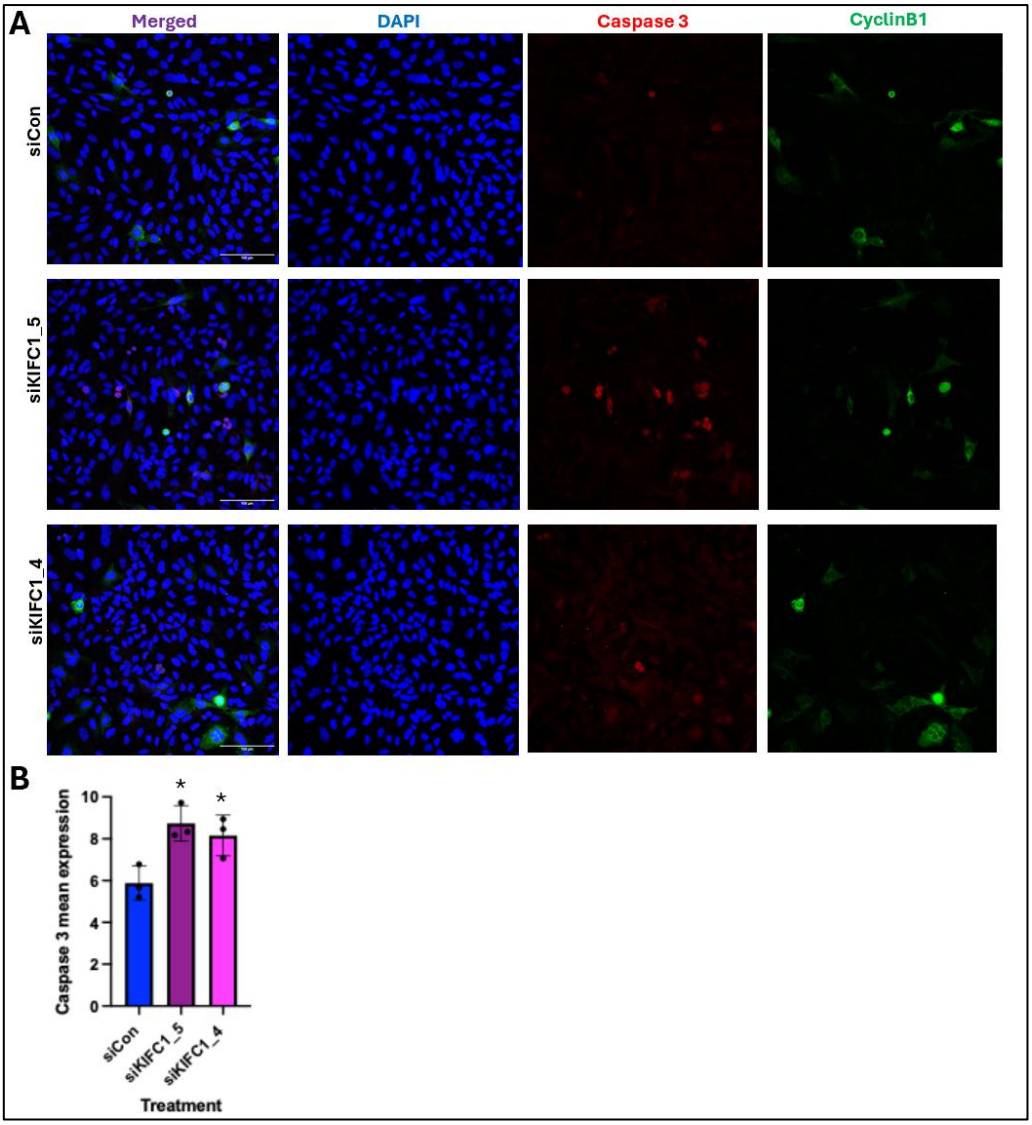

Figure 46: Cleaved caspase 3 expression in SNB-19 cells increased using siRNAs.

U251 cells were transfected with siControl, siKIFC1_5 and siKIFC1_4 siRNAs. They were incubated for 2 days before fixation with methanol. Cells were stained with primary antibodies: mouse anti-CyclinB1, rabbit anti-cleaved Caspase 3, followed by secondary antibodies: Goat anti-mouse 488nm, and Goat anti-rabbit 568nm. Cells were mounted with Mowiol and DAPI on a microscope slide before being stored overnight at room temperature. The cells were then imaged using a confocal microscope. **(A)** Whole fields of view of SNB-19 cells were captured and stained for cleaved Caspase 3, DAPI and CyclinB1 with a scale bar of 100µm. **(B)** Cleaved Caspase 3 intensity in Cyclin B1+ and/or Cyclin B1- cells was measured in FIJI using individual cells with three fields of view per condition. A One-Way ANOVA statistical test with Dunnett's multiple comparison test was performed, * p-value = 0.0131 (siKIFC1_5), * p-value = 0.0345 (siKIFC1_4).

Figure 46 revealed that cleaved Caspase 3 expression was significantly higher in SNB-19 cells after KIFC1 siRNA treatment. The data presented show SNB-19: p-value = 0.0131 (siKIFC1_5) and p-value = 0.0345 (siKIFC1_4).

7.0 – Discussion

Table 1: Summary of results

Table showing a result summary of Ovarian, Colorectal and Glioblastoma cell lines tested.

Cell line	**CA status**	**p53 status**	**KIFC1 baseline**	**Survivin baseline**	**KIFC1 expression (siRNA treatment)**	**Survivin expression (siRNA treatment)**	**Cell viability (siRNA treatment)**
OVCAR8	Low	Mutant	Similar to OVCAR4	Similar to OVCAR4	Decreased	Decreased	Decreased
OVCAR4	High	Mutant	Similar to OVCAR8	Similar to OVCAR8	Decreased	Decreased	Decreased
HT29	Low	Mutant	Lower compared to COLO205	Lower compared to COLO205	Decreased	Increased	Decreased
COLO205	High	Wild type	Higher compared to HT29	Higher compared to HT29	Decreased	No change	No change
SNB-19	Low	Mutant	Lower compared to U251	Higher compared to U251	Decreased	No change	Decreased
U251	High	Mutant	Higher compared to SNB-19	Lower compared to U251	Decreased	Increased	Decreased

7.1 - Introduction

This project investigated the dependency of KIFC1 in cell culture models of common cancer types, including Ovarian, Colorectal, and Central Nervous System cancers, sourced from the NCI-60 cancer cell panel. We assessed whether cancer cells are more dependent on centrosome clustering or Survivin expression. We also investigated whether these dependencies vary based on genetic or phenotypic features, such as baseline KIFC1 or Survivin levels, p53 status, and cleaved Caspase 3 expression. Six cancer cell lines were used in this project: OVCAR8, OVCAR4 (Ovarian), COLO205, HT29 (Colorectal), SNB-19 and U251 (CNS). Online bioinformatic data were collected to assess the prevalence of KIFC1 and BIRC5 gene alterations in many cancer types, as well as prognosis rates in patients. Methanol-fixed IF staining was used to quantify KIFC1 and Survivin expression, and MTS assays were used to assess cell viability. siRNAs were used in both assays to degrade KIFC1 mRNA in cells.

7.2 – KIFC1 and BIRC5 genes are key therapeutic targets in cancer

Given that numerous studies have demonstrated that KIFC1 and BIRC5 genes promote cancer cell proliferation and survival, it is worthwhile to investigate the prevalence and prognosis rates in cancer patients exhibiting abnormalities in these two genes. Using cBioportal, it was found that the KIFC1 and BIRC5 genes are highly prevalent in various cancer types, including Ovarian, Colorectal and CNS cancers. High mRNA expression and amplification were frequently apparent, suggesting that these cell lines heavily depend on these cellular characteristics rather than mutations to promote proliferation and survival. These findings also highlight that the KIFC1 and BIRC5 genes are excellent therapeutic targets. Furthermore, prognosis rates were significantly lower in cancer patients with abnormal KIFC1 and BIRC5 genes, suggesting great urgency for exploring therapeutic strategies to target KIFC1 and BIRC5, which may help suppress cancer cell proliferation and survival. Moreover, KIFC1 and BIRC5 mRNA expression showed a weak correlation, suggesting that KIFC1 protects Survivin more effectively at the protein level than at the mRNA level, which is consistent with the findings from (Fu et al., 2018).

Therefore, it is ideal to measure KIFC1 and Survivin at the protein expression level rather than at the mRNA expression level in this project. Ovarian cancer cell lines appear to have greater mRNA expression of both KIFC1 and BIRC5 genes than Colorectal cancer cell lines, which could indicate a higher reliance on these proteins for survival and proliferation in Ovarian cancer.

7.3 - OVCAR8 and OVCAR4 cells are highly sensitive to KIFC1 knockdown

The two Ovarian cancer cell lines, OVCAR8 and OVCAR4, exhibited similar KIFC1 and Survivin expression when compared between the two cell lines. This suggests that it is worthwhile to investigate whether KIFC1 depletion leads to altered Survivin expression. OVCAR8 and OVCAR4 exhibited a significant decrease in KIFC1 and Survivin expression after siRNA treatment, which was also accompanied by a corresponding drop in cell viability. The knockdown of KIFC1 results in Survivin no longer being protected from degradation at the 26S proteasome, leading to a decrease in Survivin expression, which is consistent with the findings reported by (Fu et al., 2018). The lack of Survivin expression indicates that apoptotic intrinsic pathways in cells remain active, particularly caspase enzymes that drive apoptotic signalling forward. This renders cells more vulnerable to apoptosis. Furthermore, the sharp decrease in cell viability suggests that both cell lines are more dependent on Survivin than KIFC1-mediated clustering. It is KIFC1's role in promoting Survivin stability in OVCAR8 and OVCAR4 cells that plays a dominant role in cell survival.

7.4 – COLO205 cells are highly resistant to KIFC1 knockdown

COLO205 cells exhibited a higher baseline of KIFC1 and Survivin nuclear expression when compared to HT29 cells. This may make sense in the context of CA in cancer cell lines altogether. COLO205 is known to exhibit high CA, which may indicate increased dependency of KIFC1-mediated clustering. Furthermore, the higher baseline nuclear Survivin expression could make COLO205 cells less susceptible to mitotic stress if KIFC1 is disrupted. Moreover, KIFC1 knockdown was also apparent in response to siRNA treatment, but Survivin expression did not change, which was unexpected. A

possible explanation for this resistance is that COLO205 cells possess additional cellular mechanisms to compensate for KIFC1 loss, allowing for centrosome clustering. For example, proteins such as Dynein and NuMA have been expressed in other cancer cell lines to help cluster centrosomes after KIFC1 depletion, but they are not a complete replacement for KIFC1. Dynein and NuMA have also been shown to maintain a bipolar spindle in cancer cells; thus, they could potentially increase resistance to mitotic stress after KIFC1 knockdown (Mercadante et al., 2023). Additionally, COLO205 cells exhibited no change in cell viability after KIFC1 siRNA treatment, indicating high resistance to KIFC1 knockdown.

7.5 – HT29 cells express Survivin upregulation with reduced viability

HT29 cells exhibited a lower baseline expression of KIFC1 and Survivin compared to COLO205 cells. It It is currently known in the literature that HT29 cells express low CA, which may indicate low dependency on KIFC1-mediated clustering. Furthermore, KIFC1 knockdown was evident in response to siRNA treatment; however, the expression of Survivin increased, which was unexpected. To explore this further, an MTS assay confirmed that cell viability in HT29 cells decreased, which does not align with the upregulation of Survivin. These findings suggest that the effect of KIFC1 depletion is likely not mediated via centrosome clustering (as cells have low levels of CA) or via Survivin (as Survivin levels are unaffected). Therefore, KIFC1 may act through an alternative mechanism in these cells, such as the interaction between STAT3 and Wnt. STAT3 is a transcription factor that can directly bind to the BIRC5 gene promoter, thereby increasing Survivin expression (Fernández et al., 2014). In Colon cancer, STAT3 has been shown to interact with the tubulin-β-catenin complex through the Wnt signalling pathway, thereby increasing further Survivin expression (Fernández et al., 2014). Additionally, colorectal cancer cells contain NF-kB enhancer binding sites, which can bind to the BIRC5 gene promoter to increase Survivin expression (Cui et al., 2017). Overall, these literature findings highlight that specific cellular pathways may be overactivated in response to mitotic stress, which may explain the upregulated Survivin expression observed in HT29 cells.

7.6 – Glioblastoma cell lines show mixed Survivin response, but show decreased viability

In the two glioblastoma cell lines, U251 exhibited higher baseline KIFC1 expression than SNB-19, suggesting a higher dependency on KIFC1-mediated clustering. Moreover, KIFC1 knockdown via siRNAs was apparent in both cell lines, but Survivin expression showed mixed results. In U251, Survivin nuclear expression was significantly higher after siRNA treatment, whereas in SNB-19, Survivin expression hardly changed. The reasons behind the mixed Survivin response remain to be studied in other projects. To investigate further, an MTS assay confirmed that cell viability was significantly reduced in both cell lines. SNB-19 cells showed great sensitivity to KIFC1 loss. Still, the effect of KIFC1 depletion is likely not mediated via centrosome clustering (as cells have low levels of CA) or via Survivin (as Survivin levels are unaffected). Therefore, KIFC1 may act through an alternative mechanism in these cells. To confirm that apoptosis is lowering cell viability rather than other factors, methanol-fixed IF staining for cleaved Caspase 3 was visualised. Both cell lines exhibited increased cleaved Caspase 3 expression after KIFC1 depletion, indicating that KIFC1 is inducing apoptosis, but not via Survivin.

7.7 – Role of p53 across cell lines

An important element of response may be p53 status. It has been shown in the literature that not all cancers harbour mutant p53, as apparent in the COLO205 cell line (Leroy et al., 2014). Wild-type p53 in these cells can stabilise mitosis, promote DNA repair, and enforce cell cycle checkpoints more tightly to mitigate the impact of KIFC1 depletion via siRNAs. Wild-type p53 may also promote cell cycle arrest instead of apoptosis, allowing time for cellular recovery. These are more plausible explanations as to why COLO205 cells showed no significant change in cell viability. Other cancer cell lines: OVCAR8, OVCAR4, HT29, U251 and SNB-19 harbour mutant p53. This suggests that these cell lines exhibit fully impaired cell cycle checkpoints, making cells more susceptible to mitotic defects unless other survival pathways, such as the upregulation of Survivin, are initiated and sufficient to preserve cell viability. Survivin has been shown to exhibit a counteractive relationship with p53, as explained in (Guindalini,

Mathias Machado and Garicochea, 2013). In HT29 cells, increased Survivin expression may partially compensate for the absence of wild-type p53, but not completely, as cell viability still decreases after KIFC1 knockdown. In OVCAR8 and OVCAR4 cells, where Survivin expression decreased upon KIFC1 depletion, mutant p53 likely leads to mitotic failure and apoptosis, hence the sharp decrease in cell viability. In glioblastoma cell lines, the absence of wild-type p53 in these cells is also indicative of lower cell viability after KIFC1 depletion.

7.8 – Limitations

There were several limitations of this project. The methanol-fixed Immunofluorescence staining involved automated software used for quantifying cells and protein expression. Sometimes, cells can be densely clustered, making it difficult for the software to distinguish between each cell nucleus accurately. This could have overestimated protein expression per cell in each field of view. To prevent this from happening in future projects, stricter settings in Fiji should be considered, such as further adjusting cell outline detection values or nuclei threshold to prevent inaccurate cell counting. Another limitation was time constraints. The time frame of this project was limited, resulting in a reduced number of experimental repeats and cell lines. If more time had been allocated, more replicates would have been performed to increase the statistical validity of the results, and a broader cell line panel would have facilitated better cell line comparisons. Another limitation was cell culture variability. Some cell lines were more challenging to culture than others, which potentially affected experimental consistency and limited the number of viable cells in my assays. There was also a high reliance on MTS assays for assessing cell viability. While MTS assays are excellent to a certain degree, other assays, such as clonogenic assays, would have provided a more comprehensive insight.

7.9 – Future Projects and Conclusion

This project demonstrated that many cancer cell lines require KIFC1 for proliferation and survival, which highlights key therapeutic interest. Although Survivin is known to support cell viability through

its anti-apoptotic function, most findings from this project suggest that cancer cells rely more on non-clustering cellular mechanisms. Furthermore, the relationship between KIFC1 and Survivin is complex and inconsistent across all cancer cell lines tested. Some, such as OVCAR8 and OVCAR4, exhibited knockdown of both proteins after using KIFC1 siRNAs, while others, including HT29 and SNB-19, showed mixed responses to Survivin, possibly due to alternative cellular mechanisms. Moreover, p53 status may have a significant role in cell survival. For example, COLO205 cells, which harbour wild-type p53, maintained cell viability despite no change in Survivin, possibly due to a better ability to manage mitotic stress, whereas cell lines that harbour mutant p53 were more susceptible to KIFC1 loss. In Glioblastoma cell lines, increased cleaved Caspase 3 levels indicate that apoptosis is the primary factor for low cell viability. Additionally, cBioportal results confirmed that KIFC1 and BIRC5 are excellent therapeutic targets due to their high prevalence and poor prognosis. cBioportal also confirmed that the relationship between KIFC1 and BIRC5 is at the protein level instead of mRNA level. Additionally, the relationship between KIFC1 and Survivin appears to be context-dependent and may reflect the relative contribution of centrosome-dependent versus Survivin-dependent survival mechanisms in different cell lines. For example, in cancer cells exhibiting high levels of CA, centrosome clustering may represent a stronger survival pathway, thereby reducing dependency on Survivin for cell survival. Importantly, while the data support a role for KIFC1 and Survivin in mitotic regulation, further investigation is required before definitive conclusions regarding therapeutic sensitivity can be drawn, as differential expression does not necessarily equate to therapeutic dependency. Future experiments that would enhance data findings include western blotting for measuring direct protein expression after siRNA treatment, RT-PCR for assessing and validating KIFC1 siRNA knockdown efficiency, and KIFC1 PROTACs for assessing direct KIFC1 protein knockdown.

8.0 - Appendix

Appendix 1

Well number:	**1**	**2**	**3**	**4**	**5**	**6**	**7**	**8**	**9**
OVCAR8									
Media alone (no cells or drug)	125	250	500	1000	2000	4000	8000	16000	
Media alone (no cells or drug)	125	250	500	1000	2000	4000	8000	16000	
OVCAR4									
Media alone (no cells or drug)	125	250	500	1000	2000	4000	8000	16000	
Media alone (no cells or drug)	125	250	500	1000	2000	4000	8000	16000	

Appendix 2

Paclitaxel final conc (nM). (stock conc = 100uM)	0	0.5	1	5	10	50	100	500	1000
100x working stock tubes (uM)	DMSO	0.05	0.1	0.5	1	5	10	50	100
AZ82 conc (uM)	0	0.01	0.05	0.1	0.5	1	5	10	50
100x working stock tubes	DMSO	1uM	5uM	10uM	50uM	100uM	500uM	1mM	5mM

Appendix 3

Tube 1	67.5ul RNAiMAX + 1125ul OptiMem
Tube 2	2.5ul siCon + 375ul OptiMem
Tube 3	2.5ul KIFC1_5 + 375ul OptiMem
Tube 4	2.5ul KIFC1_4 + 375ul OptiMem

Appendix 4

Plate plan:

	No cells	Mock	All stars	KIFC1_4	KIFC1_5	
	No cells	Mock	All stars	KIFC1_4	KIFC1_5	
	No cells	Mock	All stars	KIFC1_4	KIFC1_5	
	No cells	Mock	All stars	KIFC1_4	KIFC1_5	
	No cells	Mock	All stars	KIFC1_4	KIFC1_5	
	No cells	Mock	All stars	KIFC1_4	KIFC1_5	

9.0 - Bibliography

Akabane, S., Oue, N., Sekino, Y., Asai, R., Thang, P.Q., Taniyama, D., Sentani, K., Yukawa, M., Toda, T., Kimura, K., Egi, H., Shimizu, W., Ohdan, H. and Yasui, W. (2021). KIFC1 regulates ZWINT to promote tumor progression and spheroid formation in colorectal cancer. *Pathology International*, 71(7), pp.441–452. doi:https://doi.org/10.1111/pin.13098.

Cancer Research Institute. (2023). *Immunotherapy for Colorectal Cancer - Cancer Research Institute*. [online] Available at: https://www.cancerresearch.org/cancer-types/colorectal-cancer [Accessed 28 Oct. 2024].

Chaoxiang Lv, Qu, H., Zhu, W., Xu, K., Xu, A., Jia, B., Qing, Y., Li, H., Wei, H.-J. and Zhao, H.-Y. (2017). Low-Dose Paclitaxel Inhibits Tumor Cell Growth by Regulating Glutaminolysis in Colorectal Carcinoma Cells. *Frontiers in Pharmacology*, [online] 8. doi:https://doi.org/10.3389/fphar.2017.00244.

Cohen, A.L., Holmen, S.L. and Colman, H. (2013). IDH1 and IDH2 Mutations in Gliomas. *Current Neurology and Neuroscience Reports*, [online] 13(5). doi:https://doi.org/10.1007/s11910-013-0345-4.

Cui, X., Shen, D., Kong, C., Zhang, Z., Zeng, Y., Lin, X. and Liu, X. (2017a). NF-κB suppresses apoptosis and promotes bladder cancer cell proliferation by upregulating survivin expression in vitro and in vivo. *Scientific Reports*, 7(1). doi:https://doi.org/10.1038/srep40723.

Cui, X., Shen, D., Kong, C., Zhang, Z., Zeng, Y., Lin, X. and Liu, X. (2017b). NF-κB suppresses apoptosis and promotes bladder cancer cell proliferation by upregulating survivin expression in vitro and in vivo. *Scientific Reports*, [online] 7(1). doi:https://doi.org/10.1038/srep40723.

D'Orazi, G. (2023). p53 Function and Dysfunction in Human Health and Diseases. *Biomolecules*, [online] 13(3), pp.506–506. doi:https://doi.org/10.3390/biom13030506.

Dekker, E., Tanis, P., Vleugels, J., Kasi, P. and Wallace, M. (2019). *Colorectal cancer*. *Seminar www.thelancet.com*, p.1467.

Djuzenova, C.S., Fiedler, V., Memmel, S., Katzer, A., Hartmann, S., Krohne, G., Zimmermann, H., Scholz, C.-J., Polat, B., Flentje, M. and Sukhorukov, V.L. (2014). Actin cytoskeleton organization, cell surface modification and invasion rate of 5 glioblastoma cell lines differing in PTEN and p53 status.

Experimental Cell Research, [online] 330(2), pp.346–357. doi:https://doi.org/10.1016/j.yexcr.2014.08.013.

Drugbank.com. (2016). *Paclitaxel: Uses, Interactions, Mechanism of Action | DrugBank Online*. [online] Available at: https://go.drugbank.com/drugs/DB01229 [Accessed 25 Nov. 2024].

Du, B., Wei, L., Wang, J., Li, Y., Huo, J., Wang, J. and Wang, P. (2023). KIFC1 promotes proliferation and pseudo-bipolar division of ESCC through the transportation of Aurora B kinase. *Aging*, [online] 15(21), pp.12633–12650. doi:https://doi.org/10.18632/aging.205203.

Family, A., Roett, M. and Evans, P. (2009). Ovarian Cancer: An Overview. *American Family Physician*, 80(6).

Fan, G., Sun, L., Meng, L., Hu, C., Wang, X., Shi, Z., Hu, C., Han, Y., Yang, Q., Cao, L., Zhang, X., Zhang, Y., Song, X., Xia, S., He, B., Zhang, S. and Wang, C. (2021). The ATM and ATR kinases regulate centrosome clustering and tumor recurrence by targeting KIFC1 phosphorylation. *Nature Communications*, 12(1). doi:https://doi.org/10.1038/s41467-020-20208-x.

Fernández, J.G., Rodríguez, D.A., Valenzuela, M., Calderon, C., Ulises Urzúa, Munroe, D., Rosas, C., Lemus, D., Díaz, N., Wright, M.C., Leyton, L., Tapia, J.C. and Quest, A.F. (2014). Survivin expression promotes VEGF-induced tumor angiogenesis via PI3K/Akt enhanced β-catenin/Tcf-Lef dependent transcription. *Molecular Cancer*, [online] 13(1). doi:https://doi.org/10.1186/1476-4598-13-209.

The Fiji Team (2019). *Fiji: ImageJ, with 'Batteries Included'*. [online] Fiji.sc. Available at: https://fiji.sc/.

Fitzmaurice, C. (2019). Global, regional, and national burden of brain and other CNS cancer, 1990-2016: a systematic analysis for the Global Burden of Disease Study 2016. *Lancet Neurol 2019*, 18.

Fu, X., Zhu, Y., Zheng, B., Zou, Y., Wang, C., Wu, P., Wang, J., Chen, H., Du, P., Liang, B. and Fang, L. (2018). KIFC1, a novel potential prognostic factor and therapeutic target in hepatocellular carcinoma. *International Journal of Oncology*, 52. doi:https://doi.org/10.3892/ijo.2018.4348.

Gabriella, Geraldo, Faria, B.M., Soniza Vieira Alves-Leon, Marcondes, J., Vivaldo Moura-Neto, Pontes, B., Romão, L.F. and Garcez, P.P. (2022). Centromere protein J is overexpressed in human glioblastoma and promotes cell proliferation and migration. *Journal of Neurochemistry*, [online] 162(6), pp.501–513. doi:https://doi.org/10.1111/jnc.15660.

Ganesh, K., Stadler, Z.K., Cercek, A., Mendelsohn, R.B., Shia, J., Segal, N.H. and Diaz, L.A. (2019). Immunotherapy in colorectal cancer: rationale, challenges and potential. *Nature Reviews Gastroenterology & Hepatology*, 16(6), pp.361–375. doi:https://doi.org/10.1038/s41575-019-0126-x.

GraphPad (2018). *Home - graphpad.com*. [online] Graphpad.com. Available at: https://www.graphpad.com/.

Graham, H. (2022). The mechanism of action and clinical value of PROTACs: A graphical review. *Cellular Signalling*, [online] 99, pp.110446–110446. doi:https://doi.org/10.1016/j.cellsig.2022.110446.

Guindalini, R.S.C., Mathias Machado, M.C. and Garicochea, B. (2013). Monitoring Survivin Expression in Cancer: Implications for Prognosis and Therapy. *Molecular Diagnosis & Therapy*, 17(6), pp.331–342. doi:https://doi.org/10.1007/s40291-013-0048-1.

Hanahan, D. and Weinberg, R. (2000). The Hallmarks of Cancer Review evolve progressively from normalcy via a series of pre. *Cell*, 100, pp.57–70.

Hanahan, D. and Weinberg, R. (2011). Hallmarks of Cancer: The Next Generation. *Cell*, [online] 144(5), pp.646–674. doi:https://doi.org/10.1016/j.cell.2011.02.013.

Harrison, L.E., Bleiler, M. and Giardina, C. (2018). A look into centrosome abnormalities in colon cancer cells, how they arise and how they might be targeted therapeutically. *Biochemical Pharmacology*, 147, pp.1–8. doi:https://doi.org/10.1016/j.bcp.2017.11.003.

Hashemi, M., Etemad, S., Rezaei, S., Ziaolhagh, S., Rajabi, R., Rahmanian, P., Abdi, S., Koohpar, Z.K., Rafiei, R., Raei, B., Ahmadi, F., Salimimoghadam, S., Aref, A.R., Zandieh, M.A., Entezari, M., Taheriazam, A. and Hushmandi, K. (2023). Progress in targeting PTEN/PI3K/Akt axis in glioblastoma therapy: Revisiting molecular interactions. *Biomedicine & Pharmacotherapy*, [online] 158, p.114204. doi:https://doi.org/10.1016/j.biopha.2022.114204.

He, Y., Zan, X., Miao, J., Wang, B., Wu, Y., Shen, Y., Chen, X., Gou, H., Zheng, S., Huang, N., Cheng, Y., Ju, Y., Fu, X., Qian, Z., Zhou, P., Liu, J. and Gao, X. (2022). Enhanced anti-glioma efficacy of doxorubicin with BRD4 PROTAC degrader using targeted nanoparticles. *Materials Today Bio*, [online] 16, pp.100423–100423. doi:https://doi.org/10.1016/j.mtbio.2022.100423.

Hosseinalizadeh, H., Mahmoodpour, M., Samadani, A.A. and Roudkenar, M.H. (2022). The immunosuppressive role of indoleamine 2, 3-dioxygenase in glioblastoma: mechanism of action and

immunotherapeutic strategies. *Medical Oncology*, 39(9). doi:https://doi.org/10.1007/s12032-022-01724-w.

Huang, D., Sun, W., Zhou, Y., Li, P., Chen, F., Chen, H., Xia, D., Xu, E., Lai, M., Wu, Y. and Zhang, H. (2018). Mutations of key driver genes in colorectal cancer progression and metastasis. *Cancer and Metastasis Reviews*, 37(1), pp.173–187. doi:https://doi.org/10.1007/s10555-017-9726-5.

Huo, X., Zhang, W., Zhao, G., Chen, Z., Dong, P., Watari, H., Narayanan, R., Tillmanns, T.D., Pfeffer, L.M. and Yue, J. (2022). FAK PROTAC Inhibits Ovarian Tumor Growth and Metastasis by Disrupting Kinase Dependent and Independent Pathways. *Frontiers in Oncology*, [online] 12. doi:https://doi.org/10.3389/fonc.2022.851065.

Jin, J., Wu, Y., Zhao, Z., Wu, Y., Zhou, Y., Liu, S., Sun, Q., Yang, G., Lin, J., Nagle, D.G., Qin, J., Zhang, Z., Chen, H., Zhang, W., Sun, S. and Luan, X. (2022). Small-molecule PROTAC mediates targeted protein degradation to treat STAT3-dependent epithelial cancer. *JCI Insight*, [online] 7(22). doi:https://doi.org/10.1172/jci.insight.160606.

Jovanović, A., Tošić, N., Marjanović, I., Komazec, J., Zukić, B., Nikitović, M., Ilić, R., Grujičić, D., Janić, D. and Pavlović, S. (2023). Germline Variants in Cancer Predisposition Genes in Pediatric Patients with Central Nervous System Tumors. *International Journal of Molecular Sciences*, 24(24), p.17387. doi:https://doi.org/10.3390/ijms242417387.

KAFADAR, D., YAYLIM, I., KAFADAR, A.M., CACINA, C., ERGEN, A., KAYNAR, M.Y. and ISBIR, T. (2018). Investigation of *Survivin* Gene Polymorphism and Serum Survivin Levels in Patients with Brain Tumors. *Anticancer Research*, 38(10), pp.5991–5998. doi:https://doi.org/10.21873/anticanres.12947.

Kim, D.H., Ahn, J.S., Han, H.J., Kim, H.-M., Hwang, J., Lee, K.H., Cha-Molstad, H., Ryoo, I.-J., Jang, J.-H., Ko, S.-K., Yang, J.O., Lee, H.G., Lee, S., Song, E.J., Kim, J.Y., Huh, Y.H., Kwon, Y.T., Soung, N.-K. and Kim, B.Y. (2019). Cep131 overexpression promotes centrosome amplification and colon cancer progression by regulating Plk4 stability. *Cell Death & Disease*, 10(8). doi:https://doi.org/10.1038/s41419-019-1778-8.

Konstantinos Drosopoulos, Tang, C., William and Spiros Linardopoulos (2014). APC/C is an essential regulator of centrosome clustering. *Nature Communications*, [online] 5(1). doi:https://doi.org/10.1038/ncomms4686.

Kostecka, L.G., Olseen, A., Kang, K., Torga, G., Pienta, K.J. and Amend, S.R. (2021). High KIFC1 expression is associated with poor prognosis in prostate cancer. *Medical Oncology*, 38(5). doi:https://doi.org/10.1007/s12032-021-01494-x.

Kurokawa, C., H. Geekiyanage, Allen, C., I. Iankov, Schroeder, M., Carlson, B., Bakken, K., J. Sarkaria, Ecsedy, J.A., A. D'Assoro, Friday, B. and Galanis, E. (2016). Alisertib demonstrates significant antitumor activity in bevacizumab resistant, patient derived orthotopic models of glioblastoma. *Journal of Neuro-Oncology*, [online] 131(1), pp.41–48. doi:https://doi.org/10.1007/s11060-016-2285-8.

Kwon, M., Godinho, S.A., Chandhok, N.S., Ganem, N.J., Azioune, A., Thery, M. and Pellman, D. (2008). Mechanisms to suppress multipolar divisions in cancer cells with extra centrosomes. *Genes & Development*, 22(16), pp.2189–2203. doi:https://doi.org/10.1101/gad.1700908.

Lai, Y.-J., Lin, C.-I., Wang, C.-L. and Chao, J.-I. (2014). Expression of survivin and p53 modulates honokiol-induced apoptosis in colorectal cancer cells. *Journal of Cellular Biochemistry*, 115, p.n/a-n/a. doi:https://doi.org/10.1002/jcb.24858.

Leroy, B., Girard, L., Hollestelle, A., Minna, J.D., Gazdar, A.F. and Soussi, T. (2014). Analysis of TP53 Mutation Status in Human Cancer Cell Lines: A Reassessment. *Human Mutation*, [online] 35(6), pp.756–765. doi:https://doi.org/10.1002/humu.22556.

Li, J., Diao, H., Guan, X. and Tian, X. (2020). Kinesin Family Member C1 (KIFC1) Regulated by Centrosome Protein E (CENPE) Promotes Proliferation, Migration, and Epithelial-Mesenchymal Transition of Ovarian Cancer. *Medical Science Monitor*, 26. doi:https://doi.org/10.12659/msm.927869.

Li, J.W., Zheng, G., Kaye, F.J. and Wu, L. (2023). PROTAC therapy as a new targeted therapy for lung cancer. *Molecular Therapy*, 31(3), pp.647–656. doi:https://doi.org/10.1016/j.ymthe.2022.11.011.

Li, K. and Crews, C.M. (2022). PROTACs: past, present and future. *Chemical Society Reviews*, 51(12), pp.5214–5236. doi:https://doi.org/10.1039/d2cs00193d.

Li, Y., Lu, W., Chen, D., Boohaker, R.J., Zhai, L., Padmalayam, I., Wennerberg, K., Xu, B. and Zhang, W. (2015). KIFC1 is a novel potential therapeutic target for breast cancer. *Cancer Biology & Therapy*, [online] 16(9), pp.1316–1322. doi:https://doi.org/10.1080/15384047.2015.1070980.

Liu, Y., Ye, W., Miao, X. and Wang, X. (2023). KIFC1 aggravates non-small-cell lung cancer cell proliferation and metastasis via provoking TGF-β/SMAD signal. *Cellular and Molecular Biology*, 69(14), pp.293–299. doi:https://doi.org/10.14715/cmb/2023.69.14.48.

Mahmoudian-Sani, M.-R., Alghasi, A., Saeedi-Boroujeni, A., Jalali, A., Jamshidi, M. and Khodadadi, A. (2019). Survivin as a diagnostic and therapeutic marker for thyroid cancer. *Pathology - Research and Practice*, 215(4), pp.619–625. doi:https://doi.org/10.1016/j.prp.2019.01.025.

Marteil, G., Guerrero, A., Vieira, A.F., de Almeida, B.P., Machado, P., Mendonça, S., Mesquita, M., Villarreal, B., Fonseca, I., Francia, M.E., Dores, K., Martins, N.P., Jana, S.C., Tranfield, E.M., Barbosa-Morais, N.L., Paredes, J., Pellman, D., Godinho, S.A. and Bettencourt-Dias, M. (2018). Over-elongation of centrioles in cancer promotes centriole amplification and chromosome missegregation. *Nature Communications*, 9(1). doi:https://doi.org/10.1038/s41467-018-03641-x.

Mayo Clinic. (2024). *Brain tumor - Symptoms and causes*. [online] Available at: https://www.mayoclinic.org/diseases-conditions/brain-tumor/symptoms-causes/syc-20350084 [Accessed 29 Oct. 2024].

Mehdizadeh, R., Alireza Madjid Ansari, Forouzesh, F., Shahriari, F., Seyed Peyman Shariatpanahi, Salaritabar, A. and Mohammad Amin Javidi (2023). P53 status, and G2/M cell cycle arrest, are determining factors in cell-death induction mediated by ELF-EMF in glioblastoma. *Scientific Reports*, 13(1). doi:https://doi.org/10.1038/s41598-023-38021-z.

Mercadante, D.L., Aaron, W.A., Olson, S.D. and Manning, A.L. (2023). Cortical dynein drives centrosome clustering in cells with centrosome amplification. *Molecular Biology of the Cell*, [online] 34(6). doi:https://doi.org/10.1091/mbc.e22-07-0296.

Mita, A.C., Mita, M.M., Nawrocki, S.T. and Giles, F.J. (2008). Survivin: Key Regulator of Mitosis and Apoptosis and Novel Target for Cancer Therapeutics. *Clinical Cancer Research*, 14(16), pp.5000–5005. doi:https://doi.org/10.1158/1078-0432.ccr-08-0746.

Mitra, A.K., Davis, D.A., Tomar, S., Roy, L., Hilal Gurler, Xie, J., Lantvit, D.D., Cardenas, H., Fang, F., Liu, Y., Loughran, E., Yang, J., Stack, M.S., Emerson, R.E., Cowden, K.D., Barbolina, M.V., Nephew, K.P., Matei, D. and Burdette, J.E. (2015). In vivo tumor growth of high-grade serous ovarian cancer cell lines. *Gynecologic Oncology*, [online] 138(2), pp.372–377. doi:https://doi.org/10.1016/j.ygyno.2015.05.040.

Mónica Bettencourt-Dias and Glover, D.M. (2007). Centrosome biogenesis and function: centrosomics brings new understanding. *Nature Reviews Molecular Cell Biology*, [online] 8(6), pp.451–463. doi:https://doi.org/10.1038/nrm2180.

National Brain Tumor Society. (2024). *Brain Tumor Facts - National Brain Tumor Society*. [online] Available at: https://braintumor.org/brain-tumors/about-brain-tumors/brain-tumor-facts/#:~:text=For%202023%2C%20the%20highest%20number,all%20primary%20brain%20tumor%20types [Accessed 22 Apr. 2025].

Omim.org. (2015). *Entry - *603072 - AURORA KINASE A; AURKA - OMIM*. [online] Available at: https://www.omim.org/entry/603072#:~:text=The%20AURKA%20gene%20is%20overexpressed,facilitating%20oncogenic%20transformation%20of%20cells. [Accessed 2 May 2025].

Pannu, V., Rida, P.C.G., Ogden, A., Turaga, R.C., Donthamsetty, S., Bowen, N.J., Rudd, K., Gupta, M.V., Reid, M.D., Cantuaria, G., Walczak, C.E. and Aneja, R. (2015). HSET overexpression fuels tumor progression via centrosome clustering-independent mechanisms in breast cancer patients. *Oncotarget*, 6(8), pp.6076–6091. doi:https://doi.org/10.18632/oncotarget.3475.

Park, H.-W., Ma, Z., Zhu, H., Jiang, S., Robinson, R.C. and Endow, S.A. (2017). Structural basis of small molecule ATPase inhibition of a human mitotic kinesin motor protein. *Scientific Reports*, [online] 7(1). doi:https://doi.org/10.1038/s41598-017-14754-6.

Parvin, A., Hao, S.-L., Tan, F.-Q. and Yang, W.-X. (2020). Inhibition of kinesin motor protein KIFC1 by AZ82 induces multipolar mitosis and apoptosis in prostate cancer cell. *Gene*, [online] 760, p.144989. doi:https://doi.org/10.1016/j.gene.2020.144989.

Patel, N., Weekes, D., Drosopoulos, K., Gazinska, P., Noel, E., Rashid, M., Mirza, H., Quist, J., Brasó-Maristany, F., Mathew, S., Ferro, R., Pereira, A.M., Prince, C., Noor, F., Francesch-Domenech, E., Marlow, R., de Rinaldis, E., Grigoriadis, A., Linardopoulos, S. and Marra, P. (2018). Integrated genomics and functional validation identifies malignant cell specific dependencies in triple negative breast cancer. *Nature Communications*, 9(1). doi:https://doi.org/10.1038/s41467-018-03283-z.

Paul, A. (2014). The breast cancer susceptibility genes (BRCA) in breast and ovarian cancers. *Frontiers in Bioscience*, 19(4), p.605. doi:https://doi.org/10.2741/4230.

Pennington, K.P. and Swisher, E.M. (2012). Hereditary ovarian cancer: Beyond the usual suspects. *Gynecologic Oncology*, 124(2), pp.347–353. doi:https://doi.org/10.1016/j.ygyno.2011.12.415.

Prakash, A., Shishir Paunikar, Webber, M., McDermott, E., Vellanki, S.H., Thompson, K., Dockery, P., Jahns, H., James, Hopkins, A.M. and Bourke, E. (2023). Centrosome amplification promotes cell invasion via cell–cell contact disruption and Rap-1 activation. *Journal of Cell Science*, [online] 136(21). doi:https://doi.org/10.1242/jcs.261150.

Prashanth Rawla, Sunkara, T. and Barsouk, A. (2019). Epidemiology of colorectal cancer: incidence, mortality, survival, and risk factors. *Gastroenterology Review*, [online] 14(2), pp.89–103. doi:https://doi.org/10.5114/pg.2018.81072.

Qi, F. and Zhou, J. (2021). Multifaceted roles of centrosomes in development, health, and disease. *Journal of Molecular Cell Biology*, 13(9), pp.611–621. doi:https://doi.org/10.1093/jmcb/mjab041.

QIAGEN (2025a). *Hs_KIFC1_4 FlexiTube siRNA | GeneGlobe*. [online] Qiagen.com. Available at: https://geneglobe.qiagen.com/us/product-groups/flexitube-sirna-premix/SI00462581 [Accessed 22 Jan. 2025].

QIAGEN (2025b). *Hs_KIFC1_5 FlexiTube siRNA | GeneGlobe*. [online] Qiagen.com. Available at: https://geneglobe.qiagen.com/us/product-groups/flexitube-sirna-premix/SI02653210 [Accessed 22 Jan. 2025].

Qin, L., Tong, T., Song, Y., Xue, L., Fan, F. and Zhan, Q. (2008). Aurora-A interacts with Cyclin B1 and enhances its stability. *Cancer Letters*, [online] 275(1), pp.77–85. doi:https://doi.org/10.1016/j.canlet.2008.10.011.

Raab, M., Izabela Kostova, Peña-Llopis, S., Fietz, D., Kressin, M., Seyed Mohsen Aberoumandi, Ullrich, E., Becker, S., Mourad Sanhaji and Klaus Strebhardt (2023). Rescue of p53 functions by in vitro-transcribed mRNA impedes the growth of high-grade serous ovarian cancer. *Cancer Communications*, [online] 44(1), pp.101–126. doi:https://doi.org/10.1002/cac2.12511.

Ramachandran, S. and Ciulli, A. (2021). Building ubiquitination machineries: E3 ligase multi-subunit assembly and substrate targeting by PROTACs and molecular glues. *Current Opinion in Structural Biology*, 67, pp.110–119. doi:https://doi.org/10.1016/j.sbi.2020.10.009.

Ravizza, R., Gariboldi, M.B., Passarelli, L. and Monti, E. (2004). Role of the p53/p21 system in the response of human colon carcinoma cells to Doxorubicin. *BMC Cancer*, [online] 4(1). doi:https://doi.org/10.1186/1471-2407-4-92.

Reilly, K.M. (2008). Brain Tumor Susceptibility: the Role of Genetic Factors and Uses of Mouse Models to Unravel Risk. *Brain Pathology*, [online] 19(1), pp.121–131. doi:https://doi.org/10.1111/j.1750-3639.2008.00236.x.

Rishfi, M., Krols, S., Martens, F., Bekaert, S.-L., Sanders, E., Eggermont, A., De Vloed, F., Goulding, J.R., Risseeuw, M., Molenaar, J., De Wilde, B., Van Calenbergh, S. and Durinck, K. (2023). Targeted AURKA degradation: Towards new therapeutic agents for neuroblastoma. *European Journal of Medicinal Chemistry*, 247, p.115033. doi:https://doi.org/10.1016/j.ejmech.2022.115033.

Ryniawec, J.M. and Rogers, G.C. (2021). Centrosome instability: when good centrosomes go bad. *Cellular and Molecular Life Sciences*, 78(21-22), pp.6775–6795. doi:https://doi.org/10.1007/s00018-021-03928-1.

Sabat-Po Spiech, D., Fabian-Kolpanowicz, K., Kalirai, H., Kipling, N., Coupland, S., Coulson, J. and Fielding, A. (2022). Aggressive uveal melanoma displays a high degree of centrosome amplification, opening the door to therapeutic intervention. *The Journal of Pathology: Clinical Research J Pathol Clin Res*, 8, pp.383–394. doi:https://doi.org/10.1002/cjp2.272.

Sameer Farouk Sait, Walsh, M.F. and Karajannis, M.A. (2021). Genetic syndromes predisposing to pediatric brain tumors. *Neuro-Oncology Practice*, [online] 8(4), pp.375–390. doi:https://doi.org/10.1093/nop/npab012.

Sauer, C.M., Hall, J.A., Couturier, D.-L., Bradley, T., Piskorz, A.M., Griffiths, J., Sawle, A., Eldridge, M.D., Smith, P., Hosking, K., Reinius, M.A.V., Morrill Gavarró, L., Mes-Masson, A.-M., Ennis, D., Millan, D., Hoyle, A., McNeish, I.A., Jimenez-Linan, M., Martins, F.C. and Tischer, J. (2023). Molecular landscape and functional characterization of centrosome amplification in ovarian cancer. *Nature Communications*, 14(1). doi:https://doi.org/10.1038/s41467-023-41840-3.

Sekino, Y., Pham, Q.T., Kobatake, K., Kitano, H., Ikeda, K., Goto, K., Hayashi, T., Nakahara, H., Sentani, K., Oue, N., Yasui, W., Teishima, J. and Hinata, N. (2021). KIFC1 Is Associated with Basal Type, Cisplatin Resistance, PD-L1 Expression and Poor Prognosis in Bladder Cancer. *Journal of Clinical Medicine*, 10(21), p.4837. doi:https://doi.org/10.3390/jcm10214837.

Shan, M.-M., Zou, Y.-J., Pan, Z.-N., Zhang, H.-L., Xu, Y., Ju, J.-Q. and Sun, S.-C. (2022). Kinesin motor KIFC1 is required for tubulin acetylation and actin-dependent spindle migration in mouse oocyte meiosis. *Development*, [online] 149(5). doi:https://doi.org/10.1242/dev.200231.

She, Z.-Y. and Yang, W.-X. (2017). Molecular mechanisms of kinesin-14 motors in spindle assembly and chromosome segregation. *Journal of Cell Science*, 130(13), pp.2097–2110. doi:https://doi.org/10.1242/jcs.200261.

Shin, A.E., Giancotti, F.G. and Rustgi, A.K. (2023). Metastatic colorectal cancer: mechanisms and emerging therapeutics. *Trends in Pharmacological Sciences*, 44(4), pp.222–236. doi:https://doi.org/10.1016/j.tips.2023.01.003.

Talib, W.H., Alsayed, A.R., Barakat, M., Abu-Taha, M.I. and Asma Ismail Mahmod (2021). Targeting Drug Chemo-Resistance in Cancer Using Natural Products. *Biomedicines*, [online] 9(10), pp.1353–1353. doi:https://doi.org/10.3390/biomedicines9101353.

Tumors, B. (2023). *Brain Tumor: Symptoms, Signs & Causes*. [online] Cleveland Clinic. Available at: https://my.clevelandclinic.org/health/diseases/6149-brain-cancer-brain-tumor [Accessed 29 Oct. 2024].

Vasquez-Limeta, A. and Loncarek, J. (2021). Human centrosome organization and function in interphase and mitosis. *Seminars in Cell & Developmental Biology*, 117, pp.30–41. doi:https://doi.org/10.1016/j.semcdb.2021.03.020.

Wallis, B., Bowman, K.R., Lu, P. and Lim, C.S. (2023). The Challenges and Prospects of p53-Based Therapies in Ovarian Cancer. *Biomolecules*, 13(1), p.159. doi:https://doi.org/10.3390/biom13010159.

Watts, Ciorsdaidh A., Richards, Frances M., Bender, A., Bond, Peter J., Korb, O., Kern, O., Riddick, M., Owen, P., Myers, Rebecca M., Raff, J., Gergely, F., Jodrell, Duncan I. and Ley, Steven V. (2013). Design, Synthesis, and Biological Evaluation of an Allosteric Inhibitor of HSET that Targets Cancer Cells with Supernumerary Centrosomes. *Chemistry & Biology*, 20(11), pp.1399–1410. doi:https://doi.org/10.1016/j.chembiol.2013.09.012.

Webb, P.M. and Jordan, S.J. (2017). Epidemiology of epithelial ovarian cancer. *Best Practice & Research Clinical Obstetrics & Gynaecology*, 41, pp.3–14. doi:https://doi.org/10.1016/j.bpobgyn.2016.08.006.

Wei, Y.-L. and Yang, W.-X. (2019). Kinesin-14 motor protein KIFC1 participates in DNA synthesis and chromatin maintenance. *Cell Death & Disease*, 10(6). doi:https://doi.org/10.1038/s41419-019-1619-9.

World Health Organization (2019). *Cancer*. [online] World Health Organization. Available at: https://www.who.int/health-topics/cancer#tab=tab_1.

Willems, E., Lombard, A., Dedobbeleer, M., Goffart, N. and Rogister, B. (2016). The Unexpected Roles of Aurora A Kinase in Gliobastoma Recurrences. *Targeted Oncology*, 12(1), pp.11–18. doi:https://doi.org/10.1007/s11523-016-0457-2.

Xiao, Y.-X., Shen, H.-Q., She, Z.-Y., Sheng, L., Chen, Q.-Q., Chu, Y.-L., Tan, F.-Q. and Yang, W.-X. (2017). C-terminal kinesin motor KIFC1 participates in facilitating proper cell division of human seminoma. *Oncotarget*, 8(37), pp.61373–61384. doi:https://doi.org/10.18632/oncotarget.18139.

Xiao, Y.-X. and Yang, W.-X. (2016). KIFC1: a promising chemotherapy target for cancer treatment? *Oncotarget*, 7(30), pp.48656–48670. doi:https://doi.org/10.18632/oncotarget.8799.

XIONG, T., WEI, H., CHEN, X. and XIAO, H. (2014). PJ34, a poly(ADP-ribose) polymerase (PARP) inhibitor, reverses melphalan-resistance and inhibits repair of DNA double-strand breaks by targeting the FA/BRCA pathway in multidrug resistant multiple myeloma cell line RPMI8226/R. *International Journal of Oncology*, [online] 46(1), pp.223–232. doi:https://doi.org/10.3892/ijo.2014.2726.

Yang, C., Xia, B.-R., Zhang, Z.-C., Zhang, Y.-J., Lou, G. and Jin, W.-L. (2020). Immunotherapy for Ovarian Cancer: Adjuvant, Combination, and Neoadjuvant. *Frontiers in Immunology*, 11. doi:https://doi.org/10.3389/fimmu.2020.577869.

Yang, L., Xie, H.-J., Li, Y.-Y., Wang, X., Liu, X.-X. and Mai, J. (2022). Molecular mechanisms of platinum-based chemotherapy resistance in ovarian cancer (Review). *Oncology Reports*, 47(4). doi:https://doi.org/10.3892/or.2022.8293.

Yohei Sekino, Naohide Oue, Koike, Y., Shigematsu, Y., Sakamoto, N., Kazuhiro Sentani, Jun Teishima, Shiota, M., Matsubara, A. and Yasui, W. (2019). KIFC1 Inhibitor CW069 Induces Apoptosis and Reverses Resistance to Docetaxel in Prostate Cancer. *Journal of Clinical Medicine*, [online] 8(2), pp.225–225. doi:https://doi.org/10.3390/jcm8020225.

Yukawa, M., Yamauchi, T., Kurisawa, N., Ahmed, S., Kimura, K. and Toda, T. (2018). Fission yeast cells overproducing HSET/KIFC1 provides a useful tool for identification and evaluation of human kinesin-14 inhibitors. *Fungal Genetics and Biology*, 116, pp.33–41. doi:https://doi.org/10.1016/j.fgb.2018.04.006.

Zeimet, A.G. and Marth, C. (2003). Why did p53 gene therapy fail in ovarian cancer? *The Lancet Oncology*, [online] 4(7), pp.415–422. doi:https://doi.org/10.1016/s1470-2045(03)01139-2.

Zhang, W., Zhai, L., Wang, Y., Boohaker, Rebecca J., Lu, W., Gupta, Vandana V., Padmalayam, I., Bostwick, Robert J., White, E. Lucile, Ross, Larry J., Maddry, J., Ananthan, S., Augelli-Szafran, Corinne E., Suto, Mark J., Xu, B., Li, R. and Li, Y. (2016). Discovery of a novel inhibitor of kinesin-like protein KIFC1. *Biochemical Journal*, 473(8), pp.1027–1035. doi:https://doi.org/10.1042/bj20150992.

Zhao, H., Ming, T., Tang, S., Ren, S., Yang, H., Liu, M., Tao, Q. and Xu, H. (2022). Wnt signaling in colorectal cancer: pathogenic role and therapeutic target. *Molecular Cancer*, [online] 21(1). doi:https://doi.org/10.1186/s12943-022-01616-7.

Zhou, K., Lin, J., Dai, M., He, Y., Xu, J. and Lin, Q. (2021). KIFC1 promotes aerobic glycolysis in endometrial cancer cells by regulating the c-myc pathway. *Journal of Bioenergetics and Biomembranes*, 53(6), pp.703–713. doi:https://doi.org/10.1007/s10863-021-09924-1.